LBL-7897

Energy and Environment Division

Filtration Of Solvent Refined Coal Suspensions

Robert Joseph Steininger II

M.S. thesis

September 1978

Lawrence Berkeley Laboratory University of California/Berkeley

Prepared for the U.S. Department of Energy under Contract No. W-7405-ENG-48

LBL-7897

DISCLAIMER

FILTRATION OF SOLVENT REFINED COAL SUSPENSIONS

Robert Joseph Steininger II

Department of Chemical Engineering
University of California
Berkeley, California

FILTRATION OF SOLVENT REFINED COAL SUSPENSIONS

Table of Contents

ACKNOWLEDGMENTS

Si la vie était sample,
Elle serait ennuyeuse.

I would like to thank Professor D. Hanson for his gentle encouragement, Professor C. J. Radke for his constant exuberance, and Carolyn Hoffman for not only making life here interesting, but also enjoyable.

FILTRATION OF SOLVENT REFINED COAL SUSPENSIONS

Robert Joseph Steininger II
Department of Chemical Engineering
University of California
Berkeley, California

ABSTRACT

The surface properties of ash from solvent refined coal filter feed are examined and modified to investigate improved ash separation from coal derived liquids.

The effect of solvent and additives on settling rates and agglomeration is observed. Little enhancement other than from solvent viscosity is found with any of the materials tried.

Introduction of water and its possible use as an extractor and/or anti-solvent are examined. Additional techniques of flotation and spherical agglomeration are attempted. No enhancement in the separation of the ash from the natural solvent is observed.

Measurements of the charge on particles in nonpolar suspensions are made quantitatively. The ash exhibits a positive zeta potential in pyridine and coal solvent of approximately 50 mV. The charge on the ash is found to be caused by soluble asphaltene components within the solvent refined coal solutions.

The measured zeta potential of the particles is correlated with the specific cake resistances of the studied suspensions. Charge

is found to be one of the number of parameters affecting the filterability of these suspensions. Although filtration rates of ash in pyridine are increased ten-fold by adding copper oleate, the same effect is not noted in the case of ash dispersed in solvent refined coal solutions. Dissolved asphaltenes in the coal solvent are found to play a major role in maintaining the charge on the ash in these dispersions.

NOMENCLATURE

a	=	particle diameter
A	=	acid molecule
A_{12}	=	Hamaker constant
B	=	base molecule
c_p	=	particle concentration g/cm^3
d	=	width of cell
D_p	=	effective particle diameter
e	=	elementary charge
f	=	fraction settled
F	=	Faraday constant
F_c	=	Hückel equation correction
F(d)	=	Force at distance d
g	=	gravitational constant
H	=	distance between particle surfaces
k	=	Boltzman constant
K	=	filtration constant
l	=	length
L	=	cake thickness
m_p	=	mass of particles
n	=	number of ions/cm^3
N_a	=	Avagadro's number
p	=	pressure
Q	=	flow rate, volume per time

r = radial distance from particle

R = distance from particle center to particle center

R_m = resistance of filtration support

R_p = effective radius of particle

s = normalized interparticle distance, R/2a

S_a = surface acid group

S_b = surface base group

S_p = specific surface area of particle/unit volume

t = time

T = absolute temperature

u = particle mobility

v = velocity

ΔV = potential difference

V = volume of filtrate

V_t = total potential energy

V_a = potential energy of attraction

V_r = potential energy of repulsion

w = weight of solids/cm^3 of dispersion

W = Fuch's stability ratio

z = valence of ion

α = specific cake resistance

γ = repulsive potential correction

ϵ = dielectric constant

ζ = zeta potential

θ = contact angle

κ = conductivity

Ω = specific conductivity

λ = Debye length

$\lambda^{o}_{\pm}$ = specific conductivity of individual ions

μ = viscosity

π = 3.14 ...

ρ_s = solid density

ρ_ℓ = liquid density

σ = surface tension

τ = tortuosity

$\psi(r)$ = potential at distance r

LIST OF TABLES

LIST OF FIGURES

I. SRC PROBLEM AND APPROACH

A. INTRODUCTION

The United States uses one third of all energy consumed in the world (1). Each day the country uses four million tons of coal, 2.7 billion liters of petroleum, and 1.5 billion cubic meters of gas (1). Despite efforts to conserve, this country cannot produce enough domestic fuel to meet its needs. Alternate sources of energy are needed. Coal is the only bountiful energy source that the United States still has in reserve, predominately because of the environmental difficulties connected with its use. Starting with the Berguis-I. G. Farben Process in Germany (2) much work has been done to develop a viable, economically feasible process to convert coal to a more usable, environmentally sound source of energy.

One method which has had limited success is the Solvent Refined Coal Process I developed by Pittsburgh and Midway Coal Mining Company (subsidiary of Gulf Oil Corporation) under the auspices of the Office of Coal Research of the United States Department of Interior. This development has subsequently led to pilot plant studies in 1972, a six ton/day plant in Wilsonville, Alabama and a fifty ton/day plant at Fort Lewis, Washington. These facilities are able to convert 85-95% of their coal feed with a total yield of 50-70% to low sulfur (0.6-0.9%), low ash (0.06-0.16%) hydrocarbon product suitable for boiler use (1)(2). In the process, the coal is upgraded in heat content from 3000-6700 kcal/kg to 9000 kcal/kg of solid. In doing so, the price of such fuel

has been estimated as $22/ton of product.

The process schematic can be seen in Figure I-1. Briefly, sub 200 mesh coal is suspended with recycle solvent of a hydrogen donating character. This is pressurized with hydrogen to 1000-3000 psi, preheated, and then reacted at 435-470 ^{o}C in the dissolver. After forty minutes, ninety percent of the coal reacts and sixty percent of the sulfur leaves as gas. The resulting product is stripped of the lighter components and then filtered to remove the inorganics. The recycle solvent is flashed fron the filtrate leaving the SRC or solvent refined coal as the final product. This solid is a black, shiny coal-like substance with a melting point of about 150 ^{o}C.

As with many coal liquefaction processes, the most difficult problem is the removal of the large amount of inorganic ash, up to ten percent of the original coal. The problem is formidable. A large amount of small particles, fifty percent of which is usually under 1 micron in diameter, must be separated from a very viscous liquid, usually at elevated temperatures and pressures. This separation must be nearly perfect to meet the Environmental Protection Agency's standards. No more than 0.96% of the sulfur and 0.15% of the ash by weight may remain in the final product. In addition, further removal would be necessary if the product is to be catalytically cracked downstream to create additional petroleum products (2).

Presently, the only method capable of this separation is the use of a rotary drum filter with a diatomaceous earth precoat. This filtration has been found to be economically unfavorable because of the

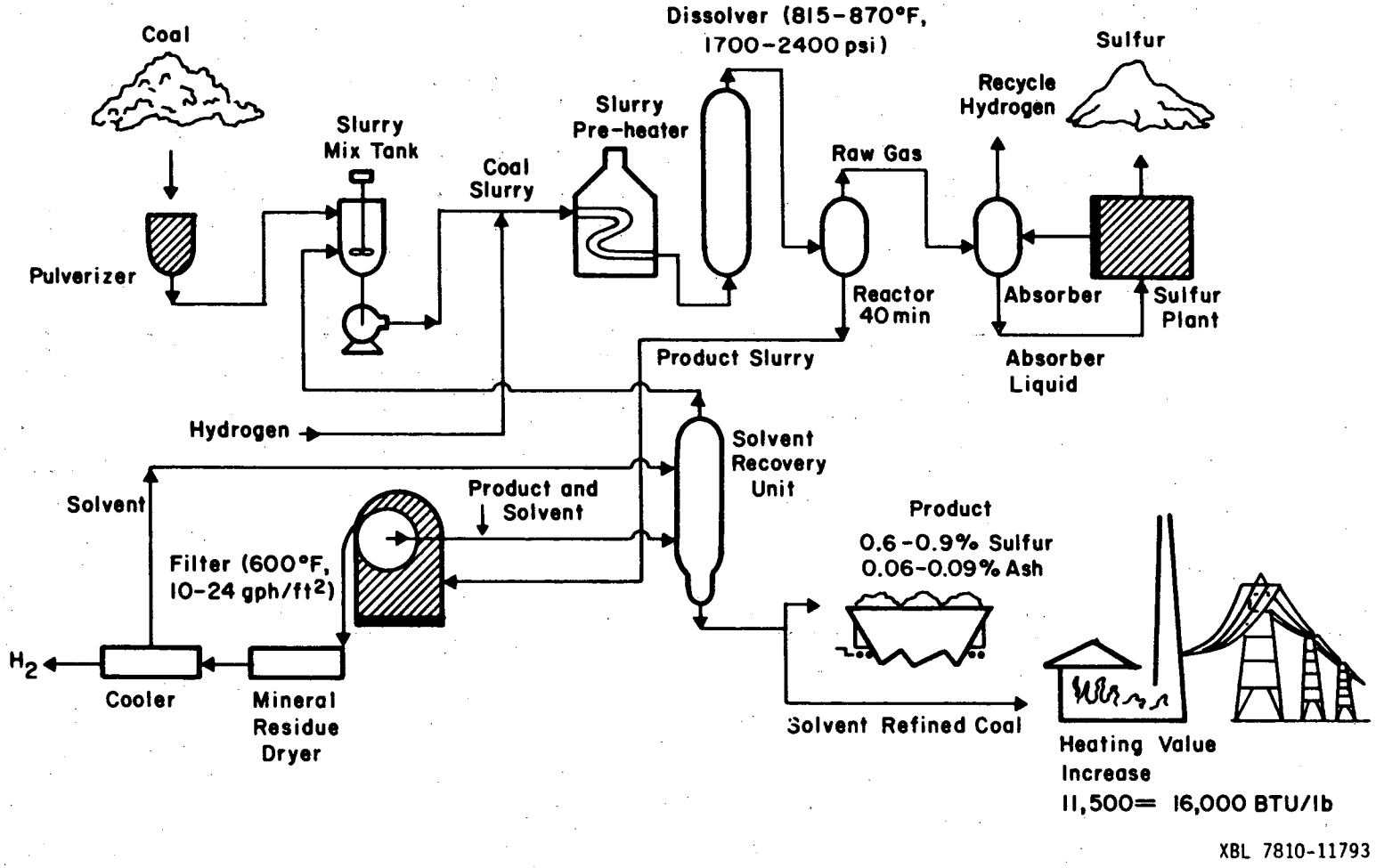

Figure I-1. Solvent refined coal process.

low flow rates and contamination of the solids with the precoat. The drum filters used in the Fort Lewis plant have at most achieved 15-20 gal/ft^2/hr, although the rate is usually lower and throughput is hampered by breakdowns. At the best sustained filter rate so far, a commercial facility processing 30,000 tons/day of coal with 10% ash would have to invest 48 million dollars for the filters alone and another $90,000/day for the precoat. Such figures indicate a mandatory ten fold increase in filtration rate if this process is to approach commercial feasibility (3).

B. PAST STUDIES

Considerable effort has been expended on attempting to improve the SRC filtration. Extensive research has been done on the effect of filtration parameters. Changes in knife advancement, immersion, precoat, differential pressure, and temperature have had little effect on the filtration rate (4)(5)(6)(7)(8)(9). Using a precoat of ground coal reduces the daily expense but does not increase the filtration rate (8).

External fields as well as alternative filtration systems have been studied. The use of high gradient magnetic separation as well as AC agglomeration has been tried but found to be unpromising (10). Cross flow and electro cross flow filtration have been proposed (11)(12). Neither has been encouraging.

Ninety nine percent removal of the ash has been achieved through the use of an antisolvent. Addition of antisolvents such as decane, toluene, and light kerosene oil to suspensions of ash in the liquefied product causes agglomeration due to the partial precipitation

of the asphaltenes and SRC in solution (8)(13)(14)(15)(16)(17)(18)(19)(20). Some success has been achieved through the addition of alkanolamines with pyridine accomplishing the same result (21). Separation is by settling in both cases. Unfortunately, these methods lose up to 30% of the SRC in the settled cake and require from 25-50% solvent when mixed with the SRC solution (15)(20)(21).

The work presented here concentrates on processes to alter the surface properties of the particles to effect agglomeration. In recent years, petroleum asphaltene solutions have been recognized as nonaqueous colloidal dispersions, stabilized by a number of different mechanisms (22)(23). The SRC liquid, although complex, might be considered similarly. Thus, traditional methods of achieving agglomeration without precipitating the asphaltenes from solution may be used to obtain a faster filtration rate.

C. THE SRC SOLUTION COMPONENTS

The SRC solution is a complex mixture of different sized, nearly exclusively aromatic compounds with a large percentage of inorganic particles. Understanding its general nature is of prime importance if one is to work to change its properties, especially those which influence the interaction of the SRC liquid and the surfaces of the suspended ash.

Since SRC is derived from coal, the number of products within the solution is enormous. Coal itself varies widely in composition and ash content. However, as an example, the elemental composition of the average coal used in making the SRC solution used in this study is given

in Table I-1. The forms of sulfur are further characterized in Table I-2. The conversion of such coal to liquids and oils has been studied and found to be a two step process (22)(23)(24). The first is the relatively fast breakdown of the coal's superstructure to form preasphaltenes and asphaltenes. The second is the slow decomposition of the asphaltene molecules to lighter products, usually considered resins and oils. During this process, the inorganics entrained in the superstructure of the coal are released as ash.

1. Ash Particles

a. Composition

Of the components of this hydrocarbon suspension, the ash is probably the best characterized for specific types of coal, although the exact composition depends on the origin of the coal. These solids are the mineral matter that was in or mined with the coal, usually consisting of clays and sands. Comparing ten coals, the elemental composition ranges are given in Table I-3. The predominate minerals are pyrites, quartz, kaolinite, hematite, calcite, gypsum, dolomite, and sphalerite (5)(25)(26).

In the SRC liquid, unreacted coal also contributes to the total mass of the particulates. This is shown in the composition analysis of the pyridine extracted ash given in Table I-4. The presence of this material is suspected to hinder high temperature filtrations (6).

TABLE I-1. Typical coal analysis (6)

Element	Weight Percent
C	71.35
H	5.07
N	1.44
S	3.50
O	7.55
Ash	10.12
Moisture	0.97

TABLE I-2. Sulfur forms (6)

Form	Weight Percent of Coal
Pyritic	1.63
Sulfate	0.09
Organic	1.76

TABLE I-3. Elemental inorganic composition of coals (25)

Element	Weight Percent
Si	1.2 - 3.0
Al	0.6 - 2.7
Fe	0.34 - 2.5
Mg	0.02 - 0.23
Ca	0.11 - 2.47
S	0.57 - 3.5

TABLE I-4. Typical mineral ash analysis

Element	Weight Percent
C	28 - 30
H	1.4 - 1.8
N	0.5 - 0.6
S	0.6 - 0.7
Residue	55.0 -64.0
Fe	9 - 10
Si	10 - 11

b. Size

The dimensions of the ash particles are extremely small. In recent studies by Johns Manville, extensive measurements of particle size were made on samples of SRC filter feed ash from three different liquefied coal samples (5). Using scanning electron microscopy, they found the average size of all ash particles to be less than or equal to 0.65 microns. Those particles greater than 0.2 microns followed a log normal distribution. In addition, a large number of sub 0.2 micron particles were found but not included in the average particle size calculation. These small particles are highly agglomerated and are difficult to separate from the SRC filter feed.

2. Coal Solution

The coal liquid is much more complicated in composition; it has a large variety of aromatic compounds as the result of the conversion process. Most of the molecules have a high molecular weight and are slightly polar due to varying amounts of hetero-atoms such as oxygen, nitrogen, and sulfur. There are very few aliphatic chains larger than three carbons long. The compounds are usually divided into three groups: the oils; the resins; and the asphaltenes. These divisions are arbitrary, primarily determined by solubility properties (27)(28)(29). In actuality, there is a gradual reduction of molecular size and polarity as one goes from asphaltenes to the oils (30)(31).

a. Oils

The oils are the clear, light fractions of the coal liquid, soluble in hexane. Usually, they include molecules of C_{15}-C_{18} in size

with a large variation in aliphatic hydrogen (29). Because 2-4 ring structures predominate, the oils have been closely associated with the composition of creosote oil (31). These compounds probably make up the light ends of the SRC recycle solvent.

b. Resins

The resins are the intermediary compounds which will dissolve in the coal oils (32). These red, oily liquids have a characteristic phenolic odor and are soluble in benzene-hexane mixtures and other slightly polar solvents (27)(28). In most cases, they are susceptible to dipole-dipole interactions due to the presence of hydroxyl and nitrogen functional groups (27)(32). Proposed structures for such compounds are usually of a molecular weight of 300 as shown in Figure I-2.

c. Asphaltenes

The asphaltenes are higher molecular weight resins with as much as one hetero atom per 8-10 carbon atoms (29). Traditionally, they have been defined as those components that are soluble in benzene and insoluble in pentane. However, recent work has shown that there is a significant amount of these compounds that requires more highly polar solvents to dissolve them, for example pyridine, tetrahydrofuran, and chloroform (28)(30)(33)(34)(35)(36)(37). Although these are included as asphaltenes here, others have segregated this fraction once again into the asphaltenes, soluble in hot benzene, and the preasphaltenes or carboids, soluble in pyridine and carbon disulfide (24)(31). Molecular weights of these compounds vary from 500 to as high as 20,000 (30)(33)(38). These weights undoubtably depend on the origin of the asphaltenes and the extent which the

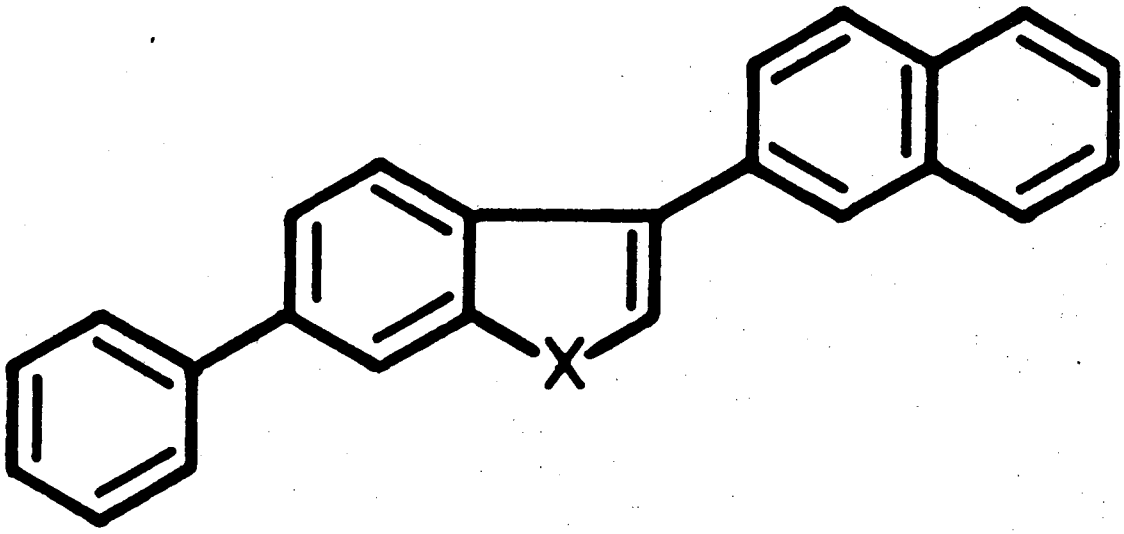

X = O, S, N–H

Average Analysis:

C = 91.8%, H = 5.4%,
S = 0.8%, N = 0.85%,
O = 1.1%

XBL 7810-11794

Figure I-2. Resin molecule.

individual molecules are associated with others (38)(39). Model compounds have been proposed for the smaller molecules such as found in Figure I-3.

Molecular weight determination is further complicated by the existence of acid-base pairs of asphaltene molecules. Because of the abundance of hetero atoms, the large molecules have an acid or basic character and have been separated as such by many authors (30)(33)(35)(40). In Sternberg's et al., original work, the acidic compounds were ascribed to phenolic hydroxyls and pyrroles; the basic were ring ethers and pyridine like structures. No oxygen has been found as carbonyl groups (34)(37). In the Kentucky Synthoil asphaltenes studied by Sternberg, these acid-base molecules occurred in a 37/63 weight ratio. The average weight of the acidic species is 550 and the basic, 368.

NMR spectra indicate that these species are hydrogen bonded to each other. The existence of these hydrogen bonds has been further established by IR and NMR spectra of basic asphaltenes with the gradual addition of a complexing model acid such as phenol (38)(41). Likewise, the addition of a pyridine base to acidic solutions shows similar bonding (27). The existence of hydrogen bonds is compatible with the solubility characteristics of the asphaltenes. In moderately polar solvents, the acid-base pairs can be solvated into their individual acids and bases. However, these pairs will precipitate from solution if the medium becomes too nonpolar.

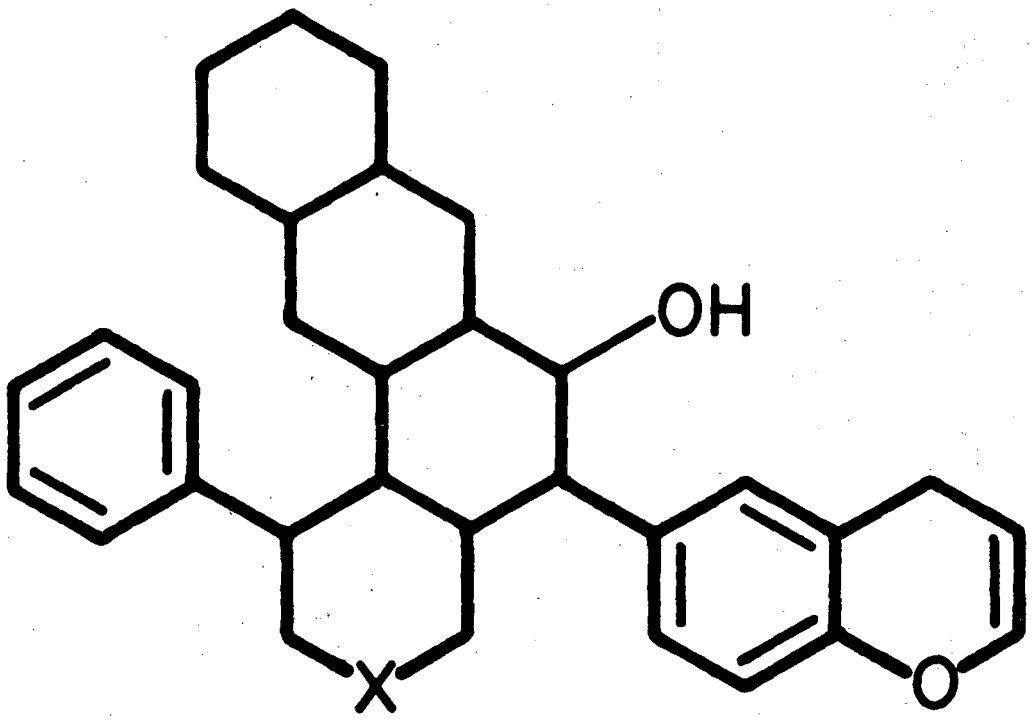

X = O, S, or N–H

XBL 7810-11795

Figure I-3. Model asphaltene.

D. THE SRC SOLUTION: CHARGED STABLE SUSPENSION OF ASH

1. Charge

The solvent refined coal unfiltered oil, SRC-UFO, which is filtered in the SRC process, is a combination of the above compounds in varying proportions. SRC itself consists of approximately 35% preasphaltenes, 40% asphaltenes, and 20% resins and oils (24). The resulting liquid and ash mixture is a stable suspension of micron and submicron sized ash particles in a viscous solvent. The viscosity is a function of the asphaltene content (24)(38).

Henry has found that the particles in this suspension possess a positive charge by applying an electric field across a sample spread on a microscope slide. He quotes an estimated mobility of 0.1 microns/sec/V/cm (26). Through similar techniques, Rogers has confirmed this charge (40)(42). This charge can be attributed to the asphaltenes and resins in the suspensions and on the solids. Asphaltenes have been known to exhibit a charge in appropriate solutions, both negative and positive depending on the solvent used (43)(44)(45). Eldib observed a pronounced increase in conductivity when comparing solutions of asphaltenes in benzene, pyridine, and nitrobenzene respectively (46). A positive charge has been found by Csanyi and Bassi on 13 of 15 bitumens suspended in benzene/methanol mixtures (47). More recently, Wright and Mesinger have done more quantitative measurements of the charge of asphaltenes in nitrobenzene. The asphaltenes were charged positive with mobilities of about 0.4 microns/sec/V/cm (48).

There are traditionally two main mechanisms which a charge might be acquired in nonaqueous media (49). They are as follows:

1. Dissociation of surface groups
2. Adsorption of an ionic solution species

Although isomorphic substitution may take place in nonaqueous dispersions, this is not suggested by observation. Particles are not found to be charged in pure nonpolar solvent (49).

a. Surface Dissociation

Dissociation is the most general method by which a surface can be charged. The surface enters into the acid-base equilibria as follows:

$$B + S_aH \rightleftharpoons BH^+ + S_a^-$$

$$HA + S_b \rightleftharpoons S_bH^+ + A^-$$

B = solvent base
A = solvent acid
S_a = surface acid group
S_b = surface base group

At a constant temperature and ionic composition, this mechanism would produce a particle surface of constant charge.

b. Solution Species Adsorption

The second method by which a particle can be charged is by the preferential adsorption of a solute over its conjugate ion. This adsorption is strongly dependent upon the physical nature of both the surface and the ion. Examples of this are amply evident in literature studies.

Copper oleate has been found to charge Fe_2O_3 in xylene (50) and Sterling in toluene positive (see Chapter IV). However, this same salt is capable of charging the surface of different carbon blacks negative in xylene (51). Aerosol OT charges rutile, alumina and calcium carbonate in xylene, and barium sulfate in cyclohexane and heptane positive; carbon blacks in xylene and benzene are again negative (53)(54)(55)(56). Those compounds that are charged positive have significant amounts of bonded oxygen. Carbon blacks with oxygens on the surface are also charged positive by divalent metal soaps in xylene and heptane (57)(58)(59).

In nonaqueous systems, trace amounts of water can drastically affect the surface dissociation. Water, with a limited solubility in most hydrocarbon solvents, is adsorbed at the solid-liquid interface. At the interface, it has a variety of effects. Water, in combination with surfactants, has been found to decrease charge and stability of nonaqueous suspensions (51)(54), increase the charge (59), first increase then decrease the charge (60)(61), reverse the charge (53), and have no effect whatsoever (53). Lyklema summarizes the effect of water as follows (49):

1. Water can charge a surface positive by itself
2. Water can be solubilized in the liquid phase by surfactants, thereby changing the adsorption equilibria
3. Thick layers of water can effect agglomeration by bridging coalescence
4. Water can create or occupy surface adsorption sites

Effects one, two, and four will be dealt with in Chapter IV. Effect three is the basis of Chapter III.

2. Stability

Particles that are as small as the ash can be stabilized by two methods. The first is due to the charge on the surface. The second results from absorbed layers of molecules causing steric stabilization.

a. Charge Stabilization

According to the theory of Deryaguin and Landau and Verwey and Overbeek, DLVO theory, small particles can be stabilized in a suspension due to a net repulsive energy. Although the theory was originally developed for aqueous suspensions, it is extendable to nonpolar media despite certain theoretical difficulties due to the small number of charged species in solution. Basically, the theory presumes the total potential of interaction is given by the addition of the attractive and repulsive potentials between the particles.

(i) Attractive Potential

The attractive force is based on the contribution of the London attractive potentials of all the atoms in one particle with all those in another. It is assumed that these forces are additive and can be summed by integration. The theory developed by Hamaker expresses the total attractive energy for two spherical particles with the same radius as follows:

$$V_a = -\frac{A}{12}\left[\frac{1}{x^2 + 2x} + \frac{1}{x^2 + 2x + 1} + 2\ln\frac{x^2 + 2x}{x^2 + 2x + 1}\right]. \qquad \text{(I-1)}$$

a = radius of particle
x = R -2a
R = distance from center to center
A = Hamaker constant

If coagulation is to occur, this force must dominate over the repulsive force. Since this is to the first approximation a function of only the material of the colloidal particles and the intervening solvent, the attractive force is constant for a given system. Agglomeration is therefore accomplished by the reduction of the repulsive potential.

(ii) Repulsive Potential

In order to calculate the repulsive potential, a charge distribution around the colloidal particle must be assumed. In the DLVO theory, this is modeled by a Poisson-Boltzman distribution. Additional assumptions are as follows:

1. Space charge is smeared over the surface
2. The ions are point charges-the charge is the only factor influencing the distribution
3. The solvent is homogeneous and continuous-it only influences colloidal properties through its dielectric constant

Admittedly, assumption one is not as nearly correct in nonaqueous systems. Ignoring the possible difficulties that this might cause, an expression for the potential distribution of a single spherical particle can be derived. The analytical expression for this potential assuming spherical symmetry at low potentials is the Debye-Hückel approximation.

$$\psi = \psi_0 \frac{a}{r} \exp\left[-\frac{(a-r)}{\lambda}\right]. \qquad \text{(I-2)}$$

a = radius of particle
r = distance from the particle center
ψ_0 = potential at the surface

The constant λ, is the parameter known from Debye-Hückel theory as the Debye length, or the length which the potential falls to $1/e^{th}$ of its magnitude at the surface of the particle. For symmetrical electrolytes

$$\lambda = \left(\frac{8\pi F^2 n z^2}{\varepsilon RT}\right)^{-1/2} . \qquad \text{(I-3)}$$

F = Faraday's constant
n = equivalents of ions/cm^3
z = valence of ion
R = Boltzman constant
T = absolute temperature
ε = dielectric constant

From Equation I-2 and Gauss'law, the magnitude of the charge on the surface can be calculated.

$$Q = -\, 4\pi\, a^2 \varepsilon \left(\frac{\partial \psi}{\partial r}\right)_{r=a} = \varepsilon \psi_0\, a \left(1 + \frac{a}{\lambda}\right). \qquad \text{(I-4)}$$

In nonpolar media where λ is large, the potential decreases very slowly as one moves away from the surface. Therefore the surface potential is often approximated as the potential measured at the Stern or electro-kinetic slipping plane, the zeta potential. Substituting values typical of nonpolar solvents ($\varepsilon = 4.0$, $\psi_0 = \zeta = 50$ mV, $a = 0.1$ micron, $a/\lambda << 1$) only fourteen unit charges per particle are needed to create a rather large potential of 50 mV (49).

The repulsive potential is the work required to bring the particle from infinity to a specific distance in the electrostatic potential field on the second particle. For particles with constant

charged surfaces and equal radii, the repulsive potential can be represented by

$$V_r = \gamma \frac{a^2 \psi_0^2 \varepsilon}{H + 2a} \exp - \left(\frac{H}{\lambda}\right) \qquad \text{(I-5)}$$

H = shortest distance between particle surfaces

where ψ_0 is the common surface potential when the particles are infinitely separated.

This equation is strictly valid only for small surface potentials, but the error introduced at higher potentials is not great (63). γ is a complicated function of the separation distance, the Debye length, and particle radius. Verway and Overbeek report values between 0.6 and 1.0 (64). Its value can be neglected in the case where no great precision is required. In addition, the exponential term may also be approximated as one if the Debye length is large. Once again, assuming that the potential at the surface is nearly equal to the zeta potential, Equation I-6 can be simplified to

$$V_r = \frac{a^2 \zeta^2 \varepsilon}{H + 2a} . \qquad \text{(I-6)}$$

This is simply Coulomb's law which ignores the existence of a double layer in view of the very few ions existing in solution.

Considering Equation I-6, a decrease in repulsion energy can be accomplished energy by modifying either λ or ψ_0. The Debye length can be reduced by the addition of more ions. Although a major means of coagulation in aqueous media, this effect is small in

nonpolar suspensions because ionization is limited. However, there is a very strong dependence on the surface potential, and as calculated, the net number of surface ions responsible for this potential is small. Thus, any method which results in altering the surface properties of the particles or the equilibrium adsorption of the ions, could greatly affect the stability of the suspension. It is not surprising that the effect of a specific ionizable salt in nonpolar media can be so different depending on the nature of the particles and solvent.

(iii) Total Potential

A considerable amount of work has been done to approximate the total potential function to examine the parameters which affect stability. Using the simplified repulsive potential expressed in Equation I-6 and the attractive potential derived by Hamaker, Equation I-1, Koelman and Overbeek calculated curves for the total potential. Table I-5 reproduces their results. As seen, the potential barrier to coagulation is strongly dependent on the particle size. A barrier of 15 kT is usually taken as a requirement to overcome thermal energy and achieve stability (64). It is doubtful whether particles with less than 0.1 micron radius can be charged enough to maintain a stable dispersion. This is a possible explanation for why the very small ash particles in SRC are agglomerated as noted in Section C of this chapter.

b. Steric Stabilization

Stabilization by long chain molecules adsorbed on the particle surface is well known to occur in dispersions. The molecules need not carry a charge but must be long and asymmetric with one section "liking"

TABLE I-5. Maximum total potential as a function of particle size

ζ mV	V_{max}/kT a = 1 μm	a = 0.1 μm	a = 0.01 μm
25	13	---	---
35	26	1	---
50	62	4	---
75	152	11	---
100	286	20	1
150	662	54	4

a = particle size

$\varepsilon \approx 2$

$\lambda >> 1$

$A = 10^{-12}$ ergs

$kT = 4 \cdot 10^{-14}$ ergs

the solvent, and the rest, the solid surface. The protective barrier is a result of two effects (65):

1. Osmotic - due to an increased concentration of protective agent between the particles.
2. Volume restrictive or entropic- the result of the reduction of the configurations possible of the tail of the stabilizer with close approach of the particles

The parameters varied to increase stability are molecular weight, concentration, and solvent quality. Calculations by Koelman and Overbeek show that this is a particularly good way to stabilize small particles (50). A number of people have modeled this stabilization statistically. Their work is summarized in References (66) and (67).

The stabilization of hydrocarbon suspensions has been attributed to these effects. Swanson found that asphaltenes derived from petroleum asphalts must have resin molecules present in order to be dispersed in the natural oils (32). In better characterized systems, carbon black can be stabilized in aromatic solvents using alkybenzene and alkylnapthalene derivatives. The alkyl substitute had to be at least eight carbons in length before such stabilization occurred (68), (69)(70). It is possible that the ash in the coal liquids is dispersed by this mechanism, but there are very few long chain molecules in coal solvents.

Long chain molecules, especially polymers, can also destabilize dispersions. In minute concentrations, usually on the order of parts per million in aqueous solutions, these molecules will adsorb on

many different particles causing bridging and flocculation (71). Physically, there is no reason why a similar destabilizing effect cannot be used in nonaqueous media. There is, however, a paucity of data on polymer destabilization in these systems, although some enhancement in settling has been observed for rutile in heptane and hexane using polyalkyl methacrylates as the flocculants (72).

E. STABILITY, COAGULATION, AND FILTRATION

Altering the surface properties to effect agglomeration will only be desirable if, in the process, filtration is also enhanced. An expression for the rate of flow through a porous media, can be derived using the assumptions of Kozeny and Carmen. Modeling the system as liquid flow through a bundle of capillaries, the following assumptions are made:

1. The mean hydraulic radius is adequate to account for variations in cross sectional area
2. Fluid resistance is due to only viscous forces

For small Reynolds numbers, the pressure drop can be expressed as a function of the superficial velocity, v:

$$\Delta P = \frac{\tau^2 \mu S^2 L V}{\varepsilon^3} \qquad \text{(I-8)}$$

μ = viscosity of the fluid
S^2 = specific surface area
L = length of bed
ε = porosity of bed
v = superficial velocity of fluid in channels

In this expression, τ is approximately equal to 4.2 and is defined as the empirical tortuosity factor which accounts for the complex path the fluid must take to travel through the bed. Assuming spherical particles, the specific surface area can be related to an effective diameter.

$$D_p = 6(1-\varepsilon)/a. \qquad \text{(I-8)}$$

The familiar Kozeny-Carmen equation can be obtained by substituting into Equation I-8.

$$\Delta P = \frac{36\ \tau^2 \mu L V}{D_p^3} \frac{(1-\varepsilon)^2}{\varepsilon^3}. \qquad \text{(I-9)}$$

This can be arranged to the following

$$v = \frac{\Delta P}{L\mu} \frac{\varepsilon^3 D_p^2}{(1-\varepsilon)^2 36\ \tau^2}. \qquad \text{(I-10)}$$

The factors determining the rate of flow of the fluid through the filter media can be divided into those attributed to the liquid and those that are a function of the suspended particles. The following chapters will concentrate on the manipulation of the surface properties of the particles such that the specific surface area and the resulting cake resistnace to flow of filtrate are modified to increase filtration rates.

II. ADDITIVES AND AGGLOMERATION

A. INTRODUCTION

A number of simple tests were used to establish whether agglomeration might be initiated by the addition of other compounds to SRC-UFO. These are as follows:

1. Microscopic observation
2. Variation of Coagulant and Flocculant Concentrations
3. Settling

The tests are performed on solutions of SRC-UFO and dilutions with a light distilled SRC solvent and pyridine. Pyridine was chosen for its compatibility with the SRC and asphaltenes.

B. MATERIALS

1. SRC-UFO

The SRC-UFO used in these studies is obtained from the SRC pilot plant in Fort Lewis, Washington. The black, highly viscous, noxious liquid is the filter feed of the SRC process and made using a mixture of Kentucky 9 and 14 coal with approximately 10% ash and 0.65% moisture. The amount of ash in the filter feed averages 5.5% by weight as determined by extraction with pyridine. This indicates that the feed to the process was approximately half coal and half recycle solvent.

The viscosity of the SRC-UFO as a function of temperature is given in Figure II-1. These measurements were taken using a Brookfield

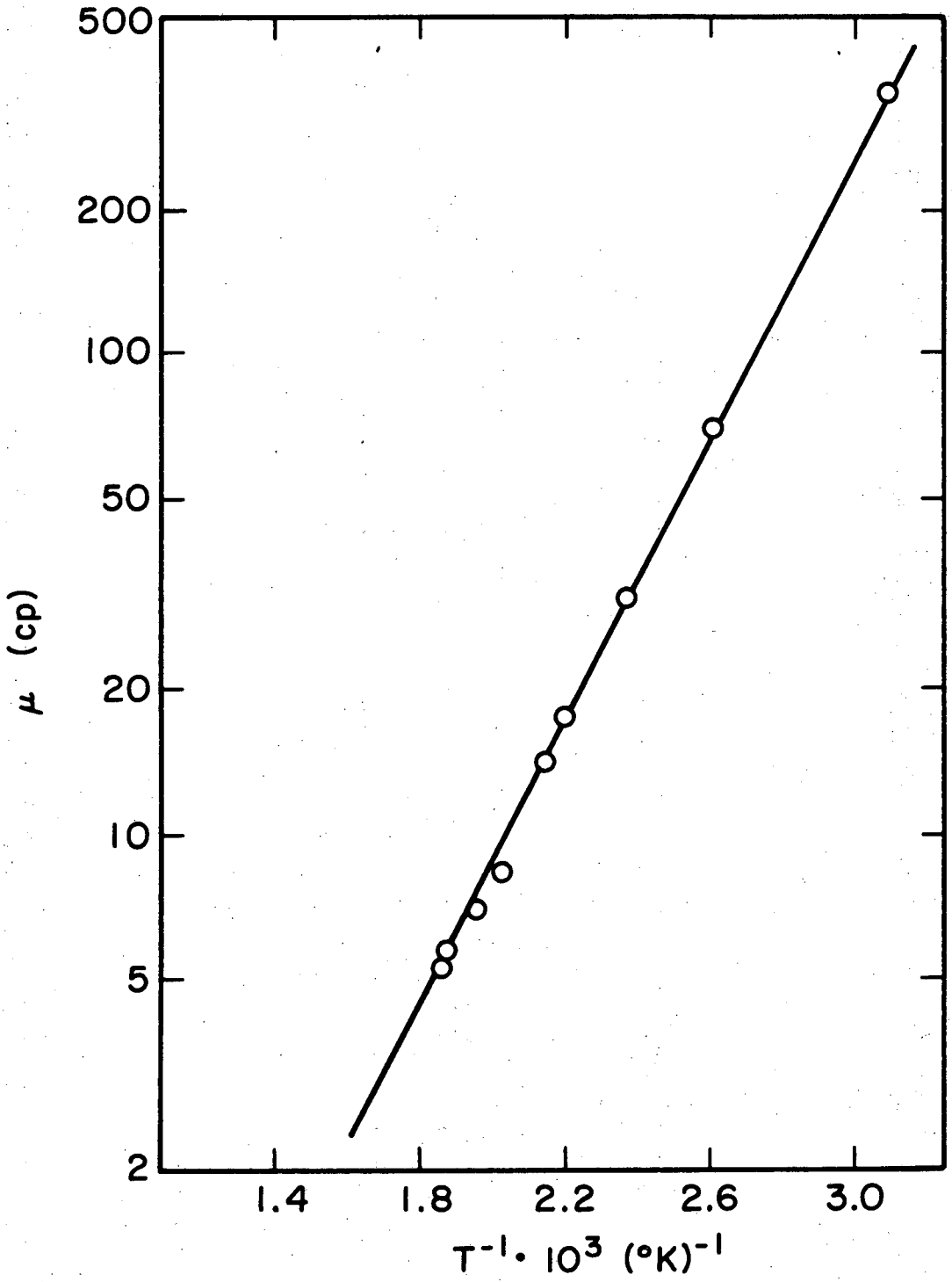

XBL 7810-11779

Figure II-1. Viscosity of SRC-UFO as a function of temperature.

Synchro-lectric Viscometer with a low viscosity attachment. This attachment was immersed in a constant temperature silicone oil bath until a stable, reproducible reading could be obtained. The viscosity-temperature profile is comparable to those reported by others (5).

The conductivity of the SRC-UFO in a 4/1 SRC/SRC solvent ratio is less than 1×10^{-9} $cm^{-1}ohms^{-1}$. This is in agreement with values reported elsewhere (40). Conductivities in these studies are measured using a Beckman Conductivity Bridge and a conductivity cell with large platinum electrodes and a cell constant of 4.78×10^{-2} cm^{-1}.

Ash particle composition found in this study after pyridine extraction have been given in Table I-4. This is comparable with those found elsewhere (4). The particles in a 70% SRC solvent/SRC-UFO dilution exhibit charged properties when placed in an electric field. Two microscope slides with aluminum electrodes 1 mm apart and a plexiglass base are used for these observations. Applying approximately 50 mV across the electrodes causes the particles to move toward the negative electrode. This motion reversed upon field reversal. Such observations confirm the results of Henry and Jacques (26).

2. SRC Solvent

The SRC solvent is the product of a vacuum distillation of the SRC-UFO described above. The distillation is carried out at 10 torr over a range of temperatures. The fraction used throughout this study is that collected with an overhead temperature of 70-135 ^{o}C. This constituted about twenty percent of the initial charge of SRC-UFO by weight and thus

represented the lighter portion of the recycle solvent used in the pilot plant.

The solvent density is 0.82 g/cm^3 at 25 ^oC and 760 torr. A dielectric constant of 4.55 is found using the Heterodyne Beat Method. This value is similar to that reported by Rogers (40). The solvent has a conductivity of approximately 2×10^{-9} cm^{-1} $ohms^{-1}$. It is miscible with most organic solvents. Its viscosity is given is Figure II-2. In addition, viscosities of various dilutions of the SRC-UFO with its solvent at 150 ^oC are found in Figure II-3. All viscosities were measured using a Brookfield Viscometer.

This solvent contains a considerable number of polar compounds, presumably similar to those described in Chapter I. The acidic compounds are separated from the solvent by extraction of a 1/1 dilution of the solvent in ethyl ether three times with 1 M NaOH. Gas chromatographs of the extracted versus unextracted liquid shows 10-20% of the solvent exists as extractable soluble acids. Infrared spectra indicate a reduction of a peak near 3350 cm^{-1} which often corresponds to the OH stretch of a hydroxyl group. (See Figure II-4 and II-5.) Addition of phenol to the extracted solvent reestablishes this peak in Figure II-6. Phenol's IR spectrum is seen in Figure II-7. NMR of the extracted and nonextracted liquids shows a disappearance of a broad band near 4.2 δ which may be due to the partial disappearance of the phenolic proton. (Figures II-8 and II-9.)

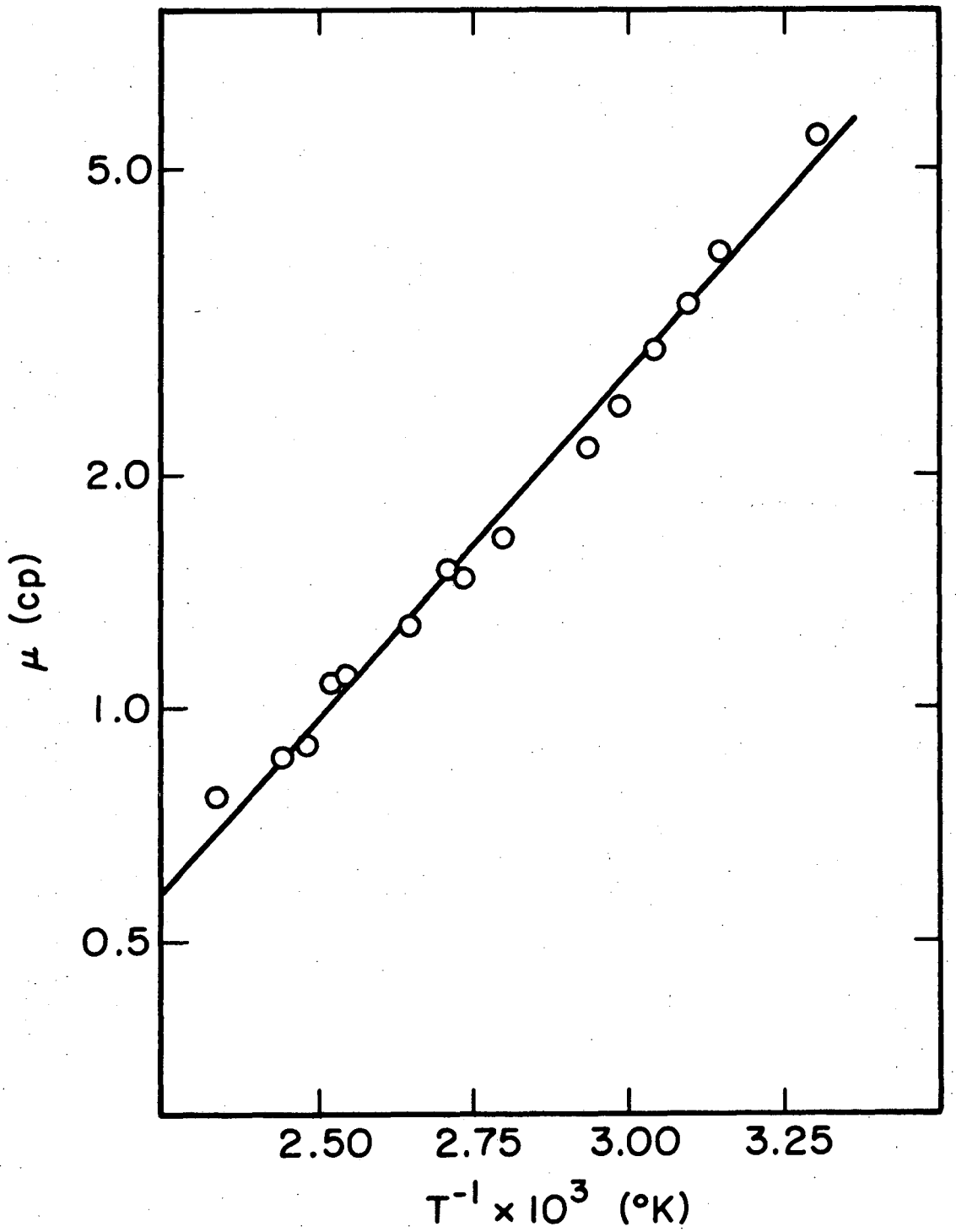

XBL 7810-11780

Figure II-2. Viscosity of SRC solvent as a function of temperature.

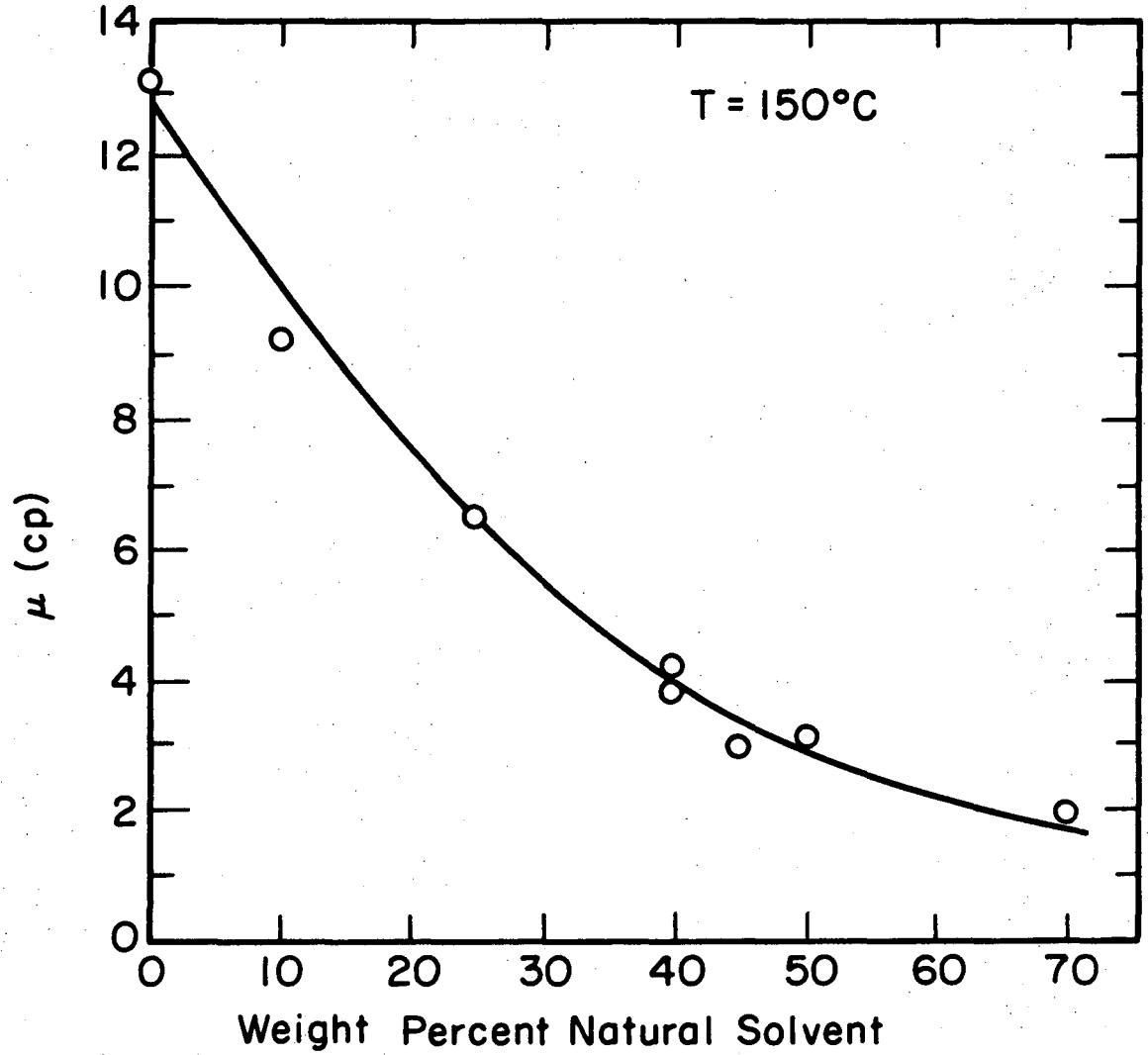

XBL 7810-11781

Figure II-3. Viscosity of SRC-UFO/SRC solvent solutions.

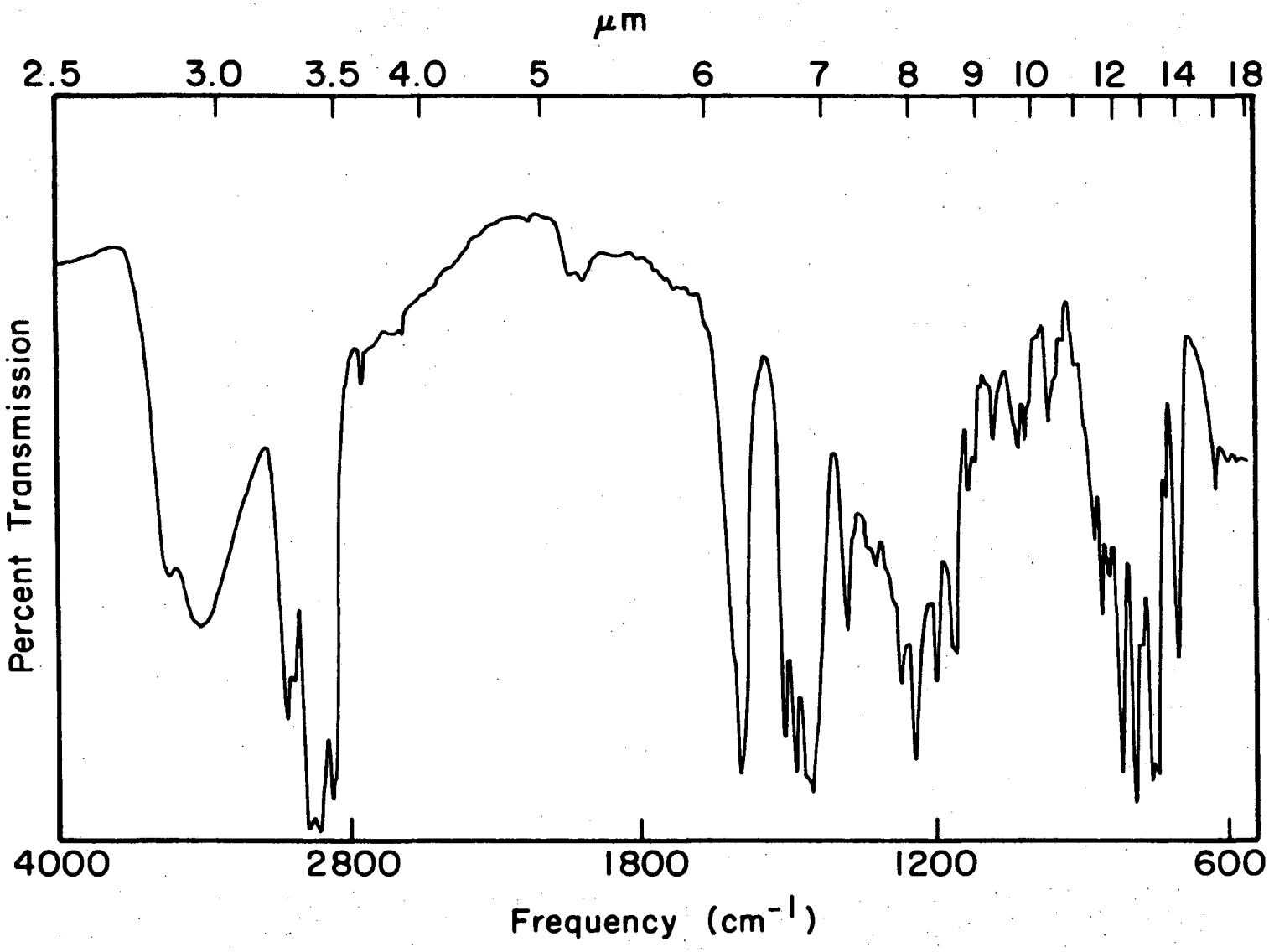

Figure II-4. Infrared spectra of SRC solvent.

XBL 7810-11782

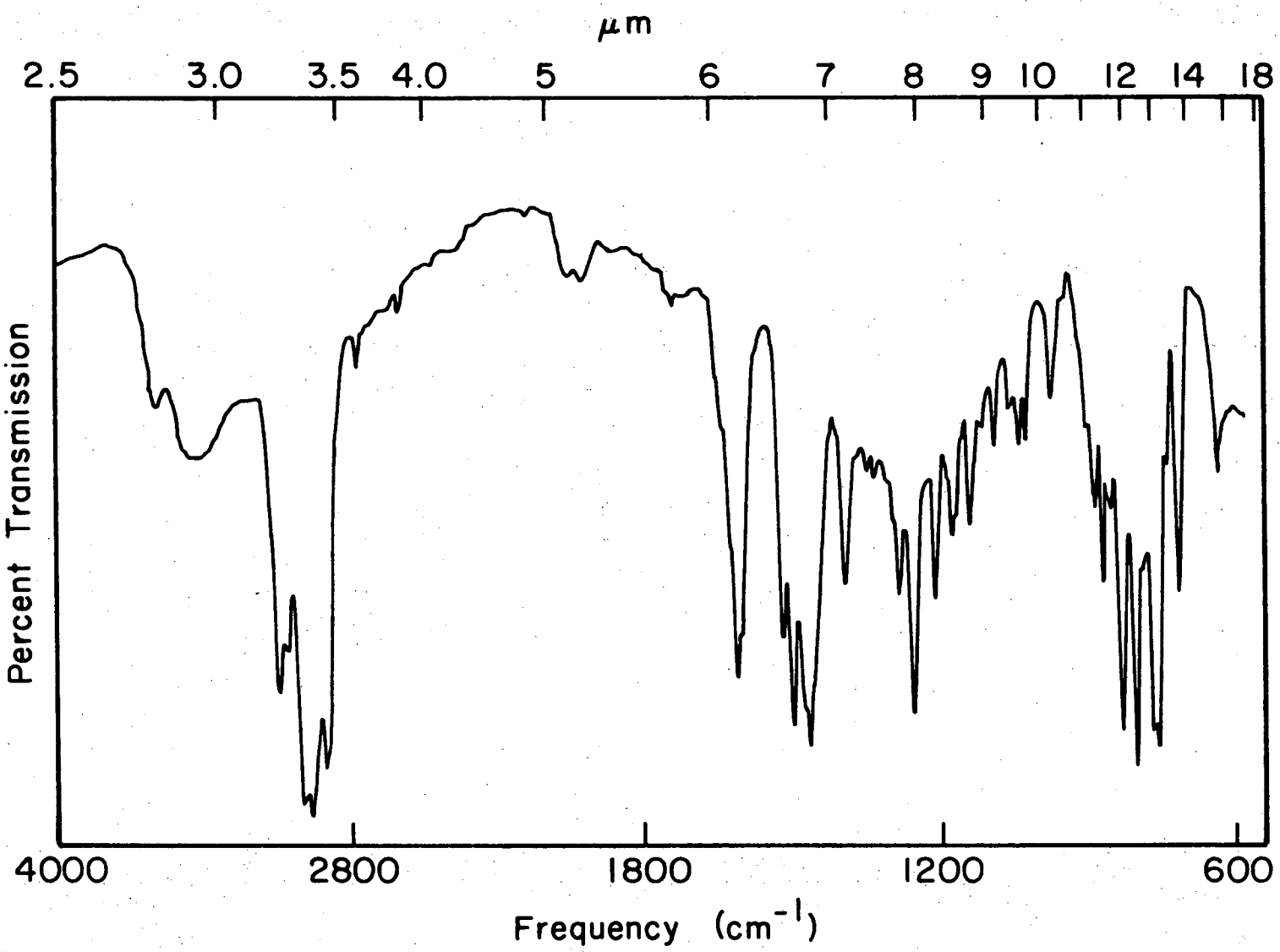

Figure II-5. Infrared spectra of extracted SRC solvent.

XBL 7810-11783

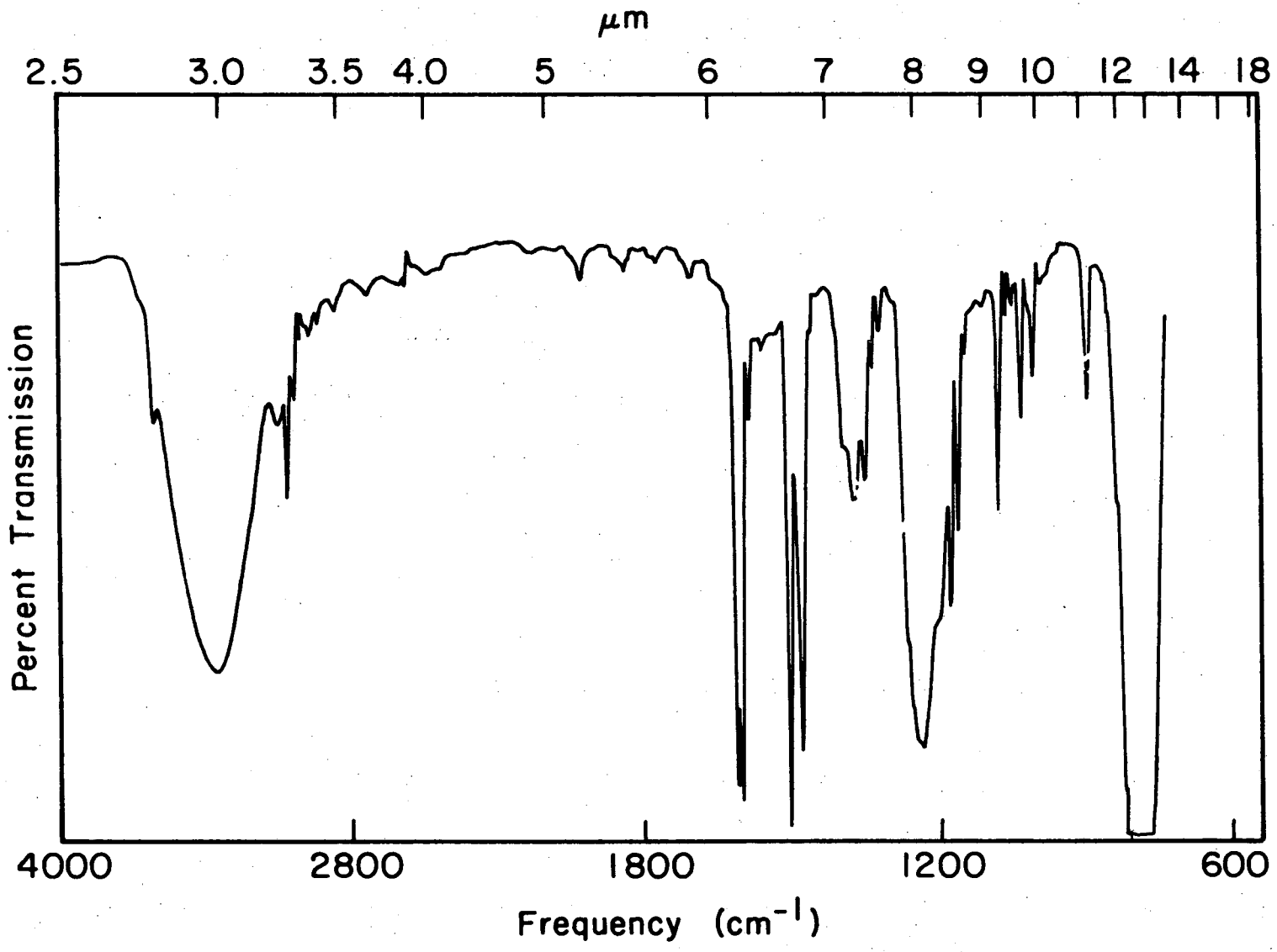

Figure II-6. Infrared spectra of phenol in carbon tetrachloride.

XBL 7810-11784

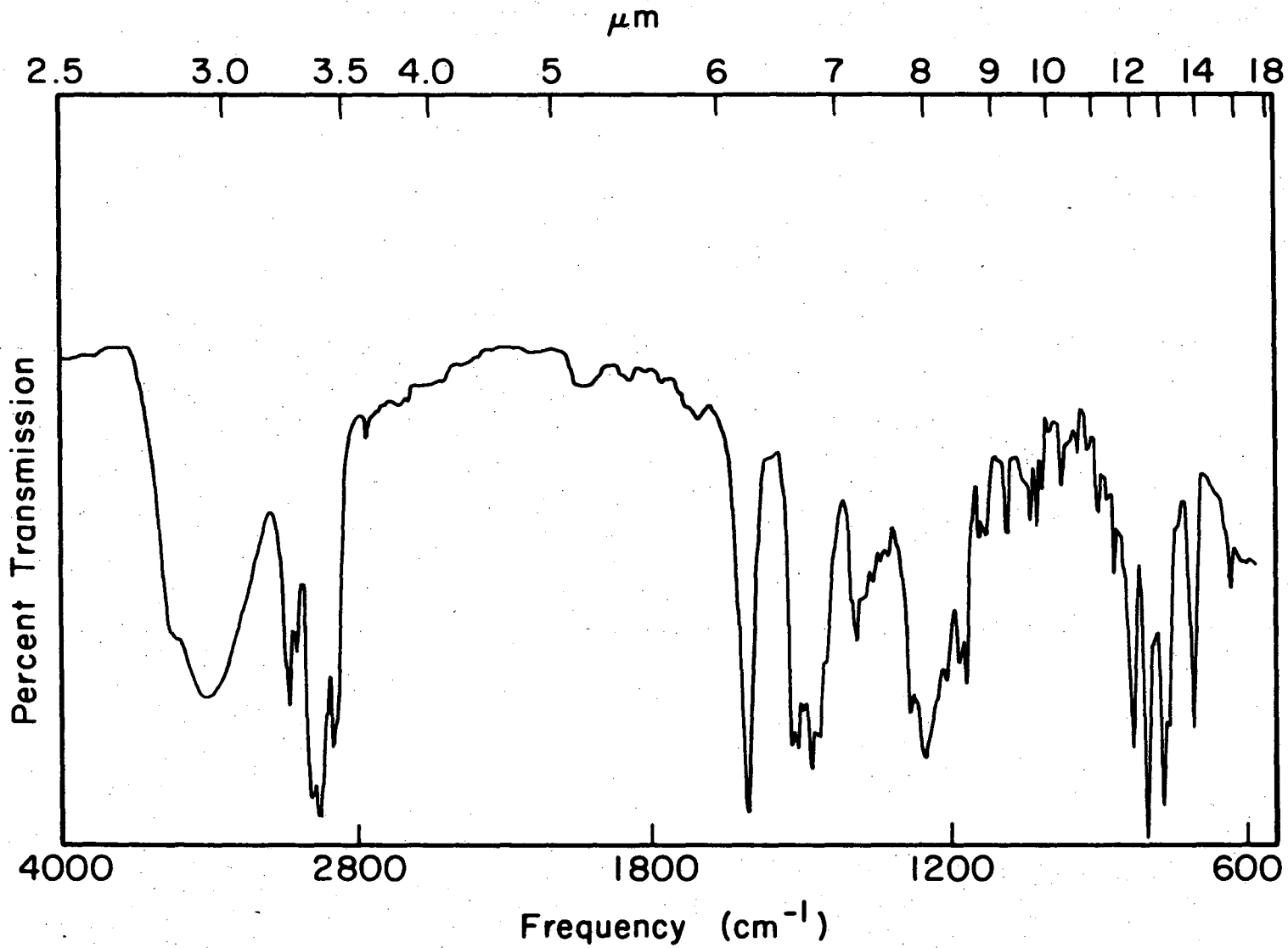

Figure II-7. Infrared spectra of phenol and extracted SRC solvent.

XBL 7810-11785

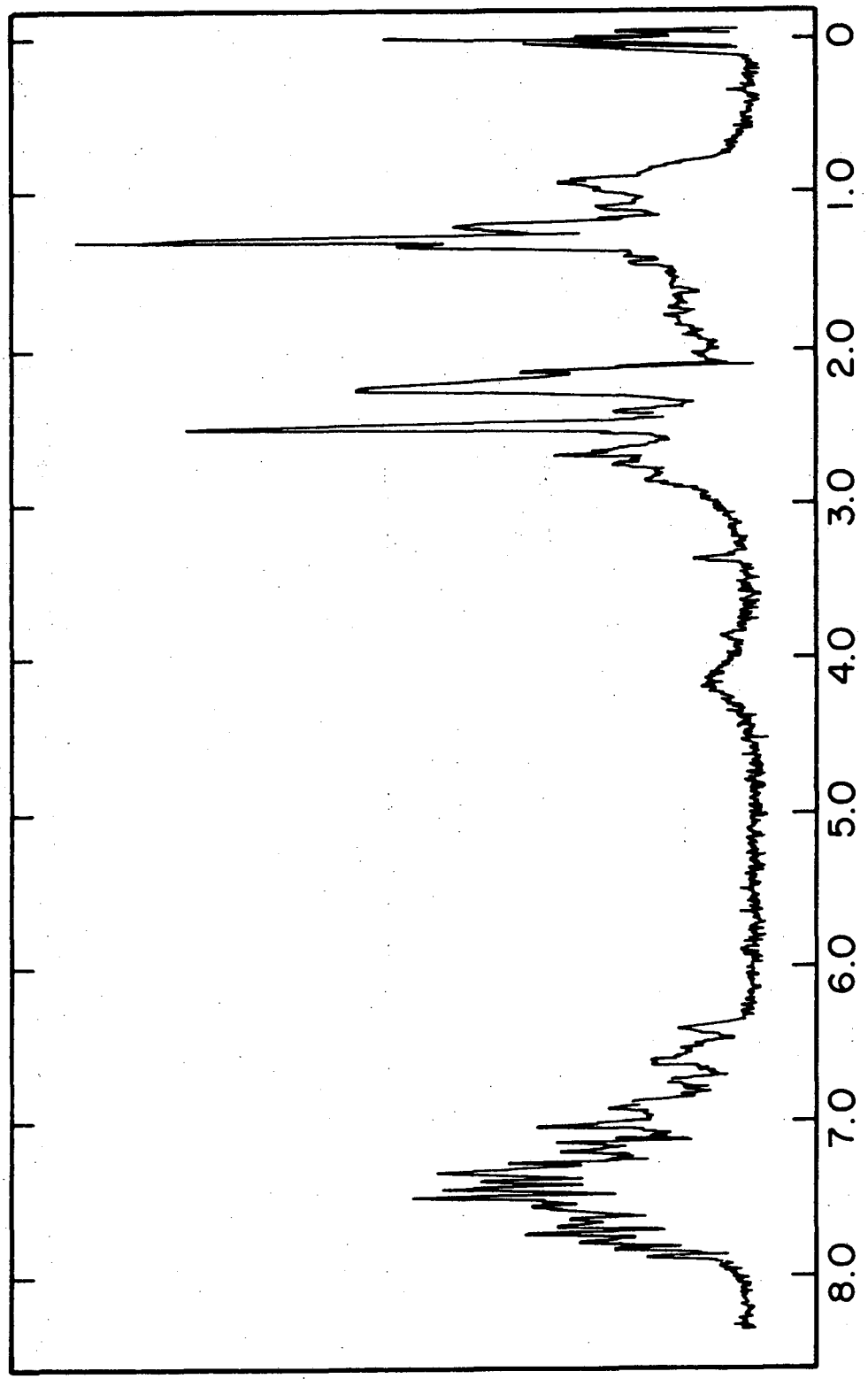

XBL 7810-11787

Figure II-8. NMR spectra of SRC solvent.

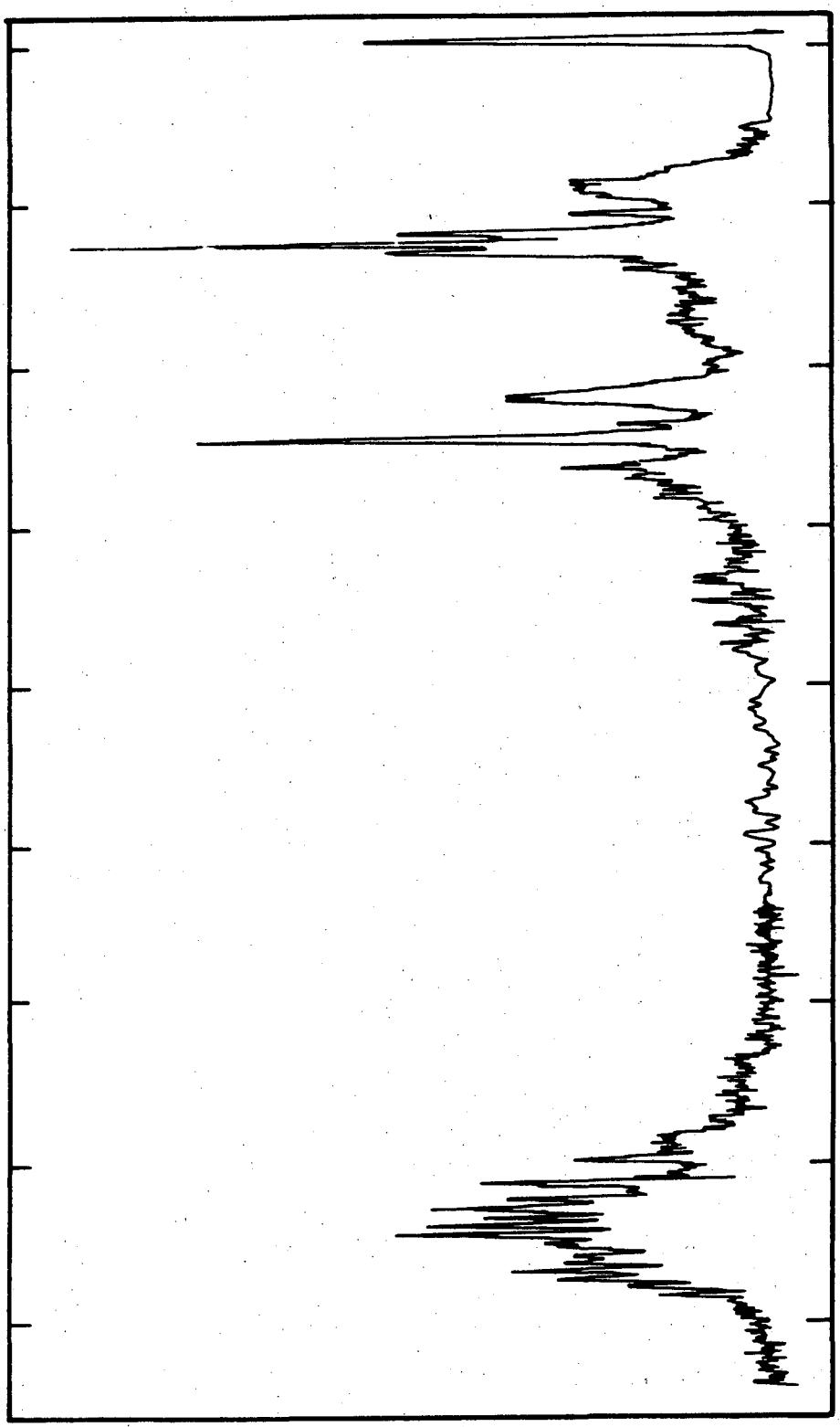

XBL 7810-11786

Figure II-9. NMR spectra of extracted SRC solvent.

3. Pyridine

Pyridine was selected as the model solvent for its rather unique compatibility with the SRC-UFO. Pyridine is known as one of the better solvents of coal, presumably because of its somewhat polar character and ring structure. Of all the solvents tried, it precipitated the least amount of particulates from the SRC-UFO, and is infinitely miscible with the SRC solvent. In all studies, Mallinkrodt Karl Fischer grade pyridine with less than 0.1% water is used. This is distilled and the overhead fraction from 114-115 ^{o}C at 750 torr is taken. The conductivity of the resulting product is about 1×10^{-7} cm^{-1} ohm^{-1}. Since pyridine itself contains no ions, this relatively high conductivity is presumably due to remaining impurities such as water.

C. COAGULATION AND FLOCCULATION OF SRC SYSTEMS

1. Effect of Solvent on Agglomeration

In this study, the purpose of the addition of a solvent to the SRC-UFO was to agglomerate the ash without precipitating the dissolved asphaltenes. By adding liquids considered to be acidic or basic, it was hoped that the acid-base character of the system would be modified such that coagulation could take place.

a. Procedure

The effect of certain liquids is ascertained by microscopic observation of the particles in a mixture of the test solvent and a 4/1 SRC solvent/SRC-UFO or pyridine/SRC-UFO solution. A small amount of this diluted solution is placed on a microscope slide to which a drop of the

studied solvent is added. A cover glass or additional microscope slide is placed on top and the solution is mixed by shear by moving the top glass. Observation is done at 420X and photomicrographs are taken when appropriate.

The extent to which precipitation occurs is tested by using a 4/1 dilution of SRC solvent/SRC-UFO which has been filtered to remove the solids. The remaining liquid is clear of any particulates and will produce dense black agglomerates if small amounts of toluene are mixed into it. Each solvent is combined with this solution to see if the same result occurs.

b. Results

The solvents tried and their effect on agglomeration are recorded in Table II-1. Only in the cases where heavy precipitation of the SRC occurs are the agglomerates dense and resistant to shear. In other cases, agglomeration can be increased but the resulting clumps of particles are easily broken up with small amounts of shear. The solids can be discerned as individual particles in point contact with numerous neighbors.

A more quantitative test of the influence of hexylamine shows that a large amount of this solvent is needed to effect the agglomeration observed. A 10% solution of pyridine and SRC-UFO was diluted with increasing amounts of hexylamine. The particles start to clump readily only when the concentration exceeded 40% by volume of hexylamine to total volume.

TABLE II-1. Solvent addition to SRC-UFO Solution

Solvent	Agglomeration	Precipitation of Asphaltenes
SRC Solvent	Loose weak agglomerates	None
Pyridine	After 5 hrs, loose agglomerates	None
Dioxane	Loose, extensive agglomerates	Slight
Toluene	Heavy agglomeration	Dense, black precipitate
Ammonia (bubbled through)	Loose agglomerates	None
Urea	Loose agglomerates	None
Hexylamine	More tightly bound agglomerates than in SRC solvent	None
Ethylenediamine	Dense agglomorates	Slight
Cyclohexylamine	Dense agglomerates	Slight
Tetrahydrofuran	Loose, weak agglomerates	None
Phenol	Loose, weak agglomerates	None
Tetralin	Heavy agglomeration	Dense, black precipitate

2. Use of Polymers and Surfactants

As noted, the stability of suspensions can be radically altered by the addition of small amounts of dissolvable compounds. These take two forms. The first is a salt which is ionizable in nonpolar media. The second is a long polymeric molecule soluble in the solvent which can floc the suspended solids. Compounds belonging to both these groups have been added to diluted SRC systems to determine their effect on particle agglomeration.

a. Procedure

The concentration and method of addition of these substances have been found to be extremely important variables in agglomeration. In most flocculation studies, a highly specific procedure is necessary such that the adsorbate contacts as many particle surfaces as possible. Doing so increases the probability of bridging. However, large amounts of either coagulant or flocculant can lead to stabilization. In the case of flocculants, entropic stability dominates as the amount of adsorption increases toward saturation. Too much coagulant, on the other hand, may permit surface charge reversal of the surface as more and more of the oppositely charged ion is adsorbed on the surface. This will lead to charge stabilization as seen in the original solution, for the stability only depends on the magnitude of the charge, not the sign. Techniques used in the previous section on visual observation are inadequate to insure proper concentrations and mixing. Two alternates methods are used here.

Initially, additives were tested in discrete amounts in test tubes. To a 10 ml test tube, an appropriate amount of the polymer or surfactant in a pyridine solution is pipetted. This is made up to a 5 ml volume with pyridine and mixed by turning it end over end. Such mixing before addition of the dispersion insures that particles will only encounter dilute concentrations of polymer. Two ml of a sonically mixed, concentrated dispersion is then added. The dispersions are pyridine- or SRC solvent-diluted SRC-UFO, or particles of ash derived from pyridine extraction, which have been found to have a charge, dispersed in these solvents. The latter dispersion is more completely described in Chapter IV. The final dispersion concentration is approximately 1-3% ash by weight. This mixture is shaken for fifteen minutes and then allowed to agglomerate while the tubes are gently rotated end over end for another thirty minutes.

The second, and quicker method to test the efficacy of a congulant or flocculant is the continuous addition of the compound to the dispersion. A dispersion of particles is prepared as above. To this stirred dispersion, a concentrated solution of a coagulant or flocculant is added dropwise. The concentration of this solution is usually ten to forty times that which is estimated to be the optimum concentration for agglomeration. If no reasonable estimate of this concentration can be made, three separate tests are done, each with a new dispersion and a ten times more concentrated polymer or surfactant solution. Addition of this solution is curtailed when the added volume amounts to 50% of the original volume in the flask.

In both cases, flocculation and coagulation had to be monitored by taking a sample of the final suspension in the case of the test tube or an intermediate sample of the dispersion of the flask test and observing its characteristics under the microscope. Although attempts were made to observe coagulation using spectrometric techniques, the solutions are all too dark to make this possible. Traditional methods to record more quantitatively the extent of agglomeration failed.

To inusre the validity of these methods, a dispersion of kaolin in water was flocculated and coagulated. Dow Separatan was used as the flocculant. Potassium chloride served as a coagulant. In both tests, the kaolin particles can be observed to be agglomerated under the microscope as well as in the test tubes and flasks. The floccules are very dense agglomerates, extremely resistant to shear. The coagulated particles are much less tightly bound, and will break with moderate shear.

The coagulants and flocculants listed in Table II-2 were tested using these methods. Copper oleate and derivatives of calcium salicylate have been known to influence charge on particles in nonaqueous media (50) (79). The calcium sulfonates are of mixed chain lengths and are precipitated with $CaCl_2$ from a mixture of sodium salts supplied by Witco Chemicals. Shell Antistatic Additive is also a mixed solution of oil soluble salts. The exact composition is proprietary. Triton X35 and Acryloid 956 are both oil soluble surface active agents made by Rohm and Haas. Triton X35 is a octyl phenoxyl polyethanol. Acryloid 956 is a poly-alkyl methacrylate used as a sludge dispersant in motor oils.

TABLE II-2. Agglomeration aids

Coagulants	
Copper Oleate	
Calcium Salicylate	
Calcium Sulfonates	
Triton X35	
Shell Antistatic Additive	
Flocculants	**Molecular Weight**
Methyl and Ethyl methacrylate	10^5
Acyloid 956	
Poly dimethyl siloxane	10^6
Polyethylene	10^4
Polystyrene	10^5

b. Results

No visual evidence of increased flocculation or coagulation was found using any of the above compounds. This cannot be construed to imply that none of these compounds had any effect on the dispersion properties. Later in Chapter IV, copper oleate's influence on ash dispersions is discussed in detail. The technique for determining coagulation here is not sufficiently precise. As stated, dispersions in pyridine or the SRC solvent seem to agglomerate weakly without the addition of any coagulant. Figures II-10 and II-11 show this to be the case in both pyridine and SRC solvent despite the particles being charged. Those particles that do clump, however, are extremely small. Secondly, the distinction between coagulated and uncoagulated systems observed under the microscope is small. Only through other more sensitive methods, such as settling and filtration can coagulation be confidently verified.

Flocculation in organic systems is equally difficult to observe microscopically. Increases in settling rates due to polymer bridging are small, and, therefore, not as dramatic as in aqueous systems (72). In addition, the polymer character necessary to achieve bridging is highly dependent upon the particle surface and solvent. No doubt, more specialized polymers could be made to enhance adsorption of the functional groups. Although all the polymers dissolved in the experimental solvents, there was no way of knowing whether any of them possesses the proper combination of molecular weight, length, polarity, and functional groups to cause flocculation.

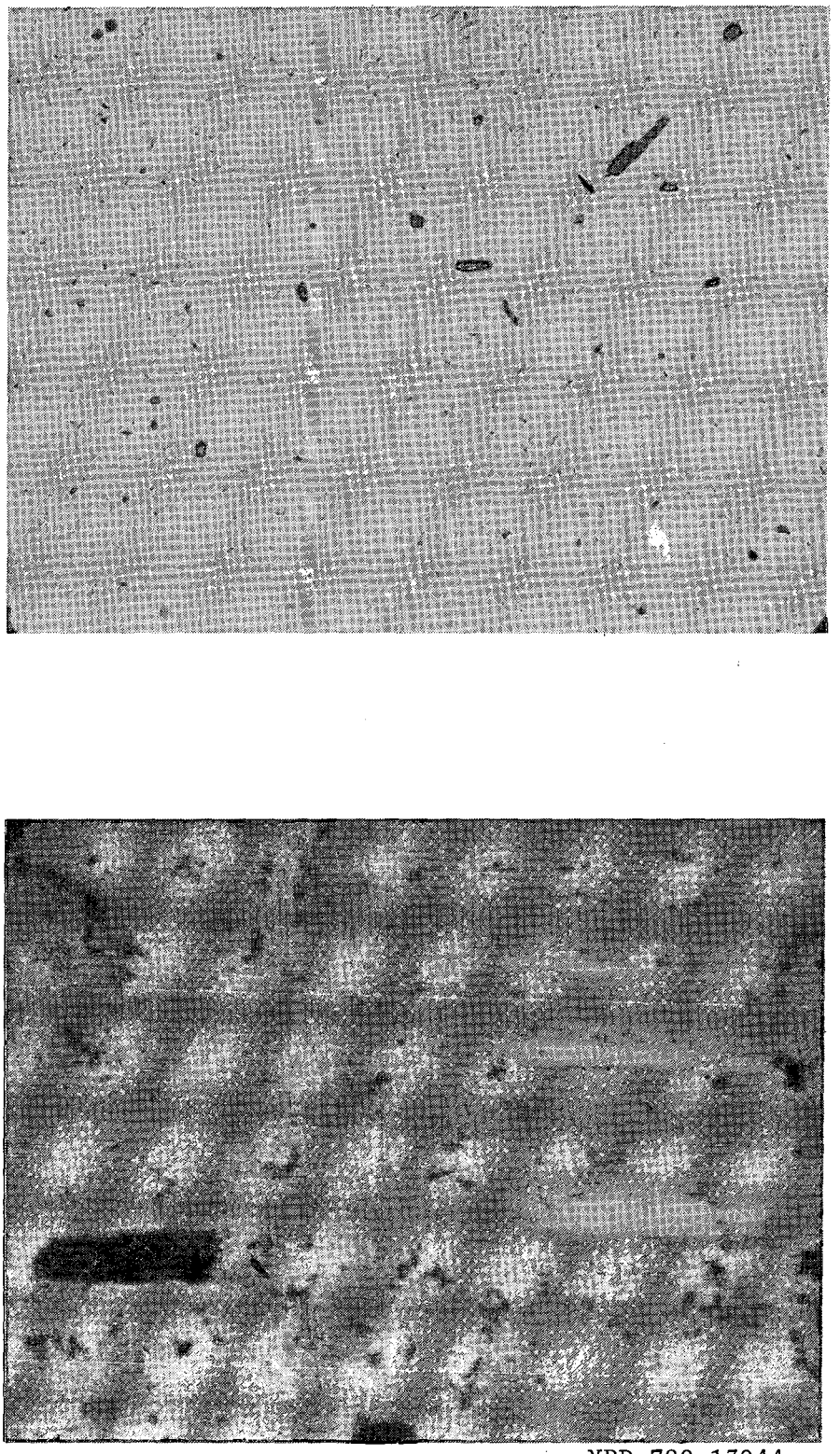

XBB 780-13044

Figure II-10. Ash coagulated in pyridine.

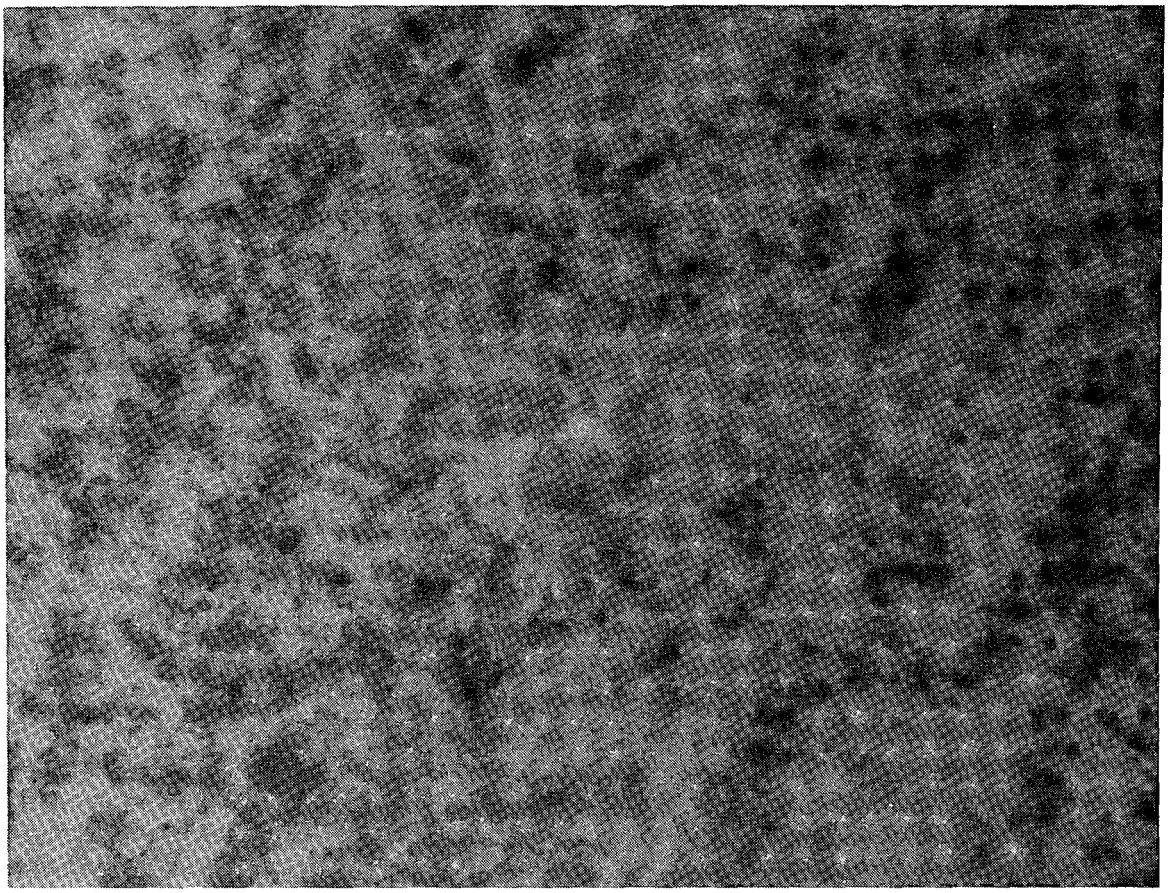

XBB 780-13041

Figure II-11. Ash coagulated in SRC solvent.

D. SETTLING

As mentioned, alternative methods must be used to determine the effectiveness of coagulants and flocculants as well as quantify the observations noted in the solvent tests. Visual techniques to monitor settling are inappropriate for the dark, opaque SRC-UFO dispersions. However, settling can be measured by noting the decrease in solids found in a given section of the settled system. In the following experiments, a given amount of suspension is allowed to settle for a fixed time at high temperatures. A known volume of sample is then drawn from the top and its solid content determined. Using this method, possible agglomeration is judged.

1. Theory

To interpret the settling results, Stokes law for unhindered, monodispersed, spherical particles is assumed. A simple mass balance around the volume (v = AL) from which the sample is drawn yields

$$Ac_p \frac{dl}{dt} = \frac{dm_p}{dt} = - \rho_p c_p Av \left(\frac{4}{3}\pi a^3\right) \qquad \text{(II-1)}$$

t = time
a = radius of particle
ρ_p = particle density
A = cross sectional area
c_p = particles/volume
l = vertical distance

where v is the Stokes terminal velocity which all particles are assumed to have reached instantaneously.

$$v = \frac{2}{9} \frac{a^2}{\mu} (\rho_p - \rho_s) g \qquad \text{(II-2)}$$

μ = viscosity of solvent
ρ_s = density of solvent

Equation II-1 applies for times less than L/v when mass still remains in the upper volume V. Integrating, equation II-1 becomes

$$m_p(t) = m_p^o - \rho_p c_p \, Avt \, (\tfrac{4}{3}\pi a^3) \qquad \text{(II-3)}$$

where m_p^o is the total mass of particles in the sample volume at t = 0.

$$m_p^o = \rho_p c_p \, V \, (\tfrac{4}{3}\pi a^3) \qquad \text{(II-4)}$$

Using the above expression, Equation II-3 can be simplified.

$$\frac{m_p(t)}{m_p^o} = 1 - \frac{vt}{L} \qquad \text{(II-5)}$$

$$vt/L < 1$$

The fraction settled can therefore be expressed as

$$f(t) = \frac{m_p^o - m_p}{m_p^o} = \frac{2}{9} \frac{a^2 \Delta\rho g t}{L\mu} \qquad \text{(II-6)}$$

Since the densities, time, and length are set by the experimental system, a ratio of fractions settled at equal times can represent an increase in particle size if the viscosities are known and t is less than the critical time.

$$\frac{\mu f}{\mu_o f_o} = \frac{a^2}{a_o^2} \qquad \text{(II-7)}$$

f_o = fraction settled with no additive

Plotting $\mu f/\mu_o f_o$ as a function of the percent coagulant added, effective changes in particle size due to agglomeration can be determined.

2. Apparatus

Figure II-12 is a diagram of the equipment used for the high temperature settling experiments. The apparatus consists of a long, hollow, copper tube, capped and O-ring sealed at the bottom. The top is fitted with a stirring assembly, again sealed with O-rings to hold an atmosphere of pressure confidently. Half way up the tube is a sample port used to remove the liquid above it. A screw valve is used fitted with an extension to facilitate opening outside the hot box that surrounds the apparatus. The sample is collected in a chamber open to the system only when the valve is open. Above the liquid level, a lead tube comes off the settling vessel so that the internal pressure can be monitored.

In most experiments, settling is done in a constant temperature, insulated hot box. The box is fitted with two resistance heaters, a fan, a thermometer, and a pressure gauge. In high temperature experiments, the settling apparatus is seated inside this container with an insulated top.

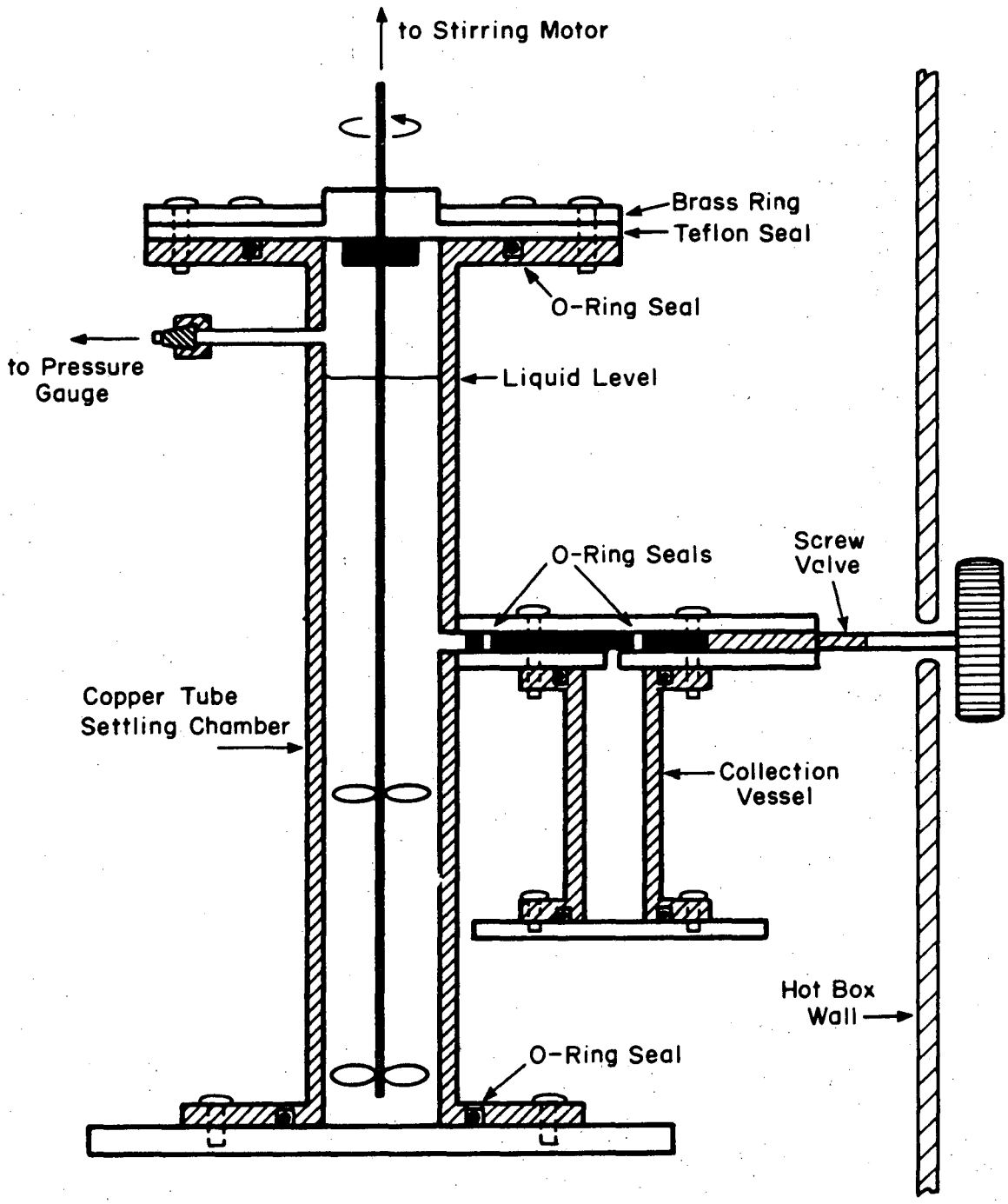

Figure II-12. Settling apparatus.

3. Procedure

A mixture of the SRC-UFO and the appropriate solvent is made up by weight and a small sample kept as a standard. The settling chamber is filled with the remaining liquid until a predetermined level is reached. The apparatus is sealed and brought to the appropriate temperature while the dispersion is gently stirred. After reaching temperature, the particles are allowed to settle for thirty minutes and then the sample port is opened to collect the upper third of the charge.

Weighed samples of the solutions before and after settling are burned down slowly in crucibles until all that remains is a red-orange ash. Using the weight of the ash in the samples before and after settling, the fraction settled is computed. In the manner described by Equation II-7, the normalized settled fraction is plotted against the amount of additive.

Extreme care must be taken in making these measurements. The solvents used are volatile and toxic, making work in a vapor hood a necessity. In addition, protective clothing is a must when working with SRC-UFO. Care must also be taken in burning the samples to ash. If not done carefully, violent splattering and/or fires are caused within the crucible. It is for these reasons that ovens are not used to reduce the liquid to ash.

4. Results

a. Solvent Addition

Using this procedure, the effect of dilution with pyridine and natural solvent was tested. In Figure II-13, the normalized settled

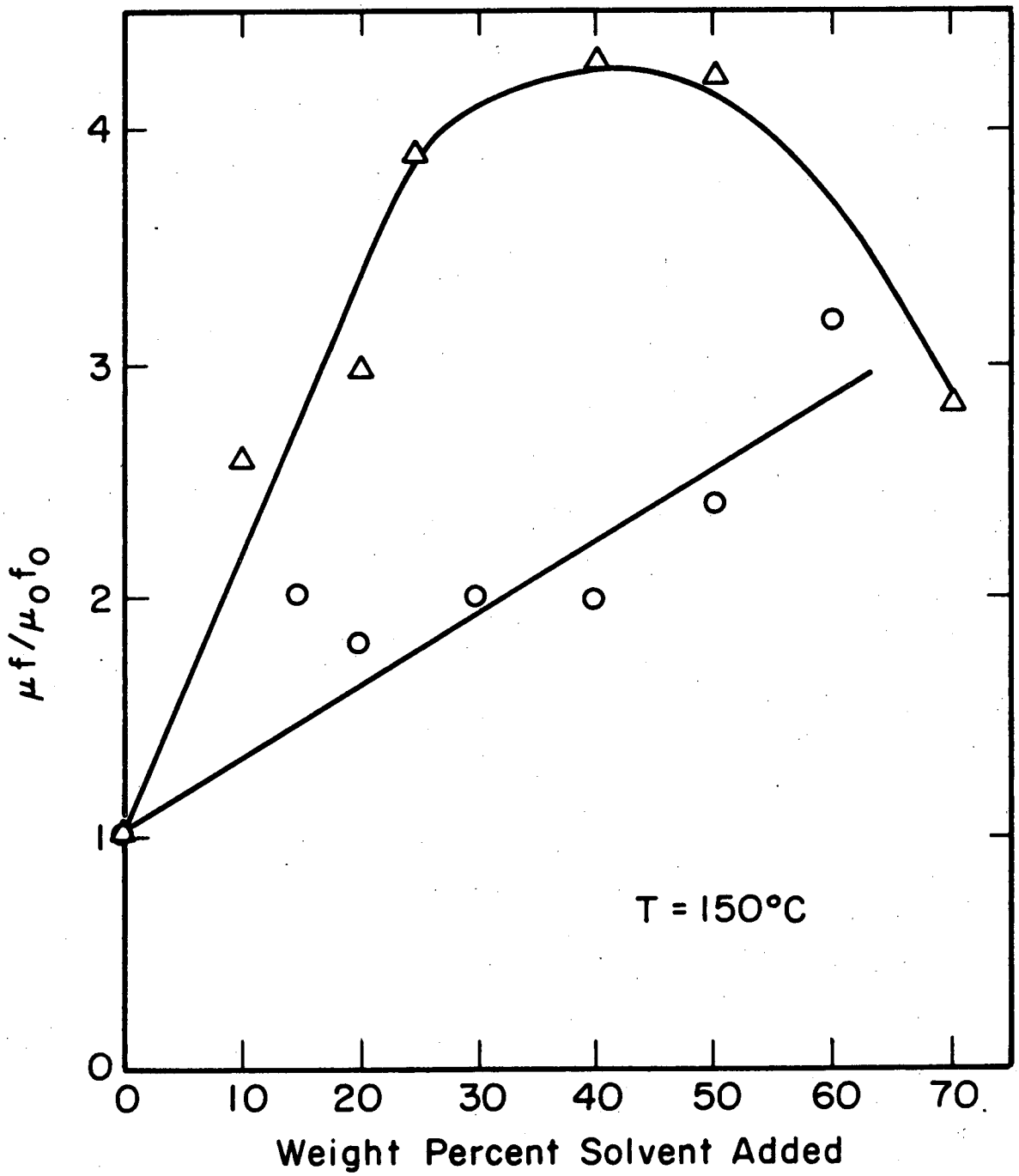

Figure II-13. Normalized settling fraction versus percent SRC solvent.

fraction versus percent SRC solvent added is plotted. The two sets of points correspond to two different runs where solvent from two different distillations was used. A slight increase in agglomeration is seen to occur in both runs. The settling rate is increased by a factor of four at its maximum. This corresponds to an effective radius increase of two, implying that any agglomeration seen microscopically is indeed very loose. The particles settle as very weakly held agglomerates. It is not surprising that small amounts of shear can break up the agglomerates.

A maximum settling rate is observed in one of these runs. At the higher dilutions Equation II-7 no longer applies, for all the solid has fallen below the sample volume. As seen in Figure II-14, all the ash, within experimental accuracy, is removed before the thirty minutes elapsed at the higher dilutions.

Pyridine's effect on settling is seen in Figures II-15 and II-16. Little if any effect besides the enhancement due to viscosity shown in Figure II-16 is noted. This concurs with microscopic observations where the amount of agglomeration is small. The 20% point is assumed to be errant because of experimental errors. Small deviations can cause large errors in the calculated fraction settled because of the comparatively large viscosities of the less diluted SRC-UFO solutions. As the concentration of pyridine increases, the settling ratio falls below one. Since the settled fraction is less than 100% (Figure II-16), one is led to conclude that either the addition of pyridine stabilizes the dispersion, or the viscosity measured does not reflect that of the dispersion while the runs were done. In support of the former explanation, visual observation discussed in Section C indicate that pyridine

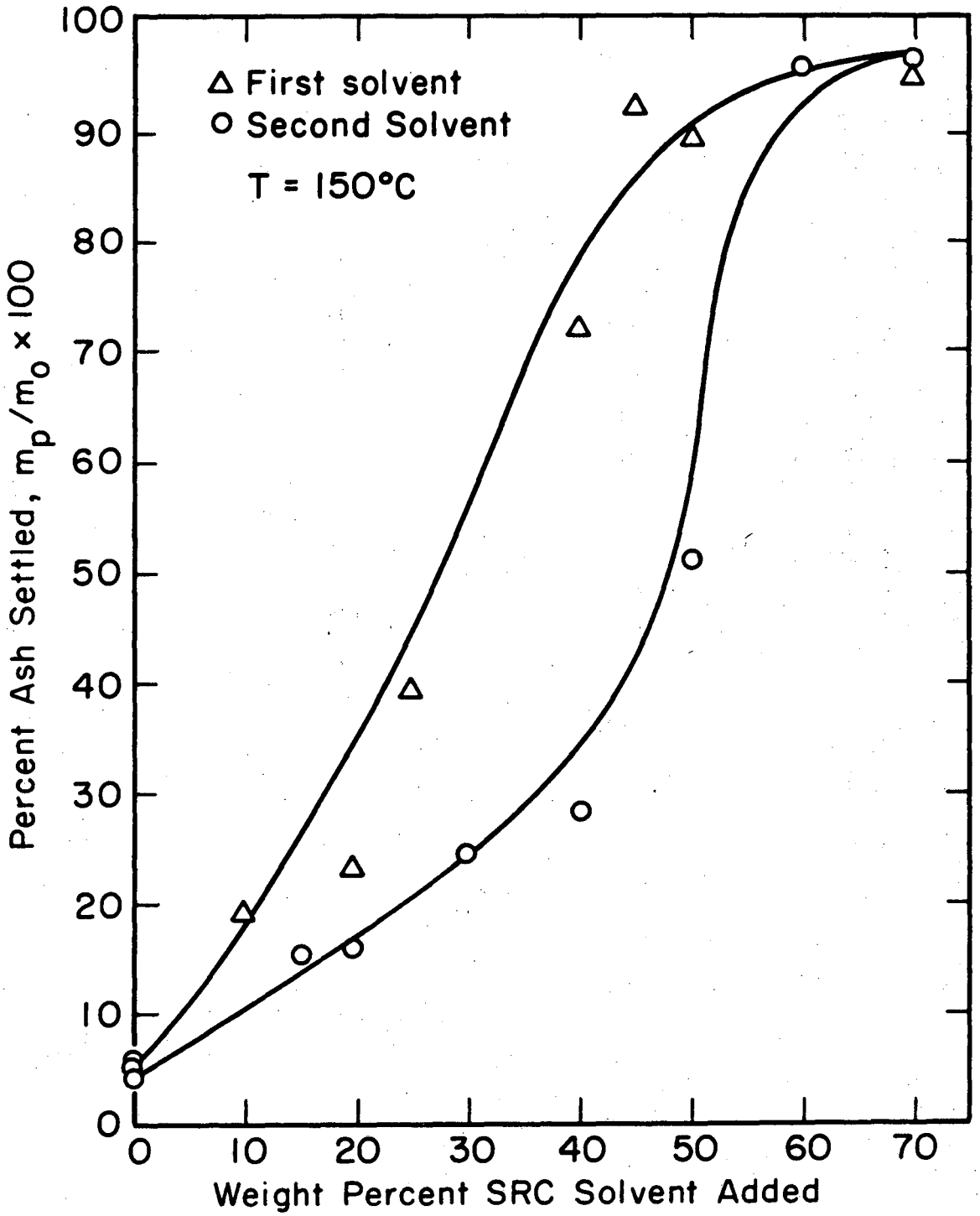

XBL 7810-11789

Figure II-14. Settling of SRC solvent/SRC-UFO solutions.

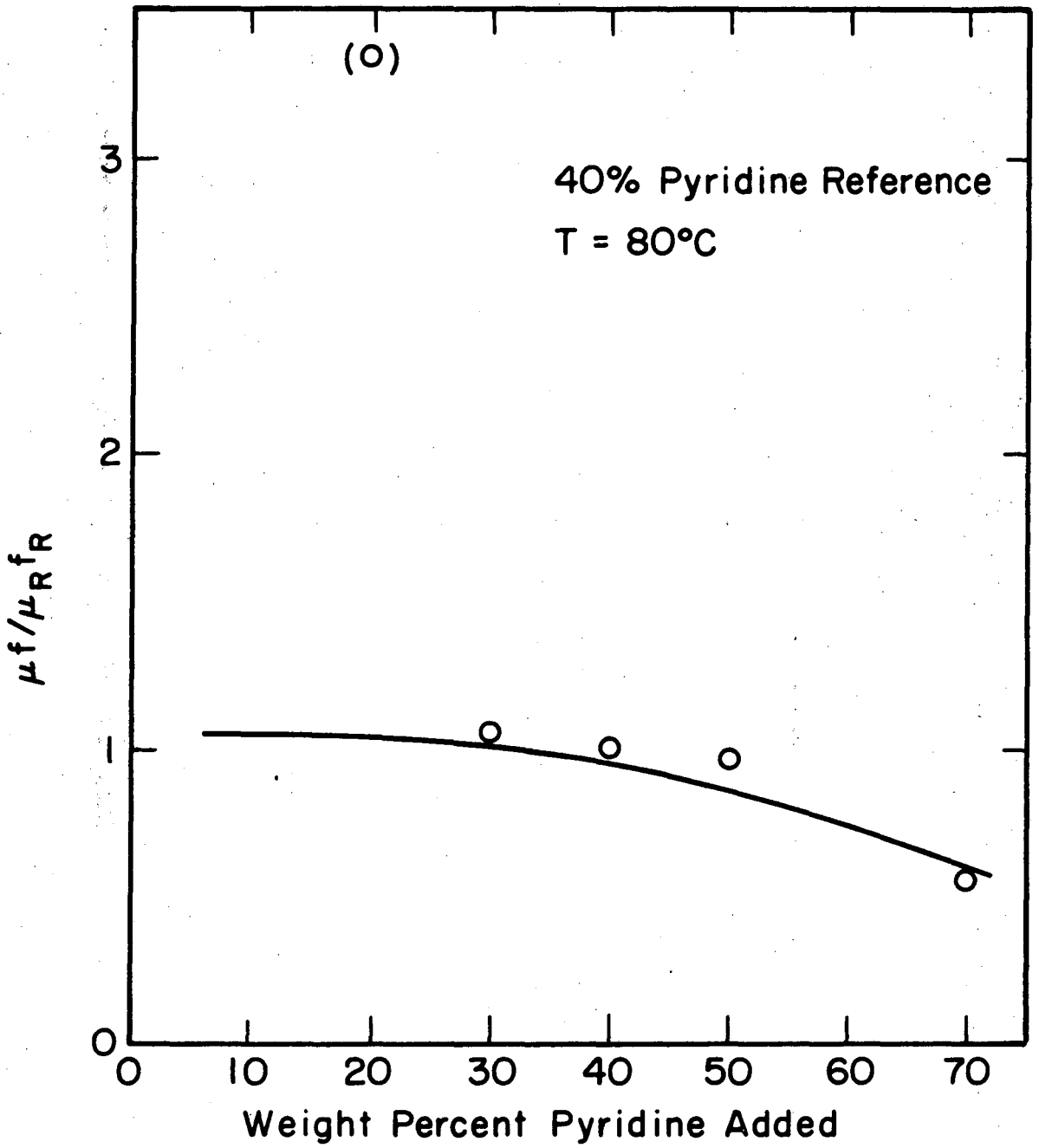

XBL 7810-11790

Figure II-15. Normalized settled fraction versus percent pyridine.

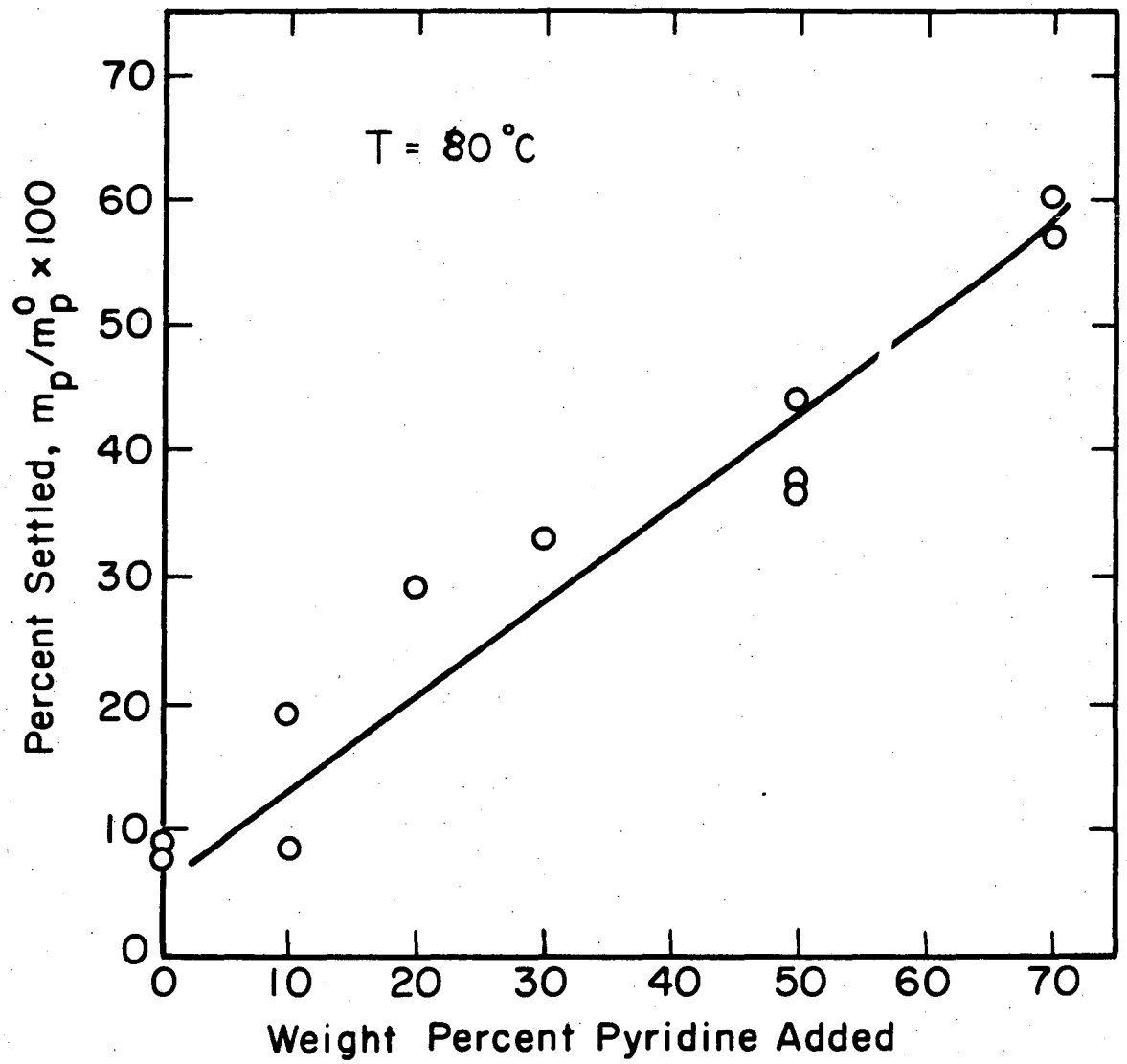

Figure II-16. Settling of pyridine/SRC-UFO solutions.

does not cause as extensive agglomeration as natural solvent.

A run was also made to determine if hexylamine had any additional effect on settling. In this run, SRC-UFO was diluted with 15% hexylamine and 15% SRC solvent. The amount settled did not differ markedly from a 30% dilution of the SRC-UFO with the pure SRC solvent.

b. Solvent Alteration

A charge of SRC-UFO was stripped of the lighter oils by bubbling nitrogen through it for two hours at 2.2 liters/min. About three ml of a clear liquid was removed by this treatment. The remaining liquid was then allowed to settle at 150 ^{o}C. Little or no agglomeration was evident after the stripping.

The solvent was also pretreated by extraction with 1 M NaOH as described in Section B. A 40% solution of the extracted solvent and SRC-UFO was used as the charge for the settler. Again, no significant increase in settling over a standard 40% SRC solvent run was observed.

c. Difficulties

Although the use of settling is a helpful tool to determine the effect of additives on dispersions, the system here is cumbersome, time consuming, and, at times, inaccurate. Burning down the sample is especially suspect. For these reasons, alternate methods were adopted to further investigate agglomeration.

III. WATER AND AGGLOMERATION

A. INTRODUCTION

Water can significantly alter the stability of dispersions in nonpolar media because of its possible preferential adsorption at the solid surface. In small quantities, this takes the form of changing the charge character of the particles. In larger concentrations, water may become influential because it exists as a separate phase.

In Chapter I, it was mentioned that water, in sufficient quantity, can form thick macroscopic layers around suspended particles causing agglomeration. This phenomenon, called spherical agglomeration, was first noted by Kruyt and Van Selms when they observed that small glass beads in halogenated hydrocarbons and coal in water agglomerates upon the addition of a third immiscible phase serves as a bridging liquid which preferentially wets the solid and forms liquid junctions when two wetted particles collide. Presently, a number of different commercial processes to make spherical pellets of fertilizer, $BaFeO_3$, ores, coal, and tungsten carbide use this principle (54)(55)(73)(74)(76)(77)(78).

The mechanism by which the particle is bridged by the added wetting solvent is based on surface tension forces. If a small particle is sitting at an oil-water interface, its position is determined by the relative magnitudes of the interfacial tensions if gravity forces are small compared to tension forces. Referring to Figure III-1, the tensions σ_{so}, σ_{sw}, and σ_{ow} will be balanced at equilibrium as given by the Young-Dupre equation.

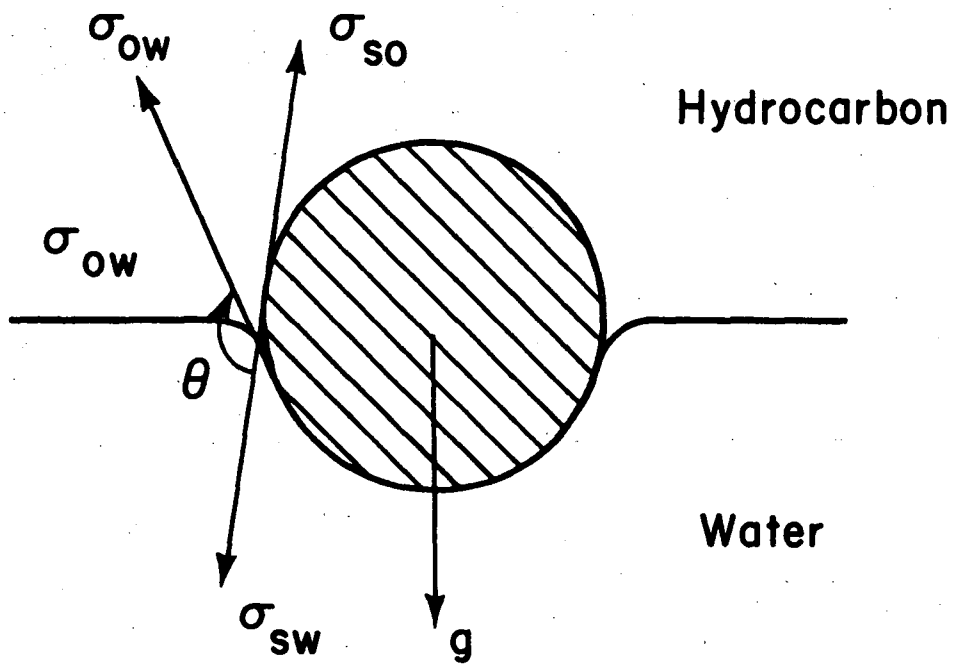

σ_{so} = surface-free energy of solid oil interface

σ_{ow} = oil-water

σ_{sw} = solid-water

XBL 7810-11778

Figure III-1. Forces on particle at a water-hydrocarbon interface.

$$\sigma_{so} = \sigma_{sw} + \sigma_{ow} \cos\theta. \qquad \text{(II-1)}$$

At the interface, the following apply:

1. If $\theta > 90^{o}$, the particle will be drawn into the oil phase
2. If $\theta = 90^{o}$, the particle will concentrate at the interface
3. If $\theta < 90^{o}$, the particle will be drawn into the water

Spherical agglomeration will occur best in suspensions in a nonpolar medium if the third criterion is met. However, whether in the water phase or at the interface, the particles could be concentrated by formation of a water phase by various methods, including AC agglomeration and flotation.

This process inherently depends on the particles themselves being sufficiently polar to be wetted by water. Because of their charge, SRC ash particles may prefer a polar interface. Based on this hope, the following experiments were made.

B. EXPERIMENTS

1. Introduction of Water and Particle Location

Initially, a 50/1 mixture of pyridine extracted ash suspension in SRC solvent to water was mixed with a Waring Blender at top speed. The resulting emulsion contained 5-500 micron sized drops of water. After gently stirring for five minutes, photomicrographs were taken of the final suspension. As seen in Figures III-2 and III-3,

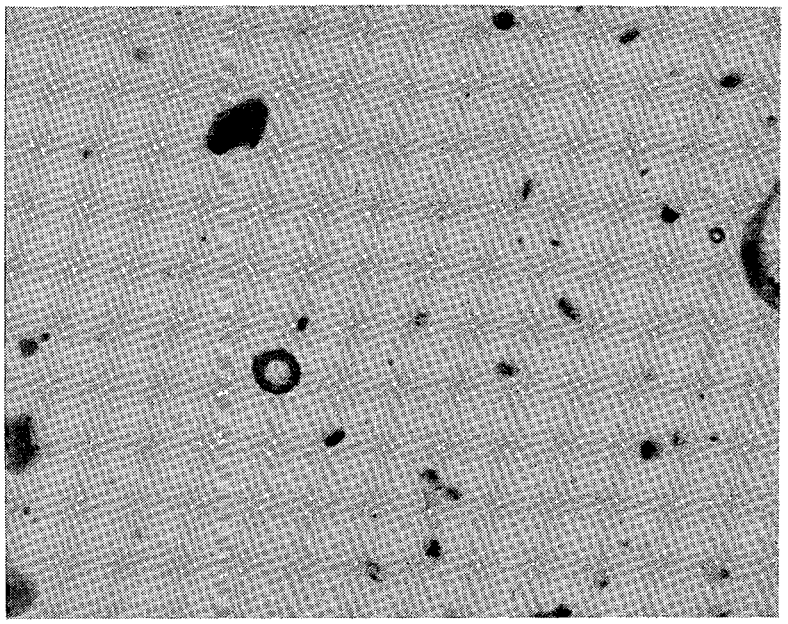

Figure III-2. SRC ash on SRC solvent-water interface.

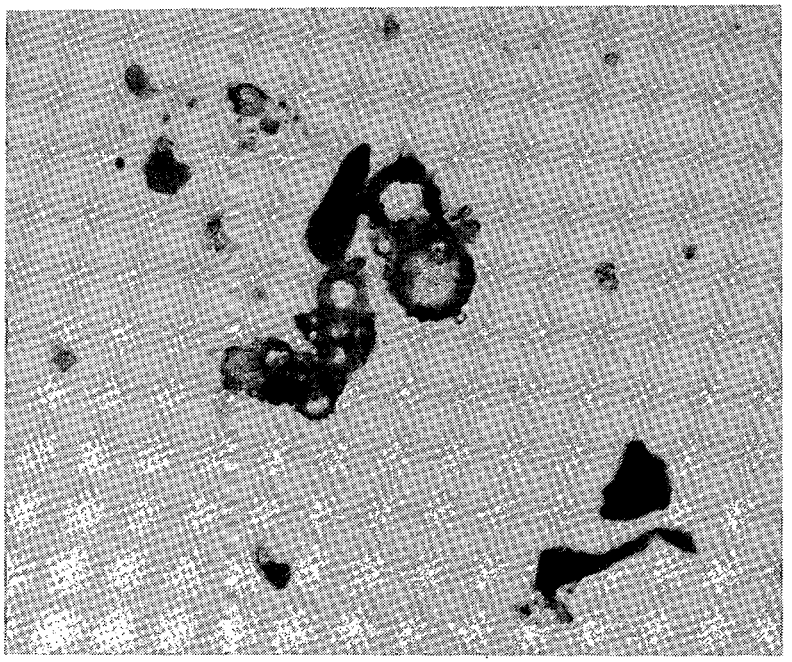

XBB 780-13042

Figure III-3. SRC ash on SRC solvent-water interface.

some particles do preferentially adsorb at the interface. Addition of Triton X35 and Acryloid 960 to change the wetting properties of the interface had no observable effect.

A more uniform emulsion with greater interfacial area can be obtained by adding small amounts of water to the SRC solvent and heating the mixture until the water boils. After saturating the oil this way, the solution is quenched by ice water. A uniform emulsion of 1-5 micron sized droplets is formed.

2. Particle Separations

a. Particles as Nucleation Sites for Water

An emulsion was created in a dispersion of pyridine extracted particles, known to have a charge, in the SRC solvent by the boiling and quenching method. Because of the ash particles' small size and charge, it was hoped that the particulates would serve as nucleation sites for the forming water droplets. The resulting emulsion once again had particles located on the surface of the droplets, but never were the particles observed to be inside them. The charge of the particles seemed to remain unaffected by the water addition.

b. Sweeping Emulsion

Aliquots of the emulsion prepared in the above method were centrifuged for various lengths of time, in order to "sweep" the particles from the oil as the more dense water drops move to the bottom of the tube, carrying particles on their surface. Although the oil and water separated, a considerable amount of ash remained in the oil layer.

The same procedure was tried with an emulsion of water in a 70% SRC solvent/SRC-UFO solution. This resulted in an even worse separation, for the oil phase was already more dense than water.

c. Water as an Anti-Solvent

In this last attempt, water was found to precipitate some of the SRC in solution during the emulsion formation. As mentioned, a great deal of work has been done to find a low cost, efficient anti-solvent so fast settling can take place. To explore water's potential, a mixture of water and a 1/4 ratio of SRC solvent to SRC-UFO was made up, stirred, and used as the charge for the settling apparatus described in Chapter II. The mixture was heated to 90°C and allowed to settle for thirty minutes. Little, if any, enhancement in the settling rate was found.

C. DISCUSSION

These results indicate that the ash particles are not as partial to water as expected, despite their charge and polar character. In fact, the asphaltene coated ash particles seem to be very hydrophobic. Introduced into water, they will coagulate into dense agglomerates. Inorganic ash particles, which are not as extensively covered by asphaltenes, are suspected to be the ash particles observed to sit at the oil-water interface. These would have more polar groups on the surface which may make them water wet (i.e., -Si- -Al-). Perhaps, if the asphaltenes were stripped from the particles, this method would be more effective.

IV. ZETA POTENTIAL AND FILTRATION

A. INTRODUCTION

The SRC ash exhibits a charge in SRC-UFO. However, the effect of this charge on the filterability and stability of these dispersions has only been inferred from their bulk properties. In this chapter, filtration enhancement is investigated by measuring a possible cause of the low filtration rate of SRC-UFO, the charge.

To date, no quantitative measurements of the charge on SRC ash have been made. More precise measurements are beneficial, serving a three fold purpose. First, the charge value, along with the particle size, is important in determining whether stability can be achieved as outlined by Koelman and Overbeek (50). Secondly, zeta potentials are indicative of the effect of additives on the potential barriers controling stability. In these studies, zeta potentials of particles in a number of nonaqueous solvents are measured, including SRC solvent. Finally, charge measurements in conjunction with filtration experiments on the same suspensions shed further light on the factors which do influence filtration rates, both in model dispersion and the SRC process filter feed. There has so far been a lack of study of the relation between zeta potential of the particles and the filtration rate of the suspensions. A preliminary review of this correlation is now presented.

B. PAST STUDIES

The importance of charge in nonaqueous media has recently been the topic of much research, primarily because of the many industrial applications that these dispersions have. Organic suspensions are essential in the paint and coating industry and are the basis of most copying processes used today.

In studying these dispersions, most work has concentrated on the effect of soluble salts on the measured zeta potential of the particles. Kitahara et al., has divided this effect into three general types as seen in Figure IV-1 (52). These curves are based on a number of studies using a wide variety of surfactants, solvents, and particulates (50)(52)(53)(57)(79). It is thought that curve A is the fundamental result and B is A shifted to the left. The particles in B are originally charged by impurities in the solvent. Curve C is probably the result of either no adsorption or nonspecific adsorption of both ions on the particle surface.

The compounds which can effect a charge are varied, but all are large organic salts capable of dissociation in nonaqueous media. This dissociation is apparent in conductivity studies of these solutions (80)(81). A partial list of these compounds is found in Table IV-1. Not only the effect of concentration on charge, but also chain length, ion size, amount of water, and combination of surfactant have been investigated (53)(57)(58)(60)(79). The last of these is most interesting. In this work by van der Minne and Hermanie, carbon black particles in benzene were charged positive by the addition of calcium diisopropyl

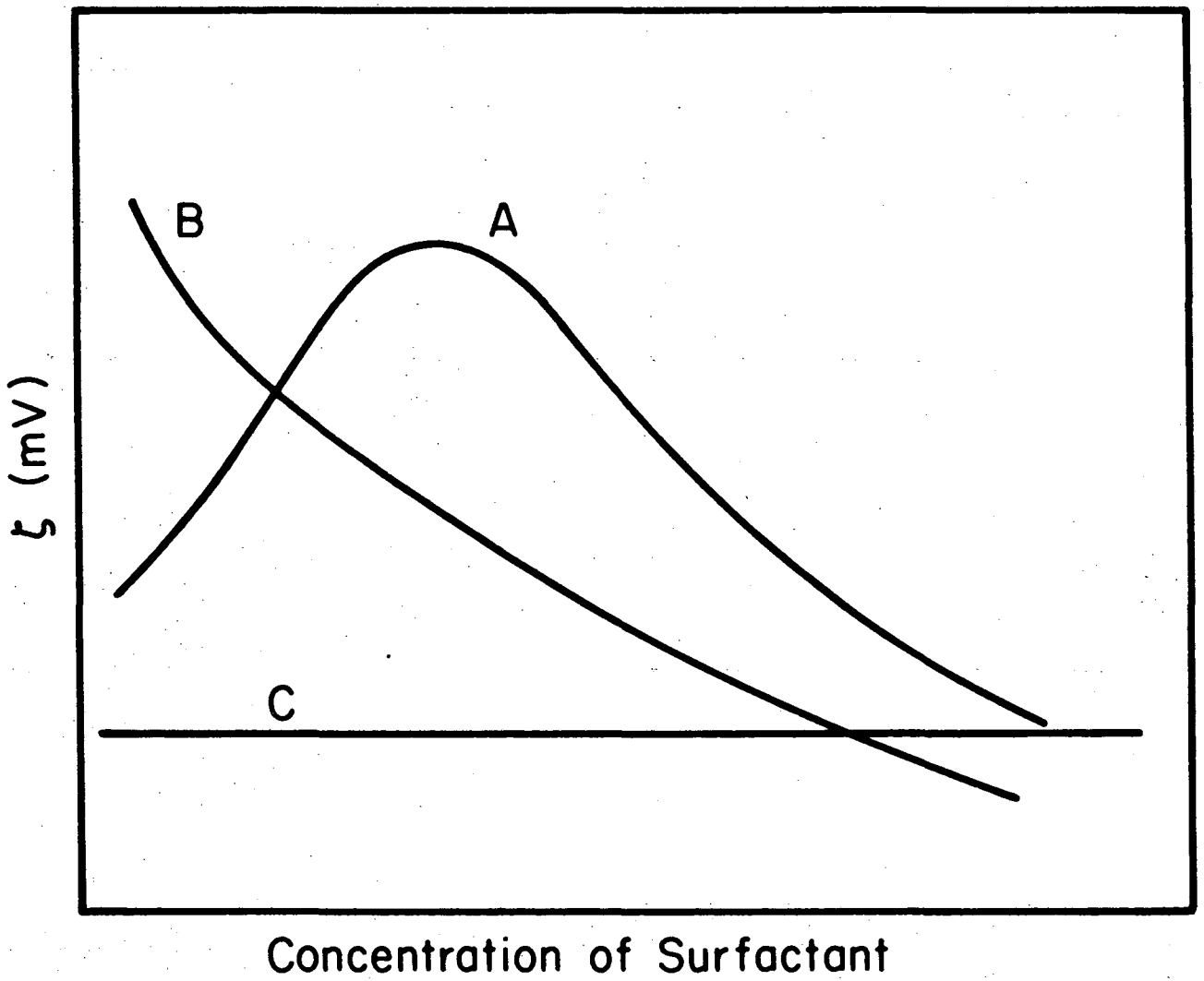

Figure IV-1. Effect of organic surfactant on measured zeta potential.

XBL 7810-11777

TABLE IV-1. Surfactants for nonpolar dispersions.

Copper Oleate
Calcium diisopropyl salicylate
Aerosol OT (Al, Ba, Na, Ca salts)
2-Ethyl hexoate (Mg, Zn salts)
Tetra-1-amyl ammonium picrate

salicylate, Cadips. Addition of tetra isoamyl ammonium picrate, tiap, charged the same particles negative. However, the positive charge of the particles was gradually reduced and eventually reversed by adding tiap. On the other hand, Cadips had no effect on the negatively charged particles. These results not only indicate ion adsorption, but also preferential adsorption of a specific surfactant ion.

Efforts have been made to experimentally verify the theoretically predicted magnitude of potential necessary to stabilize such nonpolar dispersions. Koelman and Overbeek found that very modest potentials of around 30 mV are adequate to disperse one micron sized Fe_2O_3 and Al_2O_3 particles in xylene. This zeta potential corresponds to a potential energy barrier to coagulation (Vmax) of about 15 kT. As stated earlier, this is thought to be the minimum to insure a stable suspension (64).

However, McGowan et al., observed stable aggregates of 0.1-0.5 micron particles if the zeta potentials were in excess of 50 mV. The potential curve for dispersions of particles with a, the particle radius, equally 0.1 microns show a calculated V_{mas} equaling 6.5 kT (50) (53). In the work of Cooper and Wright, 30 mV seemed adequate to stabilize particles of copper phthalocyanine in hexane (45). For the 0.3 micron sized particles used, the corresponding potential barrier is about 5 kT.

In the above studies, the stability ratios obtained from optically measured rates of coagulation are compared with the theoretical values as suggested by Fuchs based on the theory of slow coagulation (64) (83).

The shapes of the curves of zeta potential versus both experimental and theoretical stability ratios agree. At a specific potential, there is a dramatic increase in the stability ratio.

A sample plot of this theoretical stability ratio versus zeta potential for a suspension of particles of the ash in SRC solvent is given in Figure IV-2. In calculating W, the modification suggested by Parfitt et al., was used (84).

$$W = \int_2^\infty \exp \frac{V_t dS}{kT S^2} \Big/ \int_2^\infty \exp \frac{V_a dS}{kT S^2} \qquad \text{(IV-1)}$$

where $S = (R/a)$, R is the center to center distance between particles, V_a is the attractive potential given by Equation I-1, and V_t is the total potential of interaction, $V_t = V_a + V_r$. A simple Coulombic repulsive energy given in Equation I-7 is assumed. This overemphasizes the repulsive potential making the calculated barriers to coagulation somewhat higher. The radius used in the calculations is 2500 ^{o}A, the approximate average radius of the ash particles. The Hamaker constant is taken as 5×10^{-13} ergs and kT is equal to 4×10^{-14} ergs. The exact values calculated for W for specific zeta potentials are given in Table IV-2.

Very few workers have correlated stability and/or zeta potential with the filtration character of the suspensions, optical techniques being the more direct approach. One exception is Smelie and La Mer who, working with flocculated phosphate slimes in aqueous media, derived an expression relating the refiltration rate of the cake to the concentration of the polymer (85)(86). The refiltration rate was calculated from

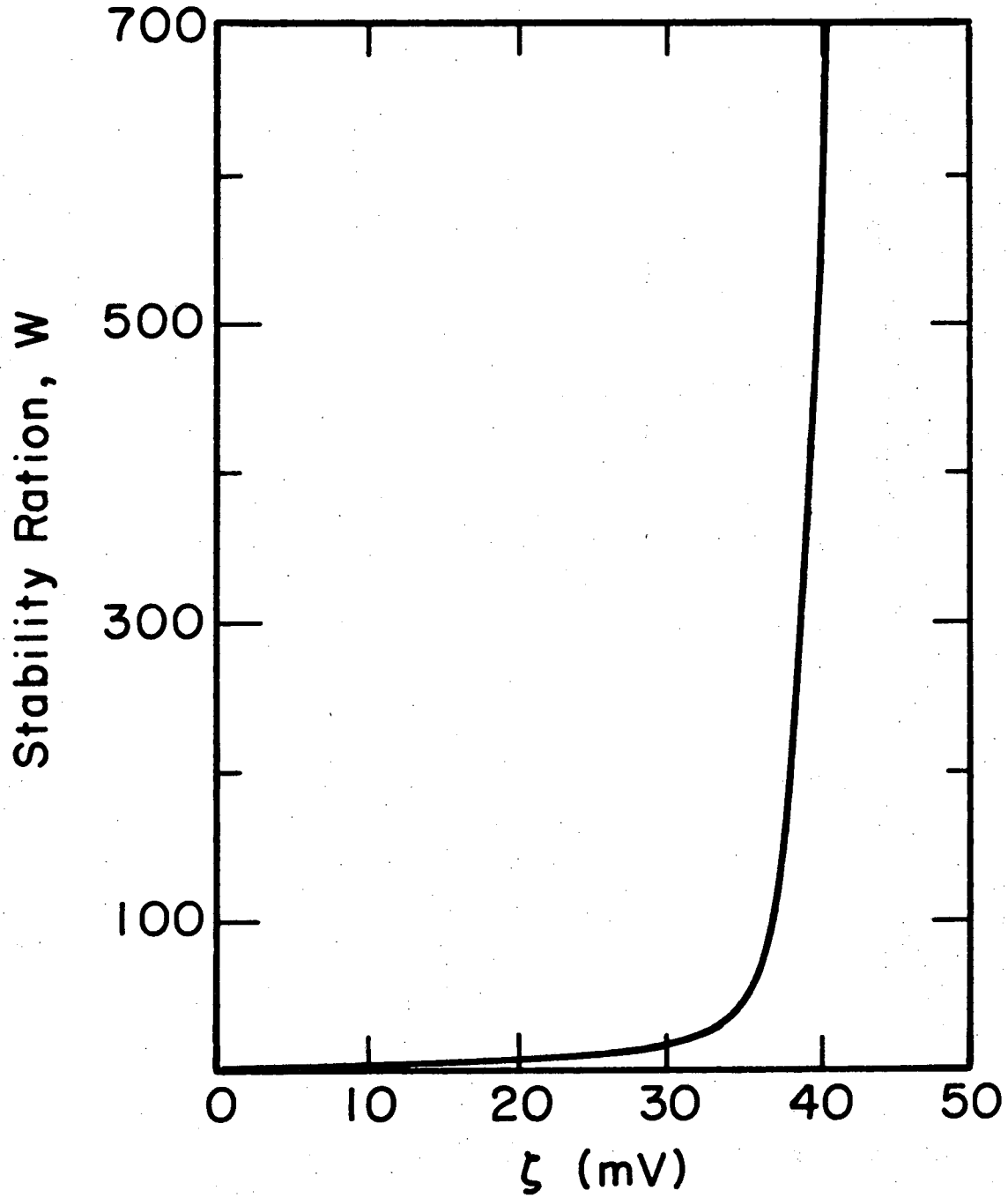

XBL 7810-11776

Figure IV-2. Stability ratio versus zeta potential.

TABLE IV-2. Stability parameters in ash in SRC solvent dispersions

mV	Stability Ratio, W
10	1.34
20	3.03
30	15.8
40	536
50	2.53×10^4
60	6.87×10^5
70	1.73×10^8

the time measured for a volume of filtrate to pass through a premade cake. In their derivation, an steady-state radius of a floc is calculated assuming a rate of flocculation due to polymer adsorption and of deflocculation because of shear. Their surface coverage is related to the polymer concentration. In conjunction with the Kozeny-Carmen equation, which expresses the filtration rate as a function of the square of the specific surface area, an equation relating the filtration rate to the polymer concentration is derived. The derived expression indicates a maximum in filtration rate; however, it is dependent upon concentration of polymer, not charge.

There are additional problems with this derivation. Smelie and La Mer assumed the floc size, height of the filter cake, and porosity as constant. These assumptions, made in order to use the Kozeny-Carmen relationship, have been found to be incorrect for flocculated systems by Kitchener et al. In their study, they conclude that there is no advantage in using the refiltration technique for studying flocculation; measuring turbidity of the supernatant is faster and quicker (87).

Such turbidity measurements are impossible in coal solutions. In addition, coagulation produces much less loose agglomerates which allows one to make some of the assumptions of Smelie and La Mer. Therefore, the following work concentrates on stability measurements by filtration, in the hope that this method succeeds where others failed.

C. MODEL SYSTEMS

SRC-UFO, because of its toxicity, viscosity, and odor, is extremely difficult to study, especially at elevated temperatures. In order to facilitate handling and expedite experiments, a number of different organic dispersions are investigated in order to glean the importance of zeta potential on filtration.

1. Solvents

Benzene and toluene are used as examples of common aromatic hydrocarbon solvents. Both are of reagent grade containing less than 0.01% water. Neither has conductivities in excess of 10^{-9} ohm^{-1} cm^{-1}.

Pyridine is again used as the model coal solvent, and prepared in the manner described in Chapter II. The SRC solvent is used as the actual coal solvent. Its origin is similarly described in Chapter II.

2. Solids

A set of three different types of particulates are used in the suspensions. Kaolin and Sterling FT are chosen as particles to represent possible surface characteristics of the SRC ash. Kaolin is supplied as a NF colloidal powder from Mallinkrodt Chemical Works. The particles have an apparent size of 0.1-0.5 microns. Sterling FT-D3 is a carbon black with similarly sized particles.

The third particle set is the ash itself. This is introduced into a solvent in two possible fashions. To isolate the particulates, the SRC-UFO is Soxhlet extracted with pyridine for a predetermined time. Because extraction conditions are extremely important to the final ash

characteristics, the distilling pot size, size of sample, and power supplied to the heating mantle are standardized. The collected black cake is dried overnight at eighty degrees in a vacuum oven and then gently ground with a mortar and pestle until a fine powder results. All samples are easily broken down to this final form which is then used to make the suspensions.

The length of time the sample is extracted with pyridine is a critical variable determining the charge character of the resulting particles, as seen in Figure IV-3. Too little extraction produced particles whose charge could not be reduced by the addition of copper oleate to the pyridine suspension. Medium extraction yields ash particles whose charge could be reversed. Finally, particles which are extracted extremely long periods of time exhibit no charge in pyridine unless copper oleate is added to the suspension. Unfortunately, the degree of extraction in a given time is difficult to control, making ash with consistent properties difficult to obtain.

3. Surfactants

The surfactant primarily used in this study is copper oleate. This is taken from a 60% solution of the salt in an inert mineral oil. This solution is supplied by Pfaltz and Bauer Company. Aerosol OT is from Eastman Kodak Company, marketed as dioctylsulfosuccinate, sodium salt. It is of practical grade.

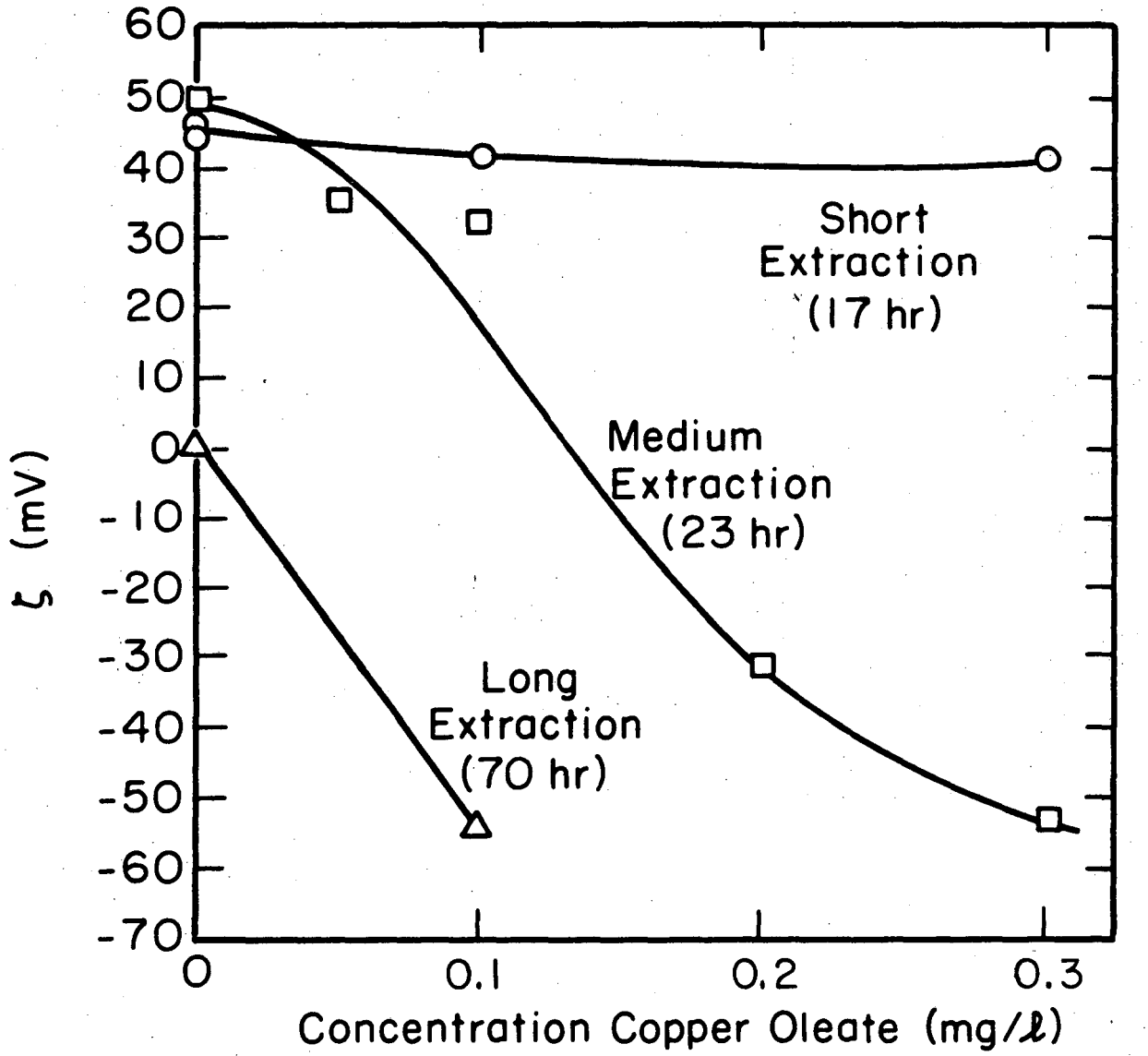

XBL 7810-11775 A

Figure IV-3. Effect of extraction on charge reduction.

D. MEASUREMENT OF CHARGE

1. Theory

In order to evaluate the magnitude of charge, zeta potentials are calculated from measured mobilities, u, of particles within an applied electric field. Mobility is defined as v/E where v is the particle velocity and E is the applied field. The zeta potential is calculated using a modified Hückel equation:

$$\zeta = \frac{3}{2} \frac{u\mu}{\epsilon} \frac{1}{F_c} \qquad \text{(IV-2)}$$

$$\mu = \text{kg m}^{-1} \text{ sec}^{-1}$$
$$\epsilon = \text{coul}^2/\text{J-m}$$
$$u = \text{m}^2/\text{V-sec}$$

The function F_c is a correction factor to take into account retardation and relaxation effects and depends on a/λ in which a is the radius of the particle and λ is the Debye length. Wiersema, Loeb, and Overbeek have tabulated the value of F_c for a wide variety of conditions (88).

The Debye length for the suspensions used in this study needs to be determined. Using the method suggested by Kitahara et al., a rough estimate of this length can be calculated. The concentration of ions in nonaqueous suspensions is estimated from conductivity data and equivalent conductivities of the ions in water. Using Walden's law and the relationship for degree of dissociation suggested by Arrhenius, the ion concentration can be expressed by

$$c\ (\frac{\text{ions}}{\text{cm}^3}) = \frac{KN_a\ \mu_{nonaq}}{(\lambda^o_+ + \lambda^o_-)\mu_{aq}} \qquad \text{(IV-3)}$$

μ_{nonaq} = viscosity of nonpolar solvent
μ_{aq} = viscosity of water
K = conductivity of nonaqueous
N_a = Avagadro's number
$\lambda^o_{+,-}$ = equivalent conductivity of ions in water at infinite dilution

Although the aqueous equivalent conductances of the oleate ions have not been measured, there is no reason that these large ions should have large equivalent conductivities. Checking Newman and Castellan, mobilities of large ions are of the order of 30-40 ($(CH_3)N^+$, $\lambda^o_+ = 45$; Picrate$^-$, $\lambda^o_- = 30.4$) (90)(91). Using these values, an approximate equivalent conductivity, Λ^o, of around 90-100 might be expected. This is of the same order of magnitude for Aerosol OT, $\Lambda^o = 120$ ohm^{-1} cm^2 equivalent (54). If water does dissociate in nonaqueous media, the limiting conductance would be expected to be higher although not of the order of magnitude found in water since proton jumping will not be a contributing factor. Considering the equivalent conductivity of hydroxyl and hydrogen ions as half of their aqueous value (arbritrarily), Λ^o would be equal to approximately 300. It will be clear that larger values will not affect the final result.

Measurements of the specific conductivity never rise above 10^{-6} ohm^{-1} cm^{-1} in pyridine and 3×10^{-9} in the natural solvent. Using these values, the rough estimates of a/λ shown in Table IV-3 are calculated. Such Debye lengths are probably the lower limit values.

TABLE IV-3. Debye length and a/λ calculations

Solvent	Λ_o(ohm^{-1}cm^{2}equi.$^{-1}$)	Ions/cm^3×10^{-14}	Debye length(A^o)	a/λ
Pyridine	300	19.8	940	2.66
	100	58.9	330	8.00
SRC Solvent	100	0.993	1540	1.62

a = 2500 A^o

ε (pyridine) = 12.4

ε (SRC solvent) = 4.55

The magnitudes of a/λ are of an intermediate value which can cause significant variations in calculating zeta potential from the mobilities. Using the tabulated values of F_c calculated by Wiersema et al., the maximum value of F_c is 1.17 for the observed 65 mV zeta potential with a a/λ of 8. In all other cases, the correction factor is very nearly one. In addition, the average value of the particle radius is probably high, since considerable number of sub 0.2 micron particles were not included in the average calculation. Smaller radii would only decrease the correction factor even more. In these experiments, all zeta potentials are calculated using the Hückel equation with $F_c = 1$.

2. Apparatus

A single particle microelectrophoresis (Rank Brothers Ltd., Bottisham, Cambridge, UK II) with dark field illumination is used for electrophoresis measurements. This is fitted with cylindrical platinum electrodes, blackened to minimize polarization. Because of the nonconducting media used for the suspensions, a flat, quartz, rectangular cell is employed for all measurements. The flat cell has the following advantages:

1. Large particles can be observed at the stationary levels while falling.
2. These large particles fall on a electro-osmotically unimportant surface and will not alter the position of the stationary levels significantly.

3. The rectangular cross section can be more readily made out of silica. This is a necessity. van der Minne and Hermanie found the fields to be inhomogeneous using glass.
4. Phase contrast is easier to arrange with the flat cell. This is important in order that the particles can be seen in the dark solutions used here.

Listed in Table IV-4 are the dimensions of the cell. The interelectrode distance used to calculate the mobility is determined by measuring the cell's conductance when filled with a solution of known specific conductivity.

Measurements are made in room temperature air, heeding the cautions of van der Minne and Hermanie about electrical leakage through any conducting phase outside the cell (79).

3. Sample Preparation

The suspension used in the cell contained 0.005-0.01% particles by weight in the appropriate solvent. At these concentrations, a large number of particles can be seen although they are observed to be distinct and unhindered in their movement. Where possible, suspensions are taken from samples to be filtered. Thus, five ml of the 1% suspension is centrifuged for 1-3 minutes and the supernatant used for electrophoresis measurements. In the case of darker suspensions, where asphaltenes caused them to be opaque, a small amount of particles (0.01% by weight approximately) is resuspended in the solvent with the appropriate concentration of surfactant. This is sonified and placed in the electrophoresis cell for mobility measurements.

TABLE IV-4. Cell dimensions

Dimension	Length (mm)
Length	30
Flow width	1
Flow Height	10
Inter-electrode distance	63.2

4. Procedure

The cell is cleaned with chromic acid, washed with acetone several times, and dried in an 80 ^{o}C oven. To this cell, the suspension is added and equilibrated until no or very little drift of the particles is observed. In darker, less viscous pyridine suspensions, drift is an ever present problem. Often this is caused by imperfectly seated electrodes, allowing evaporation at one end. Care has to be taken in assuring that the light intensity is not great enough to cause large convective velocities. In some cases, the overhead lights should be turned off to minimize the light needed for observation. Usually, after a half hour of sitting, particles remain nearly motionless.

The walls of an electrophoretic cell will in general be charged in the presence of a solvent and this will lead to the migration of the oppositely-charged double-layer ions in the solvent toward the appropriate electrode. This electro-osmotic flow has to be counteracted by flow in the opposite direction since the cell is closed. The combination of opposite flows leads to a situation where there are two discrete points along the cross section of the cell where the fluid velocity is zero. Only at these stationary levels is the velocity of the particle equal to its electrophoretic velocity.

Assuming symmetry across the cell, an equivalent electro-osmotic slip velocity, and a constant zeta potential on all surfaces, Komagada derived a Fourier series expression to calculate these points depending on the dimensions of the cell (92).

$$\frac{s}{d} = 0.500 - \left(0.0833 + \frac{32}{\pi^5}\,\frac{d}{l}\right)^{1/2} \qquad \text{(IV-4)}$$

d = cell width
l = flat cell length
s = stationary level

In using this equation, a/λ must be small in comparison to the cell thickness. Also d/l should be small. Both criteria are met for the system used in these studies. In addition, the equation is only rigorously correct for observations done on the center line of the cell. However, as long as observations are made close to center, this is not critical.

Distances are measured from the inside surface inward to reduce hysteresis errors in using the positioning micrometer. The inside surface is determined using the inhomogeneities of the cell wall. For effective illumination at these levels, the light is adjusted such that it focuses at the point of observation. When in focus, the particles appear as bright sparkling points of light in a dark background. The beam itself is positioned approximately equidistant from the four sides of the rectangular viewing plate.

Mobilities of approximately ten particles are measured at both stationary levels. To minimize heating and possible electrode reactions, the field is reversed after each measurement and turned off when observations are not being made. The mean velocity is calculated by averaging the reciprocal times for each particle to transverse a given distance. Noting the applied potential, the viscosity and dielectric constant of the fluid, and this mobility, the zeta potential is calculated

from Equation IV-2.

Each particle observed must meet all the criteria for true electrophoresis:

1. The motion must be rectilinear between the electrodes
2. The velocity must be independent of particle size and location in an uniform field
3. The velocity must be directly proportional to the field strength and reverse with field reversal

Unidirectional motion characteristic of dielectrophoresis is only observed when the field strengths exceed 150 V/cm in the apparatus used here. An additional and critical test for proper electrophoresis is to plot the velocity at various cross sectional depths according to the method Van Gils describes (93). On the abcissa, the velocities at various levels are plotted; on the ordinate, the square of the relative distance from the center axis. In this way, a parabolic velocity distribution, characteristic of electro-osmotic Poiseuille flow under a homogeneous field, will fall on two straight lines. This is observed to be true in each of the suspensions studied here. Examples for the ash particles in pyridine and SRC solvent are given in Figures IV-4 and IV-5. The slopes of these lines should be equal if the flow is truly symmetric. In Figure IV-4, there seems to be some asymmetry. However, this asymmetry varies from run to run and is suspected to be caused by the particles adhering to the cell inner wall.

5. Reproducibility

The procedure for finding the mobilities is subject to a certain amount of error. Measurements of the cell thickness, and therefore, the exact location of the stationary levels vary slightly. If extremely clean, the inside surface is difficult to find and errors as large as ± 0.02 mm can be made. If the walls are not clean, there is some deviation from symmetrical flow. However, the calculated zeta potential at each level usually varies no more than 10%.

During the measurement of 18-20 mobilities of particles of a given suspension, the velocity rarely changed more than 10-15% from the average value except when there was an obvious drift in one direction. In most cases, solutions are allowed to equilibrate until this drift velocity is extremely small compared to the electrophoretic velocity. However, in some experiments, the drift was so persistent that measurements were made despite this added velocity. In these cases, never did the average of the pairs of opposite direction mobilities vary more than the above 10-15%. The mobilities of particles from similar suspensions also deviated from each other by 10-15%. The zeta potential of ash in pure pyridine has a standard deviation of ± 9 mV, while zeta potentials of the highly charged particles in SRC solvent varied by ± 7 mV. These deviations are within the experimental error of ± 10 mV as calculated from the errors listed in Table IV-5.

In measuring the smaller potentials, drift became a significant problem because the electrophoretic velocities are small. The natural solvent viscosity of 6 cp is approximately twice that determined

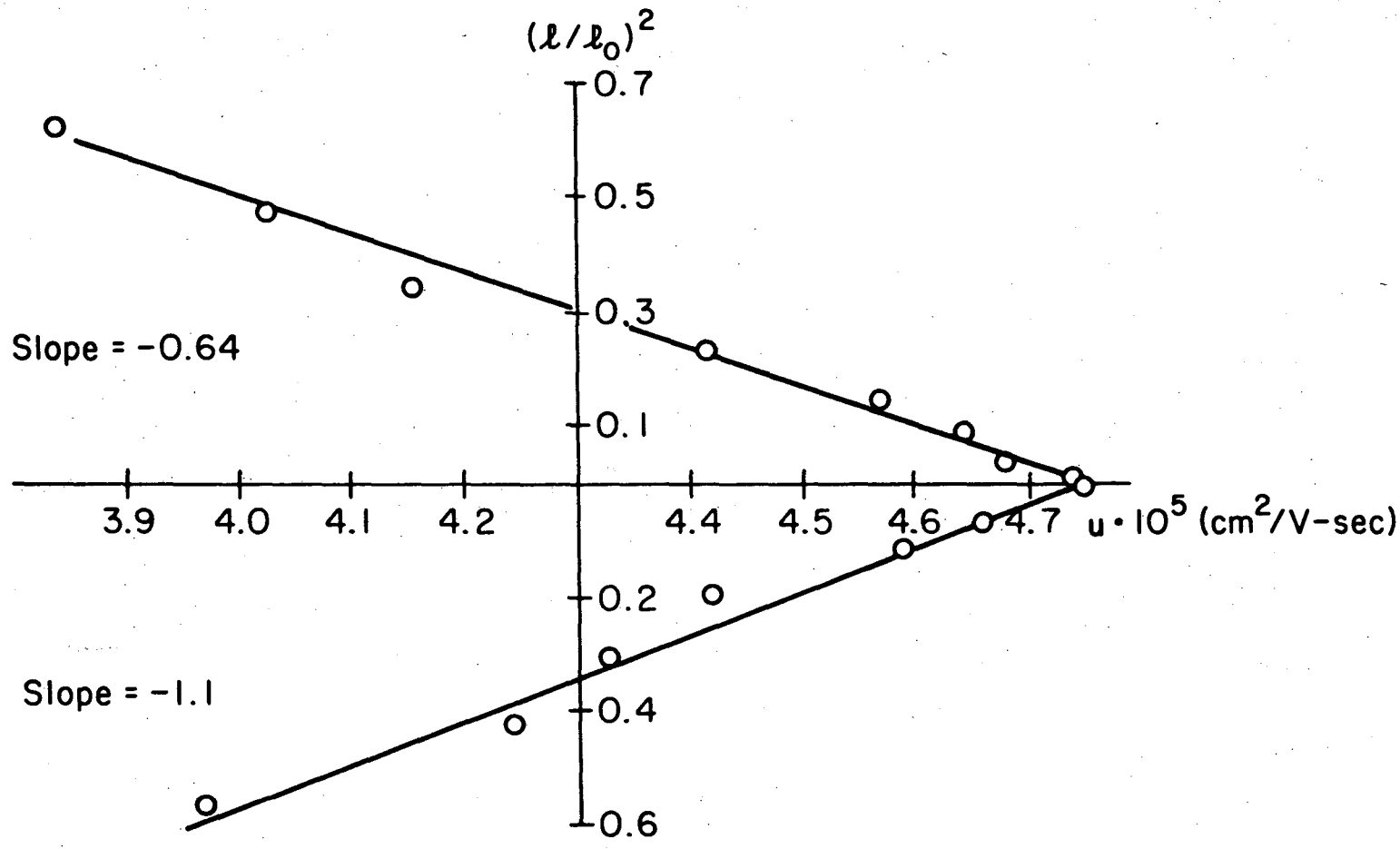

XBL 7810-11774

Figure IV-4. Velocity profile of 28 hour extracted ash in pyridine.

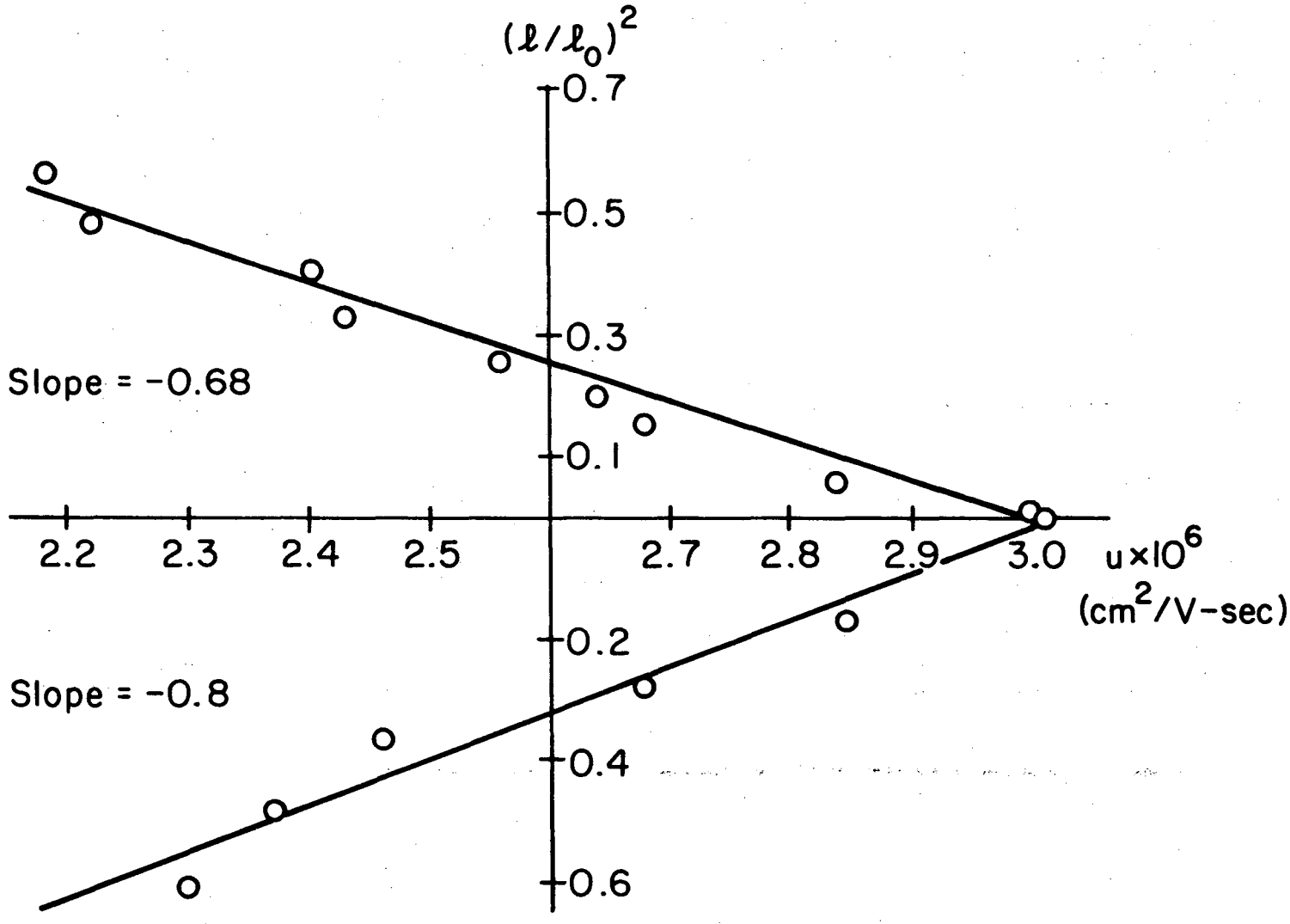

XBL 7810-11773

Figure IV-5. Velocity profile of 28 hour extracted ash in SRC solvent.

TABLE IV-5. Maximum experimental error in zeta potential calculations

$\Delta t = \pm 0.4$ sec	
$\Delta(\Delta V) = \pm 20$ V	
$\Delta l_{eff} = \pm 0.2$ cm	
$\Delta \mu = \pm 0.2$ cp	
Pyridine and Ash	$40 < \zeta_{max} < 64$
Natural Solvent and Ash	$56 < \zeta_{max} < 71$

to be the upper limit by Wright and Mesinger (48). This hampers movement to the point where convective drift nearly masks all real electrophoretic velocities.

Errors within a set of mobilities are approximately the same, but small changes in lighting, position of observation, and clarity also make determining zeta potentials less than 40 mV much less accurate in viscous systems. The reason for the difficulties can be seen schematically in Figure IV-6. When the electrophoretic velocities are large compared to the electro-osmotic, the relative error caused by being slightly away from the stationary level is small. However, when the electrophoretic velocity is small, slight errors in positioning can drastically affect the observed velocity, even reversing their direction.

E. Filtration

1. Theory

In filtration, a layer of solid particles is formed on a filter support while the clear liquid passes around the particles. The rate at which the liquid can find its way through the cake is inversely proportional to the total drag it incurs along its path of flow. As stated in the introduction, the common method to estimate this drag is based on the assumption that the cake be modeled by a set of identical conduits, each of variable cross section.

In studying a cake filtration problem, the most useful tool is the simple filtration equation derived from Darcy's law and filtrate material balance:

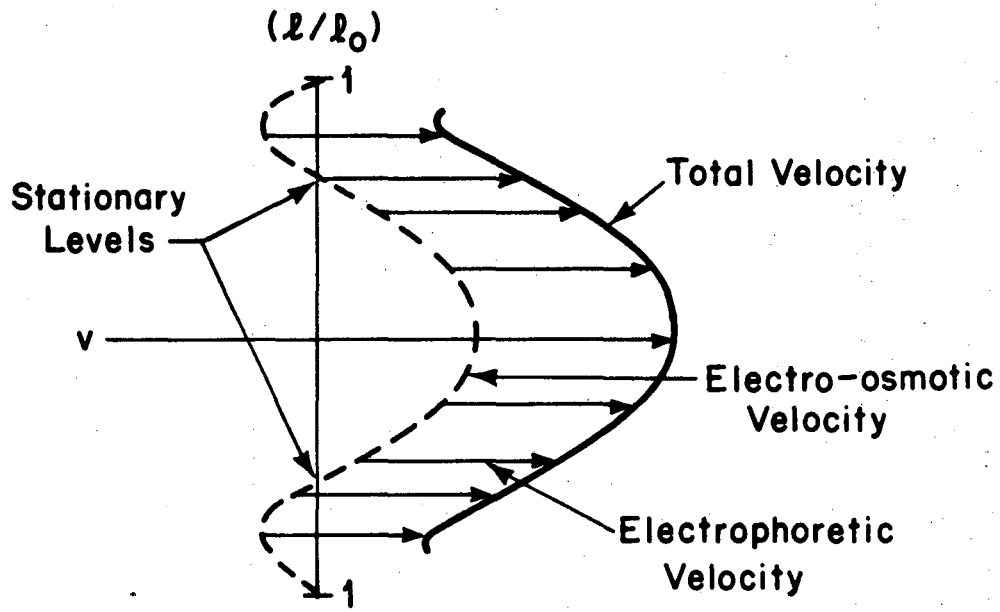

Case 1: Large Electrophoretic Velocity

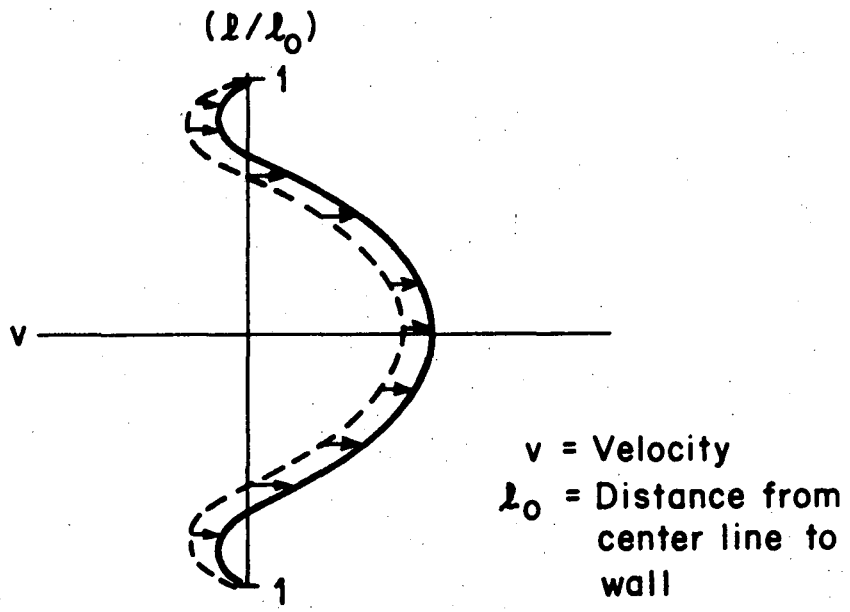

Case 2: Small Electrophoretic Velocity

XBL 7810-11772

Figure IV-6. Velocity profile of particles within an electrophoretic cell.

$$\frac{dV}{dt} = Q = \frac{A\Delta p}{\mu(\alpha\frac{wV}{A} + R_m)} \qquad \text{(IV-5)}$$

A = area of filtering surface
Δp = differentical pressure
w = mass of dry cake/volume of suspension
V = volume of filtrate
R_m = support resistance
μ = fluid viscosity

The important term in this expression is α, the average specific cake resistance or the reciprocal of the cake permeability. This resistance depends on the properties of the cake and has been better quantified by work of Carmen and Kozeny studying viscous flow through packed beds of particulate material. From Carmen-Kozeny theory, α can be written in terms of the cake properties.

$$\alpha = \frac{(1-\varepsilon)S_o^2\tau^2K}{\varepsilon^3\rho_p} \qquad \text{(IV-6)}$$

ε = porosity of cake
S^2 = specific surface area/volume of particles
τ = tortuosity
ρ_p = particle density

Theoretically, K is a constant which is a function of particle size, shape, and orientation.

The experimental difficulties in applying these equations to compressible cakes of small particles can be considerable. Although the effective pressure drop is usually held constant, the mechanical stress

on the particles varies through the cake depth, causing variations in cake porosity, and, subsequently, specific resistance. Thus, the term α is usually an average cake resistance. However, if the cake is thin, both ε and α can be assumed to be constant throughout the cake. Grace found this to be so if the thickness-to-diameter ratio does not exceed 0.6 (97). Being well below this value (thickness/diameter = 0.01), the α presented here are specific cake resistances, α_p, for the given cakes.

In order to obtain values of α, the integrated form of Equation IV-5 is used.

$$\frac{t}{V/A} = \frac{\mu \alpha V}{2 \Delta p A} + \frac{\mu R}{\Delta p} \qquad \text{(IV-7)}$$

Both α and R are calculated from plots of t/(V/A) versus (V/A) using the slope and intercept of the resulting line.

2. Apparatus

A schematic of the filter test apparatus can be seen in Figure IV-7. In these experiments, a small Büchner funnel acts as a support for a piece of Whatman 40 filter paper of known dimensions. The filtrate is collected in a graduated test tube delineated into 2.5 ml aliquots. The time to collect each volume is recorded using a resetting timer. A relative constant pressure differential of 7.5×10^8 dynes/cm^2 (740 mm Hg) is applied by evacuation of the collection vessel. The magnitude of this pressure differential is monitored by a manometer.

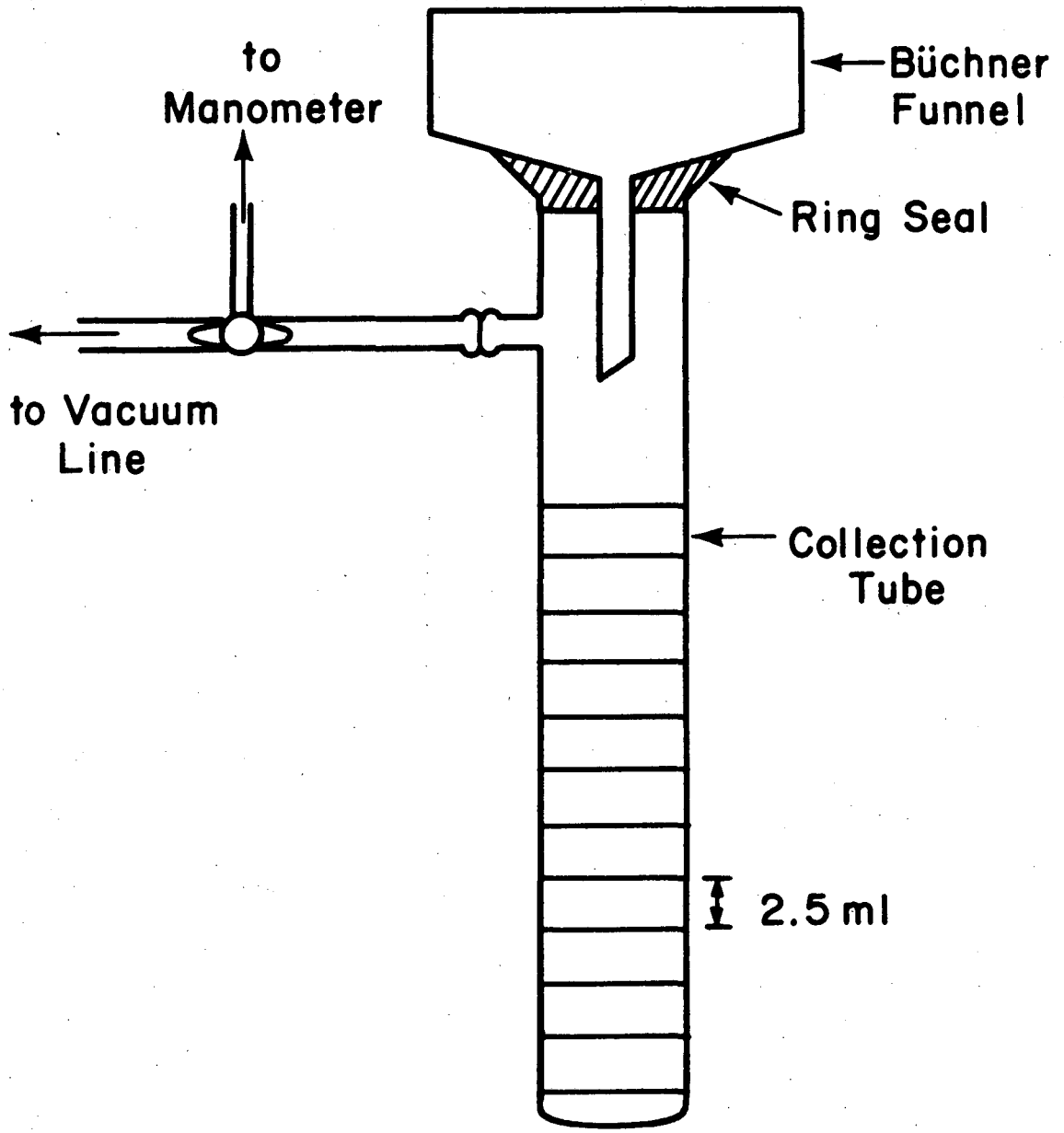

Figure IV-7. Filtration apparatus.

3. Sample Preparation

Suspensions of the desired particles and solvent are made up such that the time needed to complete the filtration is between 50 and 3000 sec. This varied the particle concentration from 10-100 g/l depending on the solvent and ash chosen. These suspensions are subjected to a given time of sonification (usually fifteen minutes) and then gently stirred for another ten minutes. This last step was not found to be critical. Despite large variations in both the time and magnitude of shear through stirring, similar suspensions filtered at the same rate. Any agglomeration is either too stable to be broken up by this method or the agglomeration takes place within the cake.

The length of sonification time is found to be an important variable determining the cake resistance. This effect is clearly demonstrated in Figure IV-8. The three lines correspond to particles subject to different times of Soxhlet extraction with pyridine. A marked increase in resistance is presumably due to a reduction of particle size. The importance of this effect decreases as the ash is extracted longer. The ash has a considerable number of small pyridine soluble asphaltene particles. Asphaltenes have been recognized as agglomerates of 20-30 Å molecules themselves (38)(39).

4. Procedure

To filter, the suspensions are added to the funnel with the vacuum on. The starting time of filtration is taken as when the solvent first moistens the filter paper. As the filtrate passes through the forming cake, the time to collect each aliquot is recorded. Plots of

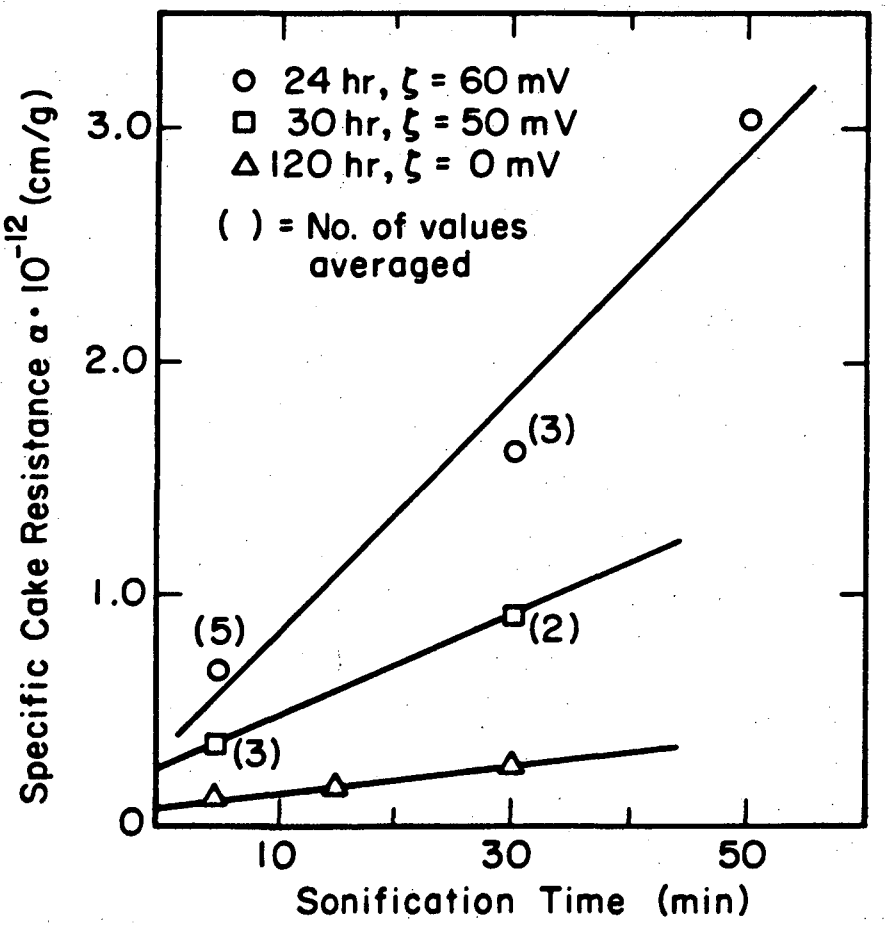

XBL 7810-11770 A

Figure IV-8. Effect of sonification on cake resistances of pyridine/SRC ash suspensions.

t/(V/A) versus (V/A) are then made and the best straight line fit using the method of least squares. Often the initial point deviates significantly from this line, presumably because of the difficulty of determining the start of filtration or the influence of the support on the packing of the first particles collected. If the correlation factor, r^2, of the fit is lower than 0.9, this point is not included in determining the final line. Figure IV-9 shows a sample plot of a set of filtration runs of partially extracted ash in pyridine.

From the slopes of these lines, the specific cake resistances are calculated. As an example, α is calculated for the 60 mg/l copper oleate run shown in Figure IV-9.

$$\alpha = \frac{2\Delta p\,(\text{slope})}{\mu w}$$

$\Delta p = 7.5 \times 10^8$ dynes/cm^2
$\mu = 0.0098$ poise
$w = 0.01$ g particles/cm^3
slope = 30.83

$$= 0.6 \times 10^{12} \text{ cm/g}$$

In this calculation, all viscosities are measured by a Brookfield rotating viscometer precise to ± 0.2 cp.

Initial cake resistances are also calculated from the intercept of the line. However, these values are primarily used to insure that gross errors are not present during the filtration procedure. Intercepts often varied by a factor of two from the fastest to slowest filtering suspensions. Once again, such difficulties are known to occur when the start of filtration is unclear.

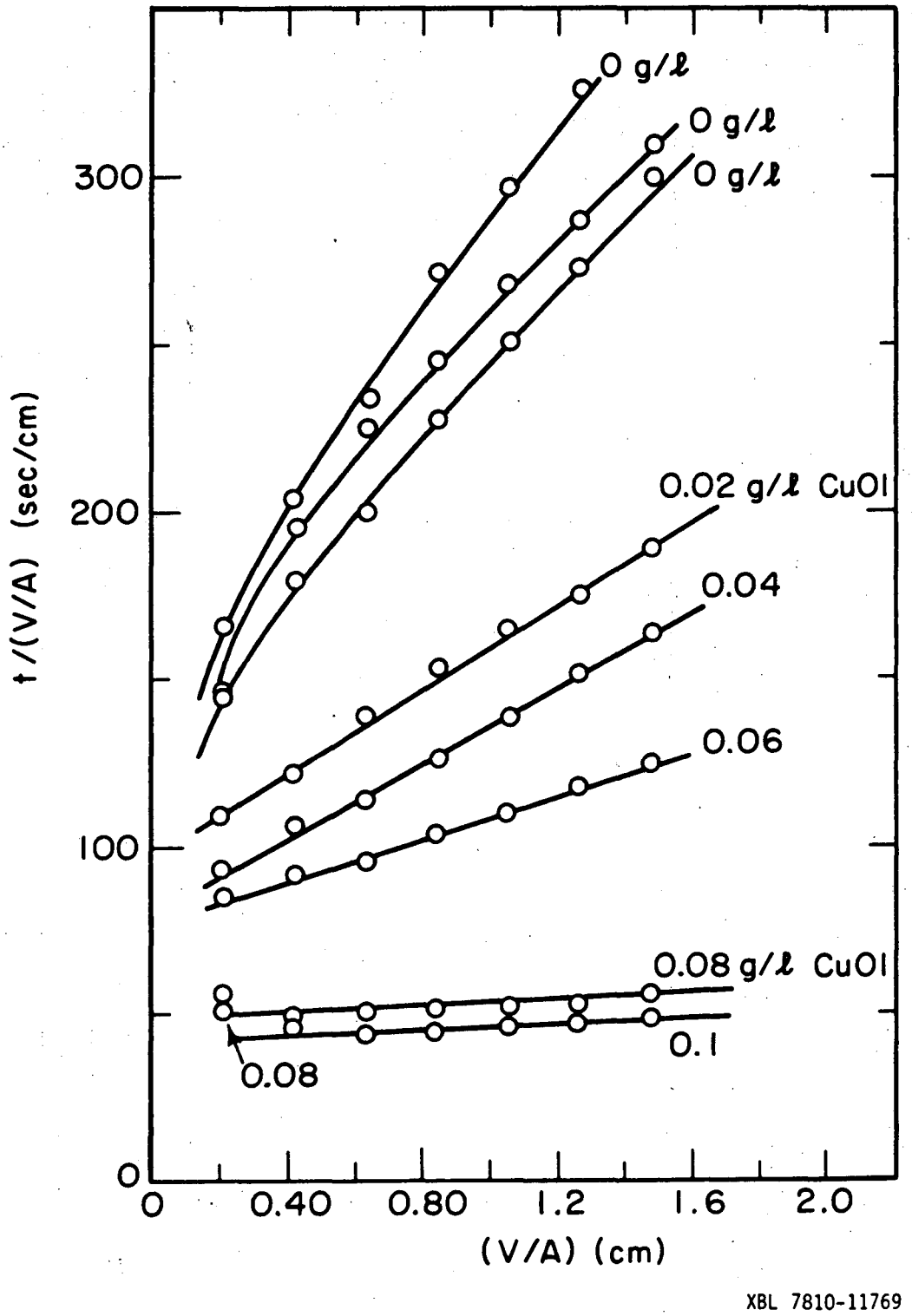

Figure IV-9. Filtration rate data.

5. Reproducibility

The reproducibility of the calculated α is found to be within ± 10% based on reproduced runs. A number of variables are suspect. The concentration and size distribution of the ash particles changes depending on how much asphaltenes dissolve and how well the sonification has dispersed the particles. Some solvent is also lost due to vaporization, affecting the measurement of time for aliquots of liquid to be collected. The latter was usually small and runs with greater than 5% loss were discarded. If one assumes errors as large as 5% in timing do take place, a maximum deviation of approximately ± 20% could be expected for the larger cake resistivities. Such large errors were never observed in duplicate runs.

F. Results and Discussion

1. Zeta Potential Measurements

Typical values of the zeta potential of those compounds observed in this study are listed in Table IV-6. These values change only slightly with time and are reproducible within ± 10 mV. Looking particularly at the SRC ash, the charge is positive in concurrence with measurements made by Henry and Jacques and by Rogers in SRC-UFO (26)(42). However, Roger's value of 15 mV is considerably lower than those found here. Since no mention was made as to how electro-osmotic velocities were taken into account in his measurements, one is led to conclude that the discrepancies might be due to such velocities.

TABLE IV-6. Zeta potential of typical suspensions

	mV
Ash in pyridine (partially extracted)	50 - 70
Ash* in SRC solvent	60
Ash* in toluene	0
Ash* in benzene	0
Kaolin in pyridine	0
Kaolin in water	-50 - -60
Sterling FT in: pyridine	0
toluene	0
benzene	0

*Partially extracted ash found to exhibit a 50 mV charge in pyridine.

The charge of the SRC ash is of the magnitude that has achieved stability in other nonaqueous dispersions. The 60 mV potential curve for ash particles in SRC solvent is seen in Figure IV-10. In calculating this curve, a coulombic repulsive and Hamaker attractive potentials were again assumed. In light of the maximum Debye lengths calculated in Section D for the suspensions, a coulombic potential will overestimate the repulsion. However, the calculated Debye lengths were the minimum values and should be significantly higher in most suspensions, especially in the SRC solvent. In this plot, the maximum is seen to occur at 15 kT, approximately that supposedly necessary to insure stability as stated by Verwey and Overbeek.

Henry proposed that the asphaltenes are primarily responsible for the charge. This is supported by varying the amount of extraction used to isolate the ash from the SRC-UFO. A plot of the zeta potential as a function of extraction time is seen in Figure IV-11. As more asphaltenes are removed, the charge drops toward zero. At this final point, the suspending pyridine solvent is completely colorless.

The magnitude of the charge is somewhat lower than found on asphaltenes in other studies. Wright and Minesinger found the mobility to be a factor of two larger with a zeta potential of approximately 100 mV. However, such differences can be attributed to the variation in particle composition and solvent purity. For example, the petroleum asphaltenes used in their study are known to have different functional groups (34)(36)(37)(97).

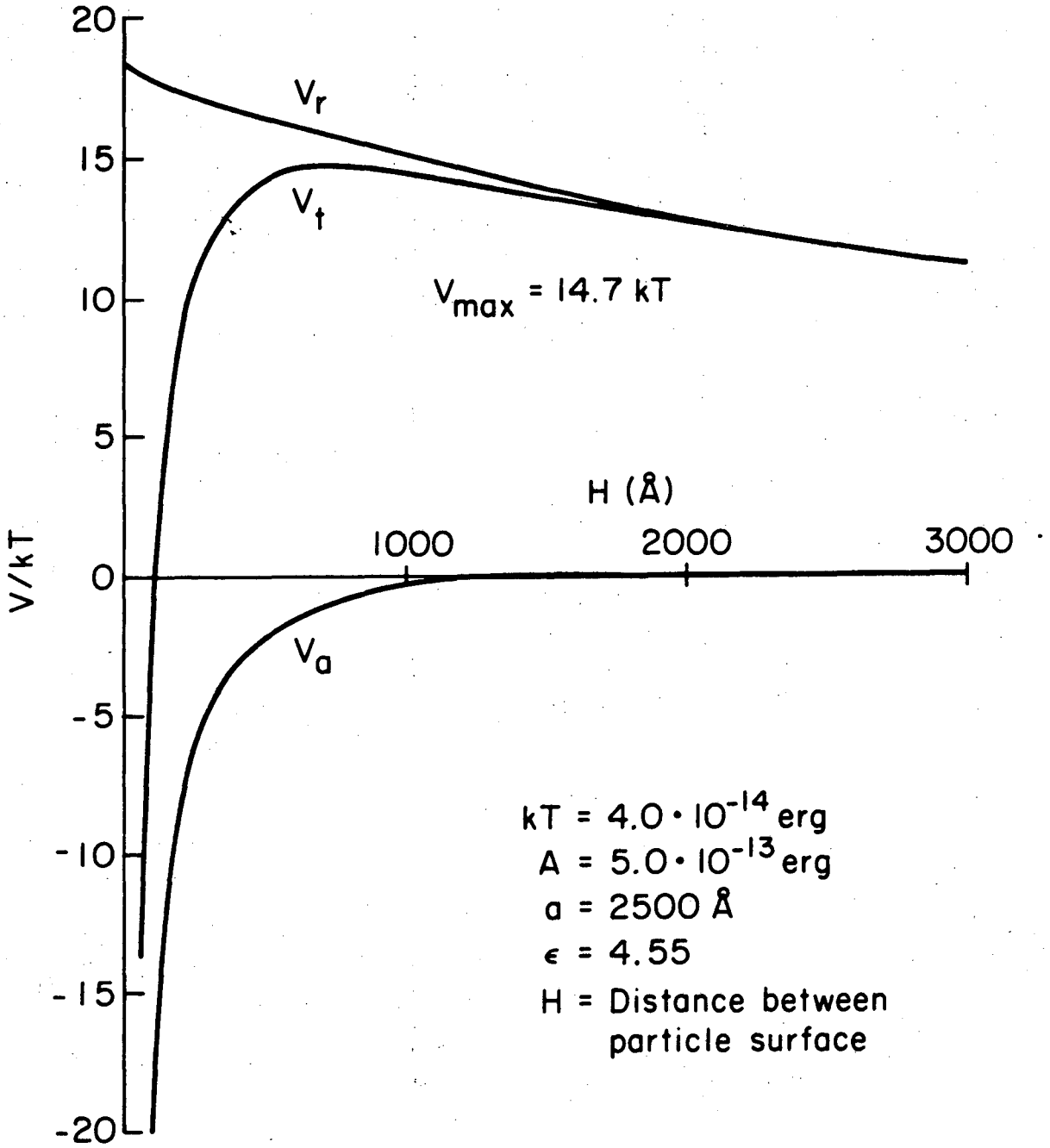

Figure IV-10. Potential curves for SRC solvent/SRC ash suspensions.

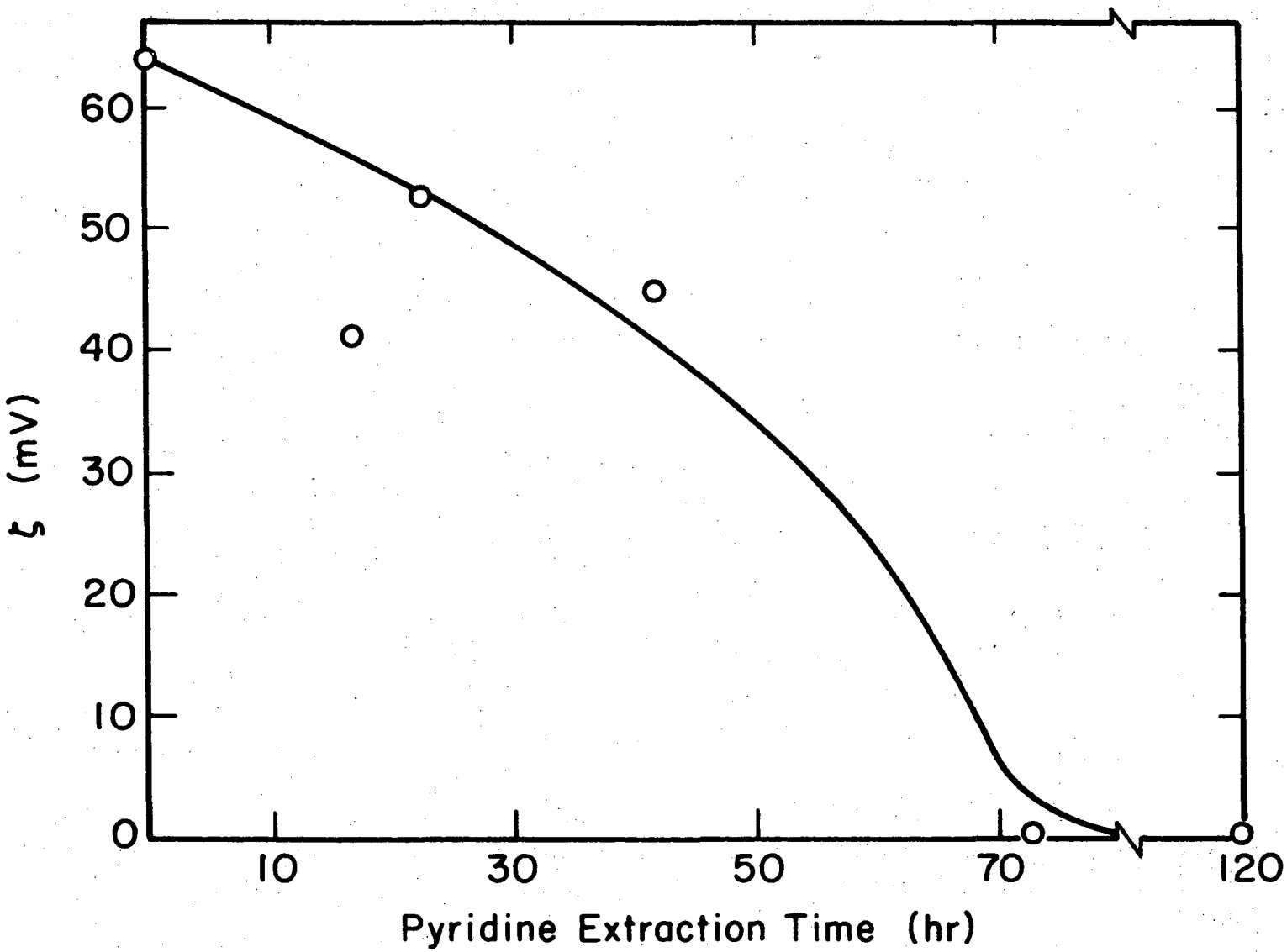

Figure IV-11. Effect of extraction on zeta potential. XBL 7810-11767

Referring to Table IV-6 again, no charge is measured when the ash is suspended in either toluene or benzene. The nature of the solvent is all important in charging the particles. The solvent must be able to solubilize the acid-base pairs of the asphaltenes. The aromatic solvents are too nonpolar to accomplish this.

In solvents that can, it is assumed that a certain degree of ionization takes place as suggested and shown by Eldib and Csayni and Bassi (46)(47). The positive charge on these particles suggests that there is an excess of basic groups on the surface which can pick up a proton, presumably through an acid-base reaction with the asphaltene acids. These negatively charged species exist solubilized by the solvent forming the double layer around the particle. Although the dissociation of an acid is undoubtably low in such nonaqueous solvents, calculations in Chapter I have shown that the extent does not have to be that large; a small number of charges on the surface gives rise to a large surface potential. The basic groups on the surface can either come from the solvent as suggested by Henry and Jacques, or be a part of the high melting carbonaceous material that has been found to be a part of the ash (5). In work to be mentioned, the former method seems to occur in pyridine suspensions of ash.

2. Correlating Zeta Potential and Filtration

a. Pure Solvents

Typical plots of zeta potential and specific cake permeability versus concentration of copper oleate for dispersions of ash in pyridine are seen in Figures IV-12 and IV-13. The filtration rate is enhanced

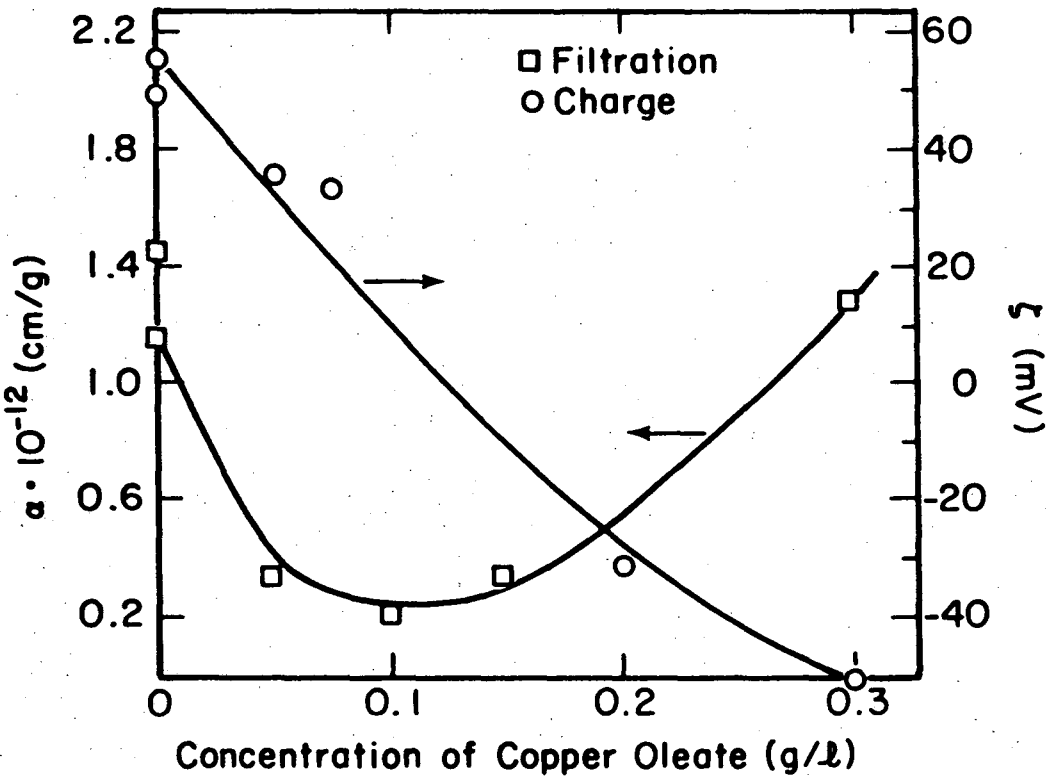

XBL 7810-11764A

Figure IV-12. Effect of copper oleate on filtration and zeta potential of suspensions of 23 hour extracted ash in pyridine.

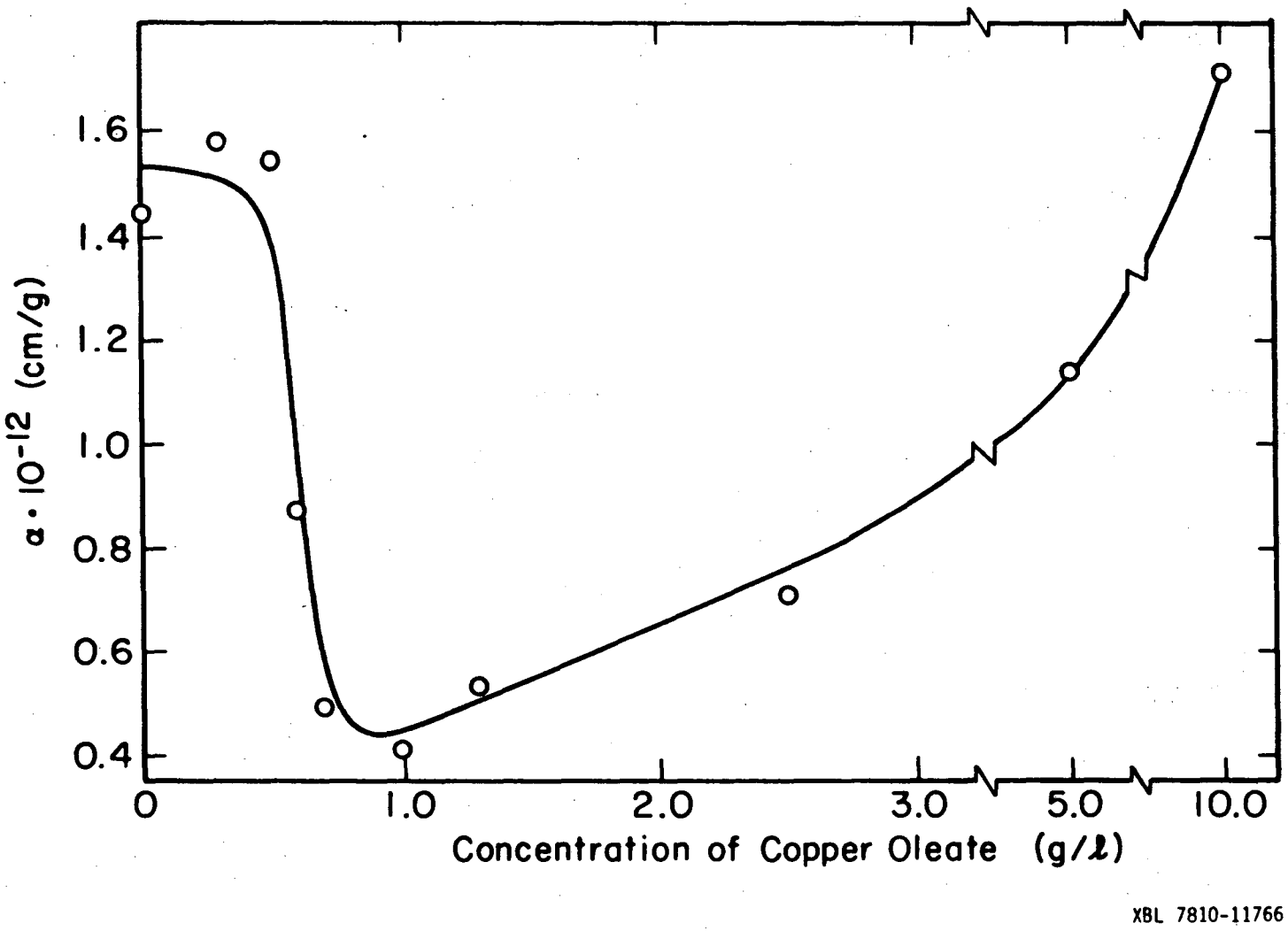

Figure IV-13. Filtration enhancement of 9/1 pyridine diluted SRC-UFO.

and then diminished as the zeta potential is reduced to zero and then increased to a high negative value. This phenomenon occurs both in dispersions of extracted ash and in dispersions with ash introduced with SRC-UFO.

The dependence of α on zeta potential is further accentuated by Figure IV-14. This graph plots zeta potential versus α of a number of different dispersions where both the concentration of the cooper oleate and time of extraction are varied to change the zeta potential. In all cases, there is a dramatic increase in the specific cake resistivity as the zeta potential approaches 40 mV. The shape of the curve is strikingly similar to the plots of the stability ratio of Fuchs versus zeta potential given in Figure IV-2.

The correlation between zeta potential and α is found to be independent of the charging or charge neutralizing mechanism. Sterling FT dispersed in toluene solutions of copper oleate also exhibits this large decrease in filtration rate as the zeta potential of the particles increases Similarly, kaolin in water, coagulated by KCl through compression of the double layer follows the same pattern. These results are plotted in Figures IV-15 and IV-16.

Photomicrographs of dispersions of particles with high and low potentials show only a small difference in the extent of agglomeration. However, these differences become more evident as the solvent is changed from an asphaltene solvent to an aromatic hydrocarbon. Figures IV-17 and IV-18 show much tighter agglomeration in toluene than in pyridine where particles do exhibit a charge.

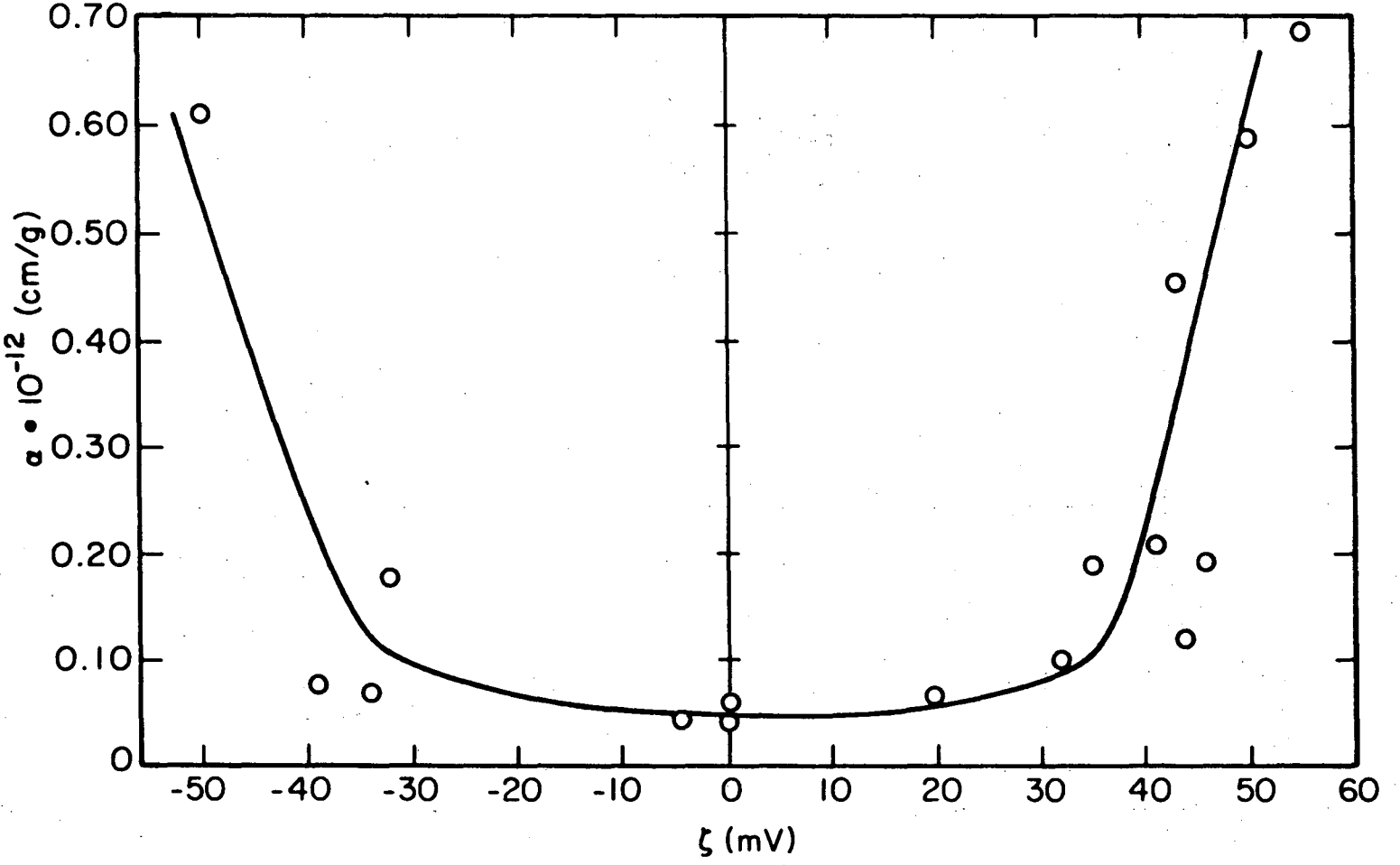

Figure IV-14. Effect of zeta potential on cake resistance of ash dispersions in pyridine.

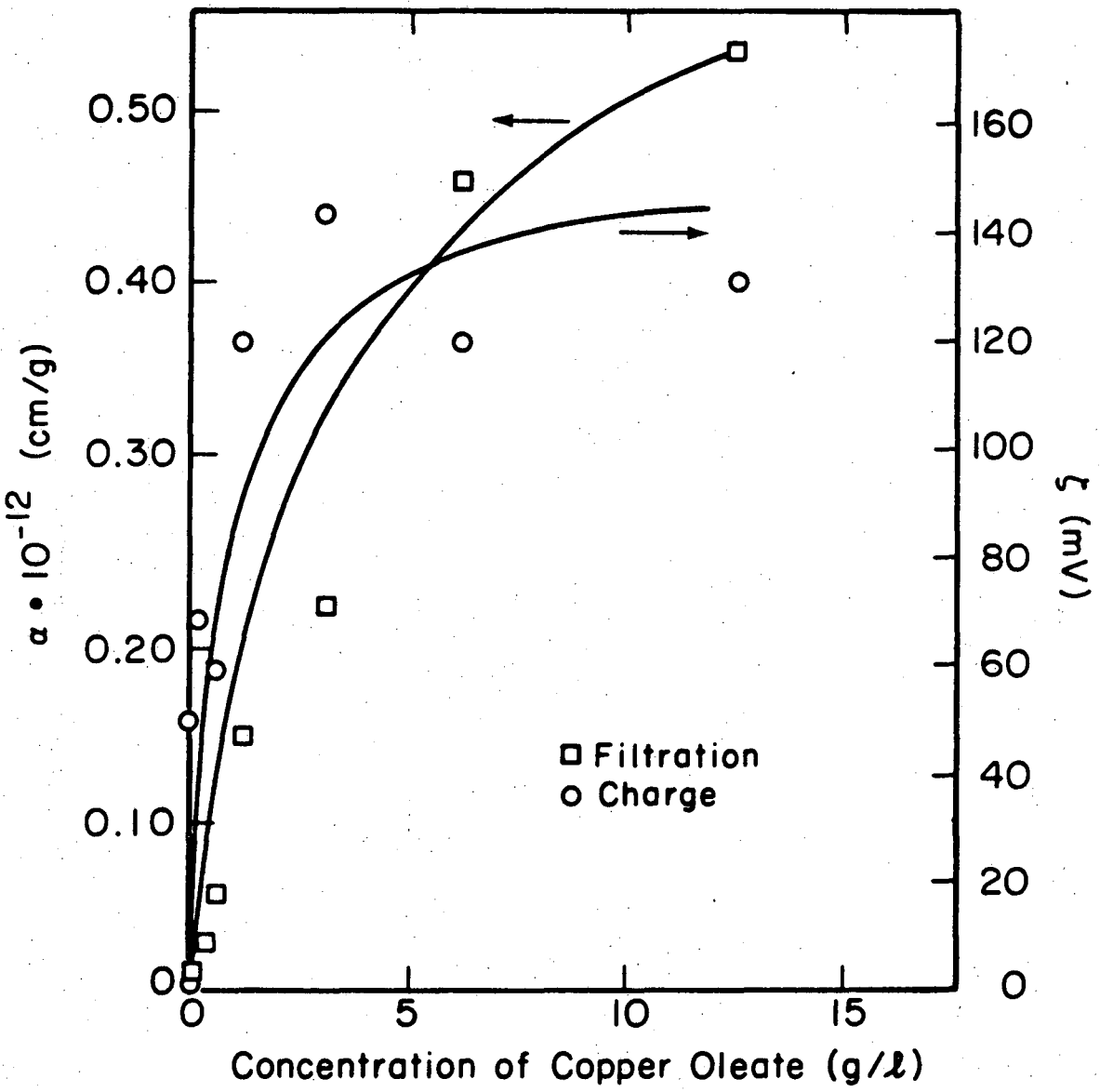

XBL 7810-11763A

Figure IV-15. Effect of copper oleate on suspension properties of Sterling FT in toluene.

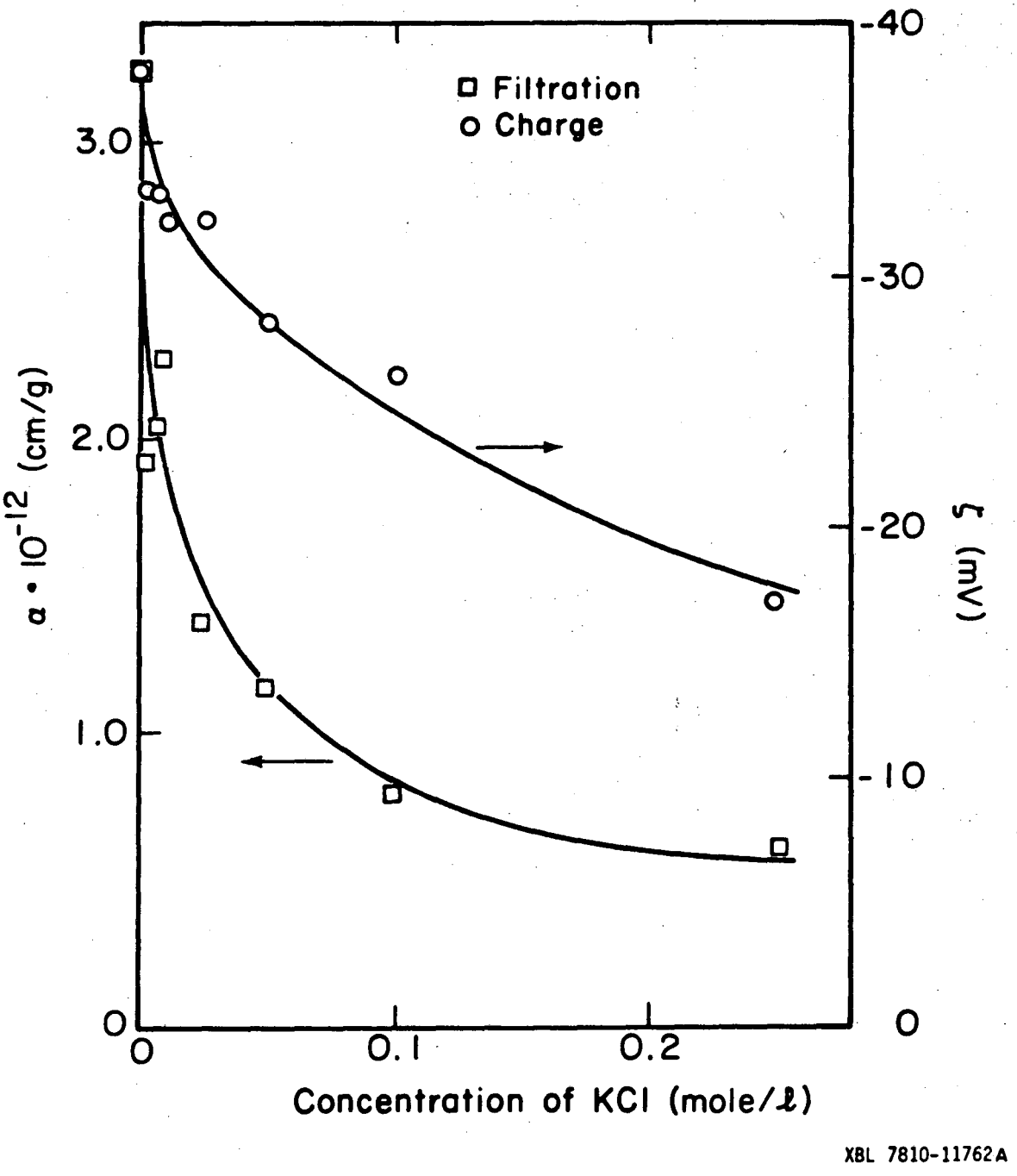

Figure IV-16. Effect of KCl on suspension properties of kaolin in water.

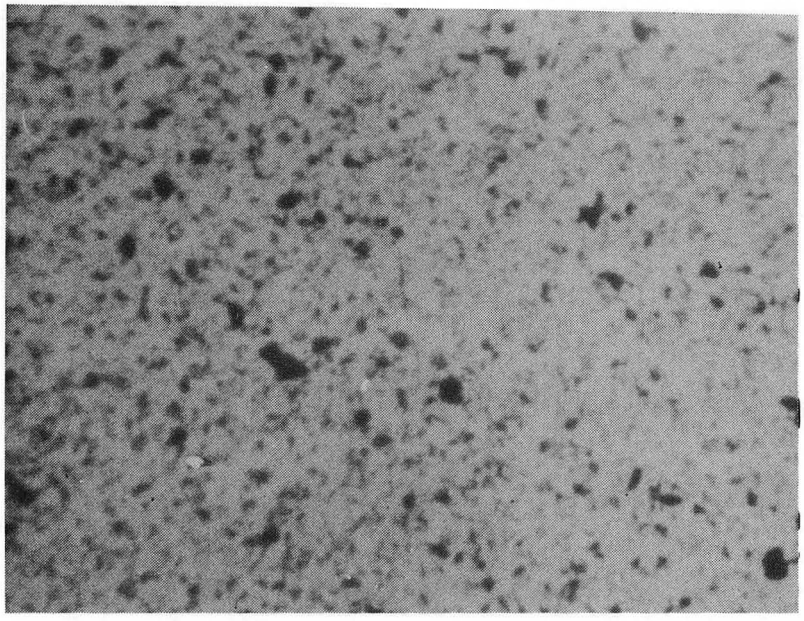

Figure IV-17. 23 hour pyridine extracted ash in toluene.

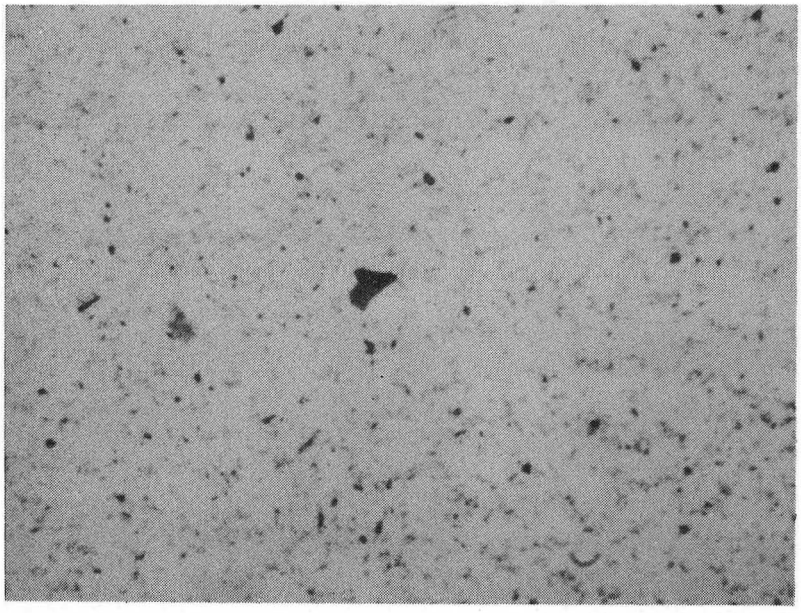

XBB 780-13043

Figure IV-18. 23 hour pyridine extracted ash in pyridine.

b. Effect of the Electrolyte

Both ions of copper oleate are known to preferentially adsorb depending on the surface characteristics. The experimental results with the ash from SRC-UFO imply a preferential adsorption of the oleate anion. Doing so, the ion not only reduces the initial positive charge, but also causes a reversal at higher concentrations. Explanation of this charge character is difficult considering the complex mixture of compounds in the dispersions. This is further complicated by the existence of water in the solvent. However, some observations can be made.

The oleate anion is undoubtedly electrostatically attracted to the positive surface. However, this is not sufficient to account for the charge reversal. Adsorption of either ion on the surface can take place due to London type interactions between the chain and the surface. The proclivity of one ion to adsorb over another is dependent on the solid surface, the structure of the ions and the characteristics of the solvent, as seen in work with Cadips and tiap (see Section IV-B). Overbeek has suggested that in the case of copper oleate, the positive ion is slightly more hydrophilic than the negative. Thus, the cation may be more likely to exist in micelles around the water present in the solvent (95)(96). This is probably only one of many factors that come into play in this system.

c. Zeta Potential's Effect in Filtration

The known effect of a reduced zeta potential, coagulation, can be combined with simple filtration theory to understand the reduction of the value of α. The average specific cake resistivity has been given

as

$$\alpha = \frac{36\, S_p^2\, (1 - \varepsilon)\tau^2}{\rho_p\, \varepsilon^3} .$$

Assuming the porosity constant, α can be considered proportional to the square of the specific surface area, S_p, of the particles. This being the case, $(\alpha^o/\alpha)^{1/2}$ is a normalized effective surface area where α^o is the specific cake resistance without an electrolyte. A decrease in surface area by a factor of 2-6 is noted in these experiments. Such aggregates are not distinguishable in photomicrographs of supposedly coagulated and non-coagulated dispersions. The calculation is, therefore, more indicative of the tendency of the small particles traveling through the cake to capture on neighbors forming agglomerates. If the small particles do cling to others, an effectively looser, more permeable cake will result. However, if they can not be captured because of electrostatic repulsion, the particles will move with the fluid until trapped by small constrictions, thereby plugging the cake and leading to large resistances.

If this capture is indeed a function of zeta potential, then the tendency for sticking should be related to the stability of the dispersion and α should be a function of the stability ratio, W. W, in this case, is a measure of the potential barrier to coagulation for two particles. Using an average radius of 2500 Å for the ash particles, the stability ratio for ash in pyridine is given at different zeta potentials in Table IV-7. The same attractive and repulsive potential functions assumed previously are used in these calculations.

TABLE IV-7. Stability ratio W as a function of zeta potential for pyridine and ash suspensions

mV	W
60	5.61×10^{17}
50	7.36×10^{11}
40	1.7×10^{7}
30	6.2×10^{3}
20	34.2
0	1.0

If the specific cake resistance is related to W, the function must be one that can negotiate the large range of values W has. One possible function is

$$\alpha = c_1 W^n \qquad \text{(IV-8)}$$

or

$$\ln \alpha = \ln c_1 + n \ln W \qquad \text{(IV-9)}$$

To determine whether any correlation is evident, the data in Table IV-7 is used in conjunction with the α versus zeta potential curve of Figure IV-14. The values chosen are shown in Table IV-8. Plotting ln W versus ln α, a good correlation results with an exponent of 0.10 as seen in Figure IV-19. This exponent, no doubt depends on the particular dispersion, but once determined, might be used to predict the effect of charge on the filterability of a suspension that coagulates in the bed.

d. Natural Solvent

The effect of copper oleate on zeta potential and of the ash in SRC solvent is shown in Figure IV-20. Similar results are obtained using Aerosol OT in the same system. Although the charge measured is of the same order of magnitude as in pyridine, no reduction of charge is found upon adding either oil soluble salt. The observation is similar to those results found by McGowan et al., where Vulcan R in xylene maintained a high negative charge despite addition of Aerosol OT (53).

TABLE IV-8. Values for plotted α versus W

mV	log W	log α
50	11.87	11.81
40	7.27	11.28
30	3.79	11.0
20	1.53	10.78
0	1.0	10.60

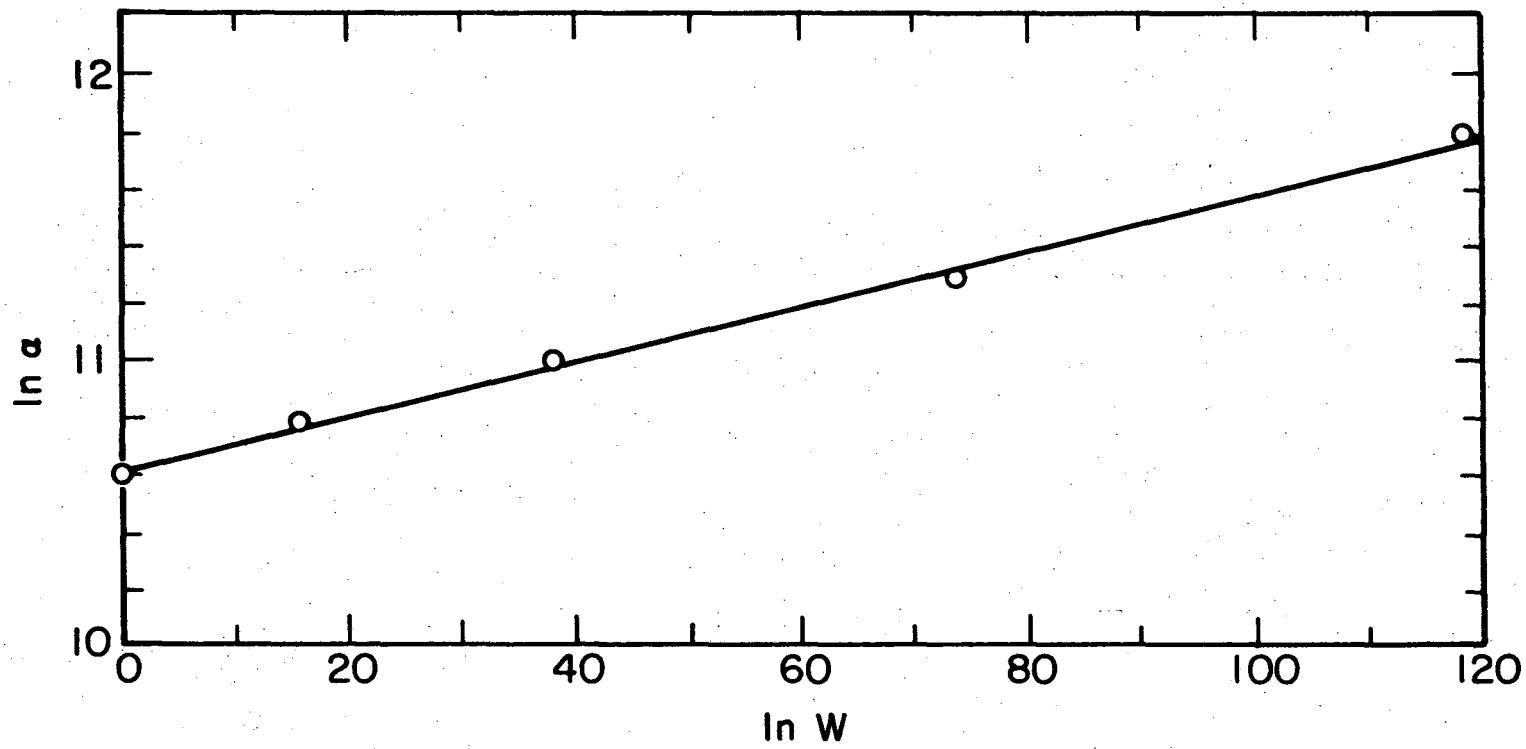

XBL 7810-11761

Figure IV-19. Correlation of stability ratio to specific cake resistance of ash in pyridine suspensions.

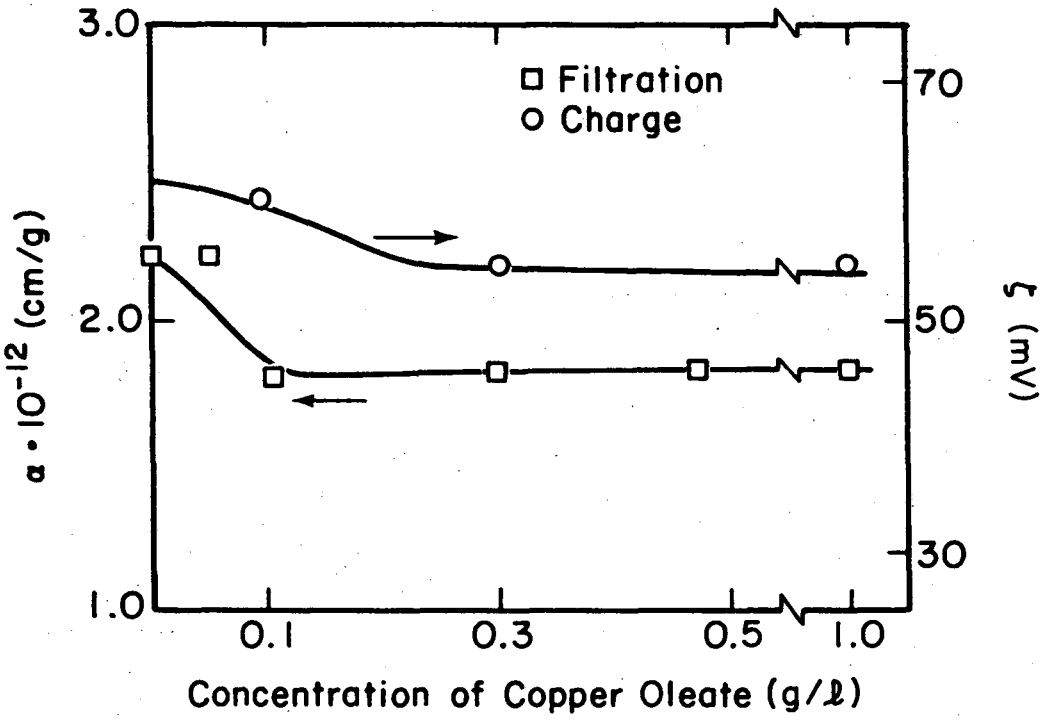

Figure IV-20. Effect of copper oleate on cake resistances of 9/1 SRC solvent diluted SRC-UFO.

The observed constant charge may be attributed to a number of physical phenomena. The charge would not be expected to change if copper oleate does not dissociate in the SRC solvent. However, conductivity measurements indicate that dissociation does take place (Sections II-A and IV-D). Furthermore, copper oleate does charge particles in less polar solvents such as benzene and toluene.

If adsorption does occur, nearly equal amounts of both the anions and cations of copper oleate must adsorb to maintain a constant charge. In the case of nonpolar dispersions, a slight preferential adsorption can cause a large zeta potential. Such nearly identical adsorptions are unlikely.

It is possible that neither oleate ion adsorbs onto the surface of the ash particles. The oleate ions may prefer the solvent rather than the solid surface. Once again, this seems to be improbable since copper oleate has been found to alter the charge on particles in both nonpolar solvents such as xylene and toluene and in medium polar solvents such as pyridine.

The adsorption of the oleate ions may be hindered, on the other hand, by the presence of other ions or molecules in the SRC solvent which adsorb preferentially onto the surface of the ash, saturating the surface adsorption sites. As pointed out earlier in this chapter, van der Minne and Hermanie observed that negative carbon black particles charged by tiap remained so, despite the addition of Ca dips which is able to charge the same particles positive if added alone to the dispersion. Although both Ca dips cation and tiap's anion are preferentially adsorbed,

the adsorption of the anion is slightly favored and maintains a rather large negative charge on the particles. Once again, the preferred adsorption does not have to be large to maintain this charge.

The results of van der Minne and Hermanie are not only similar to those found in dispersion of ash in SRC solvent, but also to observations of the suspensions of the poorly extracted ash in pyridine. Referring to Figure IV-3, the charge on the ash particles remained constant despite the addition of copper oleate in the dispersions of the poorly extracted ash. However, as more of the pyridine soluble material is removed, the ash's charge becomes more susceptible to the effect of the oleate ions in solution. In the latter case, the oleate ions are able to compete for the surface adsorption sites.

Both the SRC-UFO and the SRC solvent contain a significant amount of polar compounds (up to 10% of the solvent is base extractable) which is presumably responsible for the original charge on the ash particles. These species do dissociate (46)(47) and may serve as those compounds which preferentially adsorb on the particle surface in lieu of the oleate ions.

The adsorption of these dissolved molecules from the solvent onto the surface is substantiated by work done with suspensions of heavily extracted, noncharged particles in pyridine. These particles will become charged upon the addition of aliquots of a pyridine diluted SRC-UFO solution that is without particles. The resulting zeta potential varies from 40 to 50 mV after the suspension has been allowed to stand a short period of time. These polar compounds, presumably light asphaltenes and resins, have been found necessary to insure stability dispersions

of insoluble asphaltenes in the petroleum oils. In this work by Swanson, oil derived asphaltenes suspended in asphalt oils coagulated readily unless the resin fraction of the asphalt was added to the suspension. Unfortunately, no charge measurements were made (32).

Although derived from coal, the components of the SRC solution are not radically different from those of petroleum asphalt solutions. Even the suspended ash particles in the SRC solvent contain nearly 50% by weight carbonaceous material which has been theorized as the high molecular weight asphaltenes (4). Thus, these ash particles may be stabilized similarly by the resin/light asphaltenes absorbed on the particle surfaces. Because of the amount and possible preferential adsorption of the asphaltenes, copper oleate has little effect on the charge or stability of the SRC solvent dispersion of the ash particles.

e. Comparison of Specific Cake Resistances

Specific cake resistances of several 0.1-1.0 micron sized particle suspensions from literature are given with those fould in this study in Table IV-9. In addition, the α calculated for SRC-UFO filtration in filter leaf tests are listed. When there is evidence of stability, the α are usually higher than those found by others. The presence of very small particles in the filtration runs in these studies could significantly increase the cake resistance. Similarly small sized, dispersed kaolin particles also filter as poorly as the sonified ash.

TABLE IV-9. Comparison of specific cake resistances

Suspension	Reference	Size (μm)	Pressure (psi_a)	$\alpha \times 10^{-12}$	Condition
Polystrene lattices with 0.01 M $Al_2(SO_3)_3$	97	0.44	15	0.269	(presumed coagulated)
E-A Kaolin 50 g/l 0.01 M $Al_2(SO_3)_3$	97	0.25-2	15	0.12	(presumed coagulated)
E-A Kaolin 50 g/l 0.01 M Na_4PO_4	97	0.25-2	15	0.54	(presumed coagulated)
Fine Silica in water	97	0.1	15	1.3	(presumed dispersed)
Kaolin in water	*	1.0-0.5	15	3.2	Dispersed
Kaolin in water 250 mM KCl	*	0.1-0.5	15	0.05	Coagulated
Sterling FT in toluene	*	0.1-0.5	15	0.025	Coagulated
Sterling FT in toluene 20 mM Copper Oleate	*	0.1-0.5	15	0.53	Dispersed
SRC-UFO	4		20	0.17	T = 149 °C
			20	0.18	T = 93
SRC-UFO	5		20	0.14	T = 150 °C
			50	0.34	100
			60	0.21	150
			80	0.25	150

(TABLE IV-9.) (continued)

Suspensions	References	Size (μm)	Pressure (psi_a)	$\alpha \times 10^{-12}$	Condition
SRC-UFO	8		50	0.26	T = 150 °C Coal precoat
SRC Ash charged in pyridine	*		15	1-2	Dispersed
SRC Ash charged in pyridine 100 mM Copper Oleate	*		15	0.06-0.4	Coagulated
SRC solvent SRC-UFO 9-1 dilution	*		15	2.0	
SRC solvent charged ash	*		15	0.2-0.33	No sonification

*Experimental results from this study.

Unlike those in the high temperature studies, all suspensions in this work were subjected to ultrasonics which breaks up most of the agglomerates. Referring to Figure IV-8, the effect of charge is only manifested if the naturally occurring agglomerates are broken down to their primary particles. These particles can be dispersed by the measured charge. Without such sonification, charged ash in the SRC solvent filtered with an α of approximately $0.2\text{-}0.3 \times 10^{12}$ cm/g, about that found in the high temperature studies. Addition of copper oleate to these unsonified suspensions did not change the α.

The apparatus, size distribution of the particles, and procedure used to obtain α vary and, therefore, may account for the discrepancies between the runs presented here and elsewhere. Charge can play an important role in determining the ease of filtration, but its importance is integrally dependent on the nature of the filtered suspension.

One should also note that even if the ash can be coagulated, there seems to be a lower limit to which α approaches for particles of around 0.1-0.5 microns in diameter. Some of the small particles will always be unbounded and cause plugging of the cake even in the most agglomerated of suspensions.

V. CONCLUSIONS

The ash particles in solvent refined coal solutions have a positive charge which stabilizes the nonpolar dispersion and makes filtration more difficult. Agglomeration of these particles through the addition of common solvents and coagulants is not extensive. However, the stability and the filtration rate of nonpolar dispersions can be modified significantly by the addition of an oil soluble salt which adsorbs onto the surface of the particles. Filtration is integrally dependent on the particle charge.

Unfortunately, ash dispersions in solvents with considerable amounts of dissolved asphaltenes maintain their charge and stability in spite of copper oleate addition. Presumably, these asphaltenes are preferentially adsorbed compared to the oleate anion making charge reduction possible only when the concentration of the asphaltenes is low. This being the case, more strongly adsorbing anionic surfactants must be used if charge reduction is to increase filtration rates of ash dispersions in the solvent refined coal solvent and solutions. Nonetheless, the specific cake resistances already observed for the solvent refined coal-unfiltered oil measured at pilot plant conditions are within an order of magnitude of the best cake resistances found for suspensions of such small particles, even when coagulated or flocculated. It is doubtful whether a one order magnitude

decrease in the specific cake resistances of the solvent refined coal - ash suspensions will be sufficient to overcome the economic difficulty of filtration in the solvent refined coal process.

BIBLIOGRAPHY

1. Solvent Refined Coal, pamphlet by PAMCO-ERDA (1976).
2. Jimeson, R., Chem. Eng. March 1, (1976).
3. Rogers, B. R., and Westmoreland, P. R., "Agglomeration and Separation of Micron-Sized Particles from Coal Liquefaction Streams," presented at the 81st National AIChE Meeting.
4. Katz, S. and Rogers, B. R., Ind. Eng. Chem. Proc. Des. Dev., Vol. 15, 3, (1976).
5. Johns Manville Sales Corporation Final Report, EPRI AF 614 Project 459-1, Dec. (1977).
6. Pittsburgh and Midway Coal Mining Co., Quarterly Technical Report, January-March (1977).
7. Smith, G. R. S. and Martin, P. C., "Pressure Filtration of Liquefied Coal," Johns Manville Sales Corporation, presented at 4th Annual Int. Conference on Coal Gasification, Liquefaction and Conversion to Electricity, University of Pittsburgh, Aug. 2-4, 1977.
8. Rogers, B. R., "Filtration of Micron-Sized Particles from Coal Liquids - Carbonaceous Precoats," for presentation at the Second Pacific Chemical Engineering Congress, Denver, Co., Aug. 28-31, 1977.
9. Smith, G. R. S. and Hines, R. C., Johns Manville Corporation, FE - 2007 - 20 Sept. 1976.

10. Maxwell, E., M. I. T., ERDA/NSF/EPRI, Prin. Investigators Conference - Coal Research 3-4 Sept. 1976.

11. Snell, G. J. and Simone, A. A., EPRI AF - 234, Sept. 1976.

12. Walden Research, Massachusetts, Contract MER/2245.

13. Sze, M. C., and Snell, G. J., U. S. Patent 4,040,957.

14. Rogers, B. R., Hydrocarbon Processing, 191, May (1976).

15. Simone, A. A., Combustion, 15, May (1976).

16. Sze, M. C., Snell, G. J., U. S. Patent 3,852,182.

17. Snell, G. J., U. S. Patent 3,852,183.

18. Sze, M. CM and Snell, G. J., U. S. Patent 3,856,675.

19. Gorin, E., Kulik, C. J., Lebowitz, H. E., Industrial Eng. Chem. Process Des. Dev., 16, No. 1, 95 (1977).

20. Gorin, E., Kulik, C. J., Lebowitz, H. E., Ind. Eng. Chem. Process Des. Dev., 16, 102 (1977).

21. Farmand, J. R., Puddington, I. E., U. S. Patent 4,029,567.

22. Weller, Pelipetz, Friedin, Ind. Eng. Chem., 43, 1572 (1951).

23. Reerink and Lyzenza, J. Electroanal. Chem., 37, 215 (1972).

24. Sternberg, H. W., Raymond, R., Schweighardt, F., "The Nature of Coal Liquefaction Products," presented at the Sym. of Progress of Processing Syn. Crudes and Resins, Div. of Pet. Chem. Inc. Am. Chem. Soc., Chicago, Aug. 24-29, 1975.

25. Mitchell, R. S., Gluskoter, H. J., Fuel, 55, April (1976).

26. Henry, J. D. Jr., and Jacques, M. T., "Charged Characteristics of Particles in Coal Derived Liquids: Measurement and Origin," preprint, accepted by AIChE Journal.

27. Schweighardt, F. K., Retcofsky, H. L., and Friedal, R. A., Fuel, 55, Oct. 313 (1976).

28. Wooten, D. L., Coleman, W. M., Taylor, L. T., Dorn, H. C., Fuel, 57, Jan. 17 (1978).

29. Farcasiu, M., Fuel, 56, 9 (1977).

30. Briggs, D. E., Addington, D. V., Cameron, J. R., ERDA Contract No. EX-76-S-01-2550, quarterly report Jan.-Mar. 1977.

31. Schwager, I., Yen, T. F., Fuel, 57, 100 (1978).

32. Swanson, J. M., J. Physical Chem., 17, 141 (1941).

33. Sternberg, H.W., Raymond, R., Schweighardt, F. K., Science, 188 (1975).

34. Moschopedis, S. E., and Speight, J. G., Fuel, 55, 334 (1976).

35. Taylor, S. R., and Li, N. C., Fuel, 57, 117 (1978).

36. Moschopedis, S. E., Fryer, J., and Speight, J. G., Fuel, 55 (1976).

37. Ignasiak, T., Strausz, O. P., and Montgomery, D. S., Fuel, 56, 359 (1977).

38. Reerink, H., Ind. Eng. Chem. Prod. Res. Dev., 12, 82 (1973).

39. Dickie, J. P., Haller, M. W., and Yen, T. F., J. Colloid and Interf. Sci., 29, 475 (1969).

40. Rogers, B. R., ACS Meeting, Symposium, Anaheim, Ca. (1978).

41. Moschopedis, S. E., and Speight, J. G., Fuel, 55, 187 (1976).

42. Rogers, B. R., personal communication (1978).

43. Briant, J., Rev. Inst. Fr. Pet. Ann. Combust. Liq., 18, 1 (1963).

44. Girdler, R. G., Proc. Assoc. Asphalt Paving Technol., 34, 45 (1965).

45. Preckshot, G. W., DeLisle, N. G., Cotrell, C. E., and Katz, D. L., Am. Inst. Min. Eng. Trans., 151, 188 (1943).

46. Eldib, I. A., A.C.S. Div. Pet. Chem. Prepr., 7, 31 (1962).

47. Csayni, L. H., and Bassi, B. S., Procs. of Assoc. of Asph. Paving Technologists, 27, 52 (1958).

48. Wright, J. R., and Minesinger, R. R., J. of Colloid Sci., 18, 223 (1963).

49. Lyklema, J., Adv. in Colloid and Inf. Sci., 2, 65 (1968).

50. Koelmans, H., and Overbeek, J. Th. G., Disc. of Faraday Soc., 42, 232 (1966).

51. Damerell, V. R., and Urbanic, A., J. Phys. Chem., 48, 125 (1944).

52. Kitahara, A., Komatsuzawa, T., and Kon-no. K., J. Colloid and Polymer Sci., 255, 1178 (1977).

53. McGowan, D., Parfitt, G., and Willis, E., J. of Colloid Sci., 20, 650 (1965).

54. Kitahara, A., Karasawa, S., and Yamada, H., J. of Colloid and Interface Sci., 25, 490 (1967).

55. Kitahara, A., Komatsuzawa, T., and Kon-no. K., Proceedings of the 5th Int. Congress on Surface Active Substances, Barcelona (1968).

56. Damerell, V. R., and Mattson, R., J. Phys. Chem., 48, 134 (1944).

57. Parreira, H., J. Electroanalytic Chem., 25, 69 (1970).

58. Parreira, H., J. of Colloid and Interface Sci., 43, 382 (1073).

59. Vijayendran, B., "Colloidal Dispersions and Micellar Behavior," ACS Symposium Series 9, 211 (1975).

60. Meadus, F. W., Puddington, I. E., Sirianni, A. F., and Sparks, B. D., J. of Colloid and Interface Sci., 30, 46 (1969).

61. Micale, F., Lui, Y., and Zettlemoyer, A. C., Trans. Faraday Soc., 62, 238 (1966).

62. Hamaker, H. C., Physica IV, 10, 1059 (1937).

63. Hoskin, N. E., Trans. Faraday Soc., 49, 1471 (1953).

64. Verwey, E. J. W., and Overbeek, J. Th. G., "Theory of the Stability of Lyophobic Colloids," Elsevier, Amsterdam (1948).

65. Overbeek, J. Th. G., "Colloid and Surface Chemistry, Part 2, Lyophobic Colloids," Chapter 11, Center for Advanced Eng. Study, M.I.T., 1976.

66. Bagchi, P., and Vold, R. D., J. of Colloid Interface Sci., 33, 405 (1970).

67. Mackor, E. L., J. Colloid Sci., 6, 492 (1951).

68. van der Waarden, M., J. Colloid Sci., 5, 317 (1950).

69. Parfitt, G. D., and Willis, E., J. Phy. Chem., 68, 1780 (1964).

70. Parfitt, G. D., and Willis, E., J. of Colloid and Interface Sci., 22, 100 (1966).

71. La Mer, V. K., and Healy, T. W., "Reviews of Pure and Applied Chemistry," 13, 112 (1963).

72. Kitahara, A., and Masao, H., J. of Colloid and Interface Sci., 41, 383 (1972).

73. Puddington, I. E., and Sparks, B. D., Mineral Sci. Engng, 7, 282 (1975).

74. Kruyt, H. R., and van Selms, F. G., Rec. Trav. Chim., 62, 415 (1943).

75. Sirianni, A. F., Paillard, G., and Puddington, I. E., Can, J. Chem. Engng., 47, 210 (1970).

76. Capes, C. E., McIlhinney, A. E., and Coleman, R. D., Trans. Soc. Min. Engrs. AIME, 247, 233 (1970).

77. Melgren, O., and Shergold, H. L., Trans. Inst. Min. Metall., 25, C267 (1966).

78. Zambrana, G. Z., Medina, R. T., Gutierrez, G. B., and Vargas, R. R., Int. J. Min. Proc., 1, 335 (1974).

79. van der Minne, J. L., and Hermanie, P. H. J., J. Colloid Sci., 8, 38 (1953).

80. Strong, L., and Krause, C. A., J. Amer. Chem. Soc., 72, 166 (1950).

81. Coplan, M. A., Fuoss, R. M., J. of Phys. Chem., 68, 1177 (1964).

82. Cooper, W. D., Wright, P., J. of Colloid and Interface Sci., 54, 1, (1976).

83. Fuchs, N., Z. Phys., 89, 736 (1934).

84. Parfitt, G. D., Wood, J. A., Ball, R. T., J. of Chem. Soc. Far. Trans. I. 69(11), 1908 (1973).

85. Smelie, Jr., R. H., and La Mer, V. K., J. Colloid Sci., 23, 589 (1958).

86. La Mer, V. K., Smelie, Jr. R. H., and Lee, P., J. Colloid Sci. 12, 566 (1957).

87. Slater, R. W., Kitchener, J. A., J. Colloid Interface Sci.,

88. Wiersema, P. H., Loeb, A. L., and Overbeek, J. Th. G., J. of Colloid and Interface Sci., 22, 78 (1966).

89. van der Minne, J. L., and Hermanie, P. H. J., J. Colloid Sci., 9, 1066 (1954).

90. Castellan, G., "Physical Chemistry." Addison-Wesley Co., Reading, Mass., 1971.

91. Newman, J. S., "Electrochemical Systems" Prentice-Hall Inc., Englewood Cliff, NJ 1973.

92. Komagada, S., Nippon Kagaku Zasshi, 53, 342, 969 (1932).

93. van Gils, G. E., and Kruyt, H. R., Kolloid-Beihefte, 45, 60 (1937).

94. Selucky, M. L., Chu, Y., Ruo, T., and Strausz, O. P., Fuel, 56, 369 (1977).

95. Overbeek, J. Th. G., "Colloid and Surface Chemistry, Part 2, Lyophobic Colloids," Chapter 10, Center for Advanced Eng. Study, M.I.T. 1976.

96. Albers, W., Overbeek, J. Th. G., J. of Colloid and Interface Sci., 14, 501 (1959).

97. Grace, H. P., Chem. Engineering Process, 49, 303 (1953).

This report was done with support from the Department of Energy. Any conclusions or opinions expressed in this report represent solely those of the author(s) and not necessarily those of The Regents of the University of California, the Lawrence Berkeley Laboratory or the Department of Energy.

Reference to a company or product name does not imply approval or recommendation of the product by the University of California or the U.S. Department of Energy to the exclusion of others that may be suitable.

TECHNICAL INFORMATION DEPARTMENT
LAWRENCE BERKELEY LABORATORY
UNIVERSITY OF CALIFORNIA
BERKELEY, CALIFORNIA 94720